DEVELOPMENT OF FLUORESCENT CARBON-DOTS FOR BIOLOGICAL IMAGING

A Thesis Submitted to
the Graduate School of Engineering and Sciences of
İzmir Institute of Technology
in Partial Fulfillment of the Requirements for the Degree of

MASTER OF SCIENCE

in Chemistry

by
Tuğçe KAVURANPALA

December 2021
İZMİR

ACKNOWLEDGEMENTS

I am honored to have the opportunity to express my gratitude to these people for helping and supporting me with my master thesis program. First of all, I would like to express my sincere thanks to my supervisor Prof Dr. Serdar Özçelik for his encouragement, understanding, scientific advice, and support. As a scientist, he helped complete this thesis thanks to his very good knowledge and patience. I am very honored to be working with a scientist like him.

Besides my supervisor, I would like to thank my thesis committee: Prof Dr. Ali Çağır and Prof Dr. Ceylan Zafer for their comments and guidance during all stages of my thesis. Also, special thanks to Prof Dr. Ali Çağır for providing device support from the laboratory.

I would like to thank all the members of Özçelik research group for helping and their endless support. I would like to especially thank my supporter Seçil Sevim Ünlütürk for her advice, great motivation, and helping at all times. Also, I would like to thank Didem Taşçıoğlu for helping me in all respects and being interested in my thesis. And I would like to thank İroda Saydulleva for helping my thesis for cell culture procedure and imaging.

I would like to express my sincere gratitude to my parents Gülhan and İlker Kavuranpala, and my sister Gökçe Kavuranpala for always supporting me, encouraging, me and helping me to improve myself in my career. Also, I would like to thank my fiancee and my best friend Mustafa Kabakcı for his love, patience, and encouragement. I am very lucky to have such a family.

ABSTRACT

DEVELOPMENT OF FLUORESCENT CARBON-DOTS FOR BIOLOGICAL IMAGING

Carbon dots are called carbon quantum dots or carbon nanoparticles (NPCs), and their use has recently started to increase thanks to their good biocompatibility, unique optical properties, easy synthesis, and low toxicity. Different kinds of carbon sources and amine sources also used as different dopes of chemical create a different emission color of CDs under UV-lamp. In this study, our aim to provide a simple synthesis of carbon dots with high quantum efficiency and low toxicity for use in cell imaging. Nitrogen and sulfur-doped carbon dots were synthesized using citric acid and thiourea, and emission was obtained in the blue-green region. After the synthesized carbon dots were seeded to the A549 cell culture, intracellular viability and cell toxicity results showed that carbon dots did not affect cell viability at certain concentrations. Afterward, the carbon dots are combined with gold nanoparticles and it is aimed to attach the gold to the surface of the carbon dots. Our aim here is to increase the efficiency of carbon dots, which give an emission peak at 550 nm, thanks to gold nanoparticles. As a result of these studies, it was proved by DAPI staining that the carbon dot is directed to the nucleus of the cell. Since it does not create a toxic effect and is transported to the cell nucleus, it allows it to be used in intracellular drug transport and imaging processes in the next stages.

ÖZET

BİYOLOJİK GÖRÜNTÜLEME İÇİN FLORESAN KARBON-NOKTALARININ GELİŞTİRİLMESİ

Karbon noktalar, karbon karbon kuantum noktaları veya karbon nanopartiküller (KNP'ler) olarak adlandırıyor ve iyi biyouyumlulukları, benzersiz optik özellikleri, kolay sentezleri, düşük toksisiteleri sayesinde son zamanlarda kullanım alanları artmaya başlamıştır. Farklı kimyasal katkılı olarak da kullanılan farklı karbon kaynakları ve amin kaynakları, farklı dalga boylarında emisyon veren bir karbon noktaları UV lambası altında rengi oluşturur. Amacımız, hücre görüntülemede kullanılmak üzere yüksek kuantum verimliliği olan ve düşük toksisiteye sahip karbon noktalarını basit şekilde sentezlenmesini sağlamaktır. Sitrik asit ve tiyoüre kullanılarak nitrojen ve sülfür katkılı karbon dotlar sentezlenmiştir ve mavi yeşil bölgede emisyon elde edilmiştir. Daha sonrasında sentezlenen karbon noktaları A549 hücresine ekildikten sonra, hücre içi canlılık ve hücre içi toksiklik sonuçları carbon noktalarının belli yoğunluklarda hücre canlılığını etkilemediğini göstermiştir. Sonrasında karbon dotlar altın nanoparçacıklar ile birleştirilerek, altınların karbon dotların yüzeyine bağlanması hedeflenmektedir. Buradaki amacımız 550 nm de emisyon peaki veren karbon dotların verimini altın nanoparçacıklar sayesinde arttırmaktır. Bu çalışmalar sonucunda karbon noktalarının hücrenin çekirdeğine yöneldiği DAPI boyaması yapılarak kanıtlanmıştır. Hem toksik etki yaratmadığı hemde hücre çekirdeğine taşındığı için sonraki aşamalarda hücre içi ilaç taşınımı ve görüntüleme işlemlerinde kullanılmasına olanak sağlamıştır.

TABLE OF CONTENTS

LIST OF FIGURES

Figure **Page**

Figure **Page**

Figure **Page**

Figure **Page**

Figure **Page**

LIST OF TABLES

CHAPTER 1

INTRODUCTION

1.1. The Aim of This Study

The aim of this study synthesizes the high quantum yield of carbon dots which is blue, green, red light emission under UV irradiation. Therefore, developing and controllable synthesis to obtain high efficient carbon dots with high fluorescence quantum yield are not relatively easy to synthesize. Here, All types of CDs are used which names are blue, green, red emissive for cell imaging.

1.2. Carbon Dots

CDs, also known as carbon quantum dots, or carbon nanoparticles (NPCs), which are a sort of newly discovered fluorescent nanomaterials, have become increasingly popular over the past decade thanks to their good biocompatibility, unique optical properties, easy synthesis, low toxicity, high aqueous stability. It is possible to regulate the emission of CDs by checking. For example, chemical manipulation, condensing reaction, or most often, doping of other elements. Whereas nitrogen is the major supplier of doping, it is used in combination with nitrogen in boron, sulfur, phosphorus. Xu et. al[1] was reported to have accidentally discovered in 2004 to separate fluorescent nanoparticles from products while preparing single-walled carbon nanotubes by an arc discharge. During this time, due to the simplicity of synthesis and its unique properties, interest in the synthesis of carbon points has increased. Many different synthesis methods have been applied and these are divided into two parts of top-down and bottom-up techniques.

The carbon dots are almost spherical nanocrystals and are formed by combining atoms in the form of some molecules or nanoclusters with diameters below 10 nm. When carbon dots are compared with quantum dots, where quantum points are larger particles, the carbon size is generally several nanometers. Carbon points generally have -OH -

COOH -NH and other clusters on their surfaces. (Figure 1.1) Provide the carbon points with high water solubility and polymerization of various inorganic or biologically active materials.

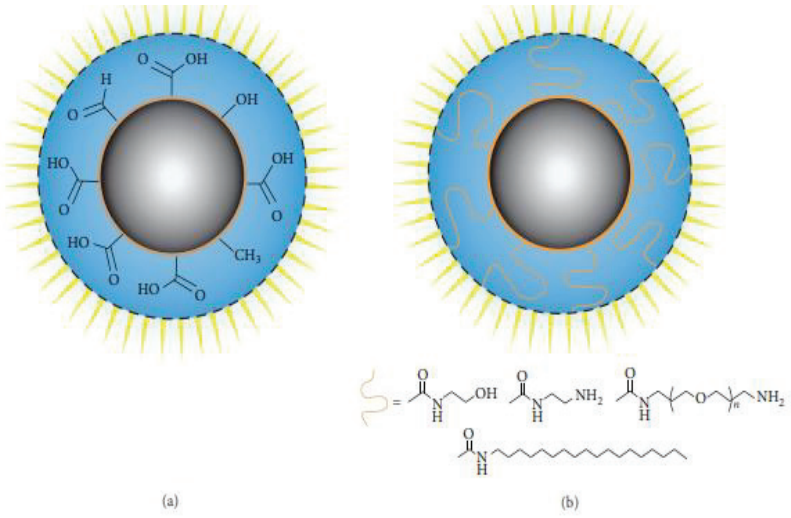

Figure 1.1. Depiction of C-Dots a) after surface oxidation treatment and b) after functionalization with surface passivation reagents. (Preparation and Application of Fluorescent Carbon Dots)

Carbon dots have strong absorption in the ultraviolet region and this region can extend into the visible region, whereas after the modification of the passivity, the absorption region can switch to red. Carbon dots have some properties, they have high fluorescence stability due to their optical properties, they contain adjustable excitation and emission wavelengths that do not bind, making a significant contribution to all areas of fluorescence nanomaterials.

The reactions were modified and reaction conditions were changed to prepare the carbon dots. In addition, carbon dots radiating at different wavelengths were synthesized. The best example of this is the first single-pot full-color light emitters reported by Ding et al. Here it is thought that the luminescence on the surfaces of carbon dots is due to conjugate bonding of atoms and variations created by these bound oxygen atoms.

In addition, if oxygen is added to the structure between the highest occupied molecular orbital (HOMO) and the lowest empty molecular orbital (LUMO), the bandgap narrows,

eventually the PL starts to shift to the red region as shown in Figure 1.2. (Full-Color Light-Emitting Carbon Dots with a Surface-State-Controlled Luminescence Mechanism)

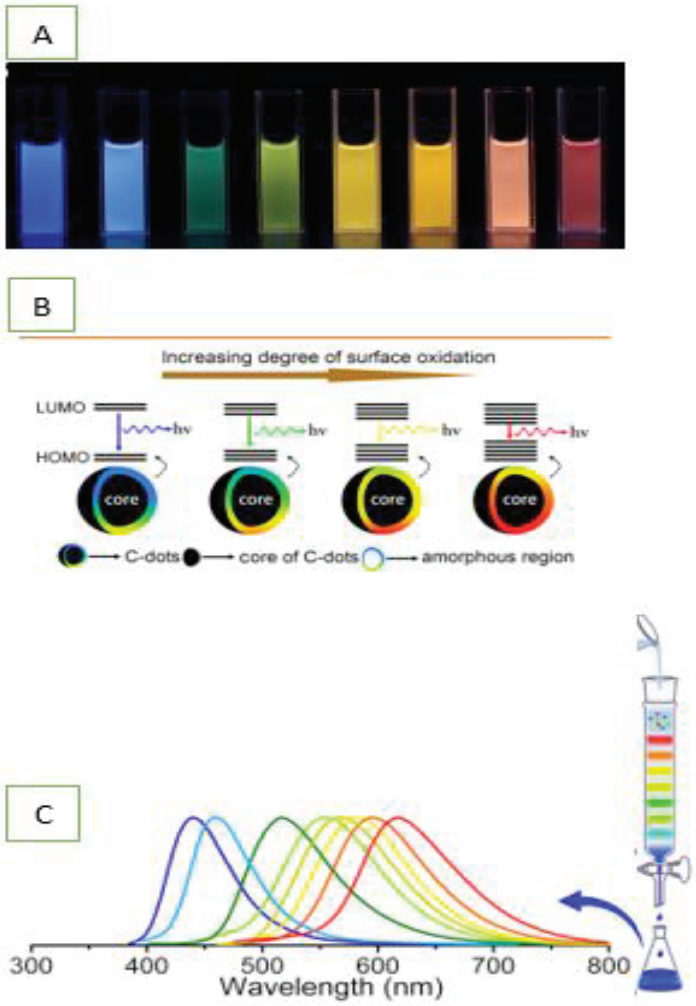

Figure 1.2. a)Eight CD samples under 365 nm UV light. b)Model for the tunable PL of CDs with different degrees of oxidation c) Corresponding PL emission spectra of the eight samples, with maxima at 440, 458, 517, 553, 566, 580, 594, and 625 nm.[2]

1.3. Types of Carbon Dots (CDs)

Carbon points have certain chemical properties which are easy, cost-effective, size control can be made, and thanks to these features, it is possible to produce large-scale carbon dots with different compositions. Depending on the direction of size development, the generation of carbon points can be classified into two approaches which names are top-down'' and ''bottom-up methods.

According to the top-down approach, carbon dots are generally formed through chemical or physical cutting procedures. These procedures of relatively, microscopic carbon structures, comprise arc discharge, laser ablation/passivation, electrochemical synthesis, and chemical oxidation most common representative sources for these techniques are carbon nanotube and graphite. Also, bottom-up methods produce carbon dots from molecular precursors such as citric acid, sucrose, and glucose via microwave patterned pathways and plasma treatment.

Carbon dot types and their classifications, merits, and demerits features are shown in Table 1.1

(Recent progress on carbon quantum dots: synthesis, properties, and applications in photocatalysis)

Table 1. 1. Carbon dot types and their classifications, merits, and demerits[3]

	Methods	Merits	Demerits
Top-Down	Laser ablation	Controllable morphology and size	The complicated operation, high cost
	Electrochemical oxidation	High purity, high yield, controllable size, good reproducibility	Complicated operation
	Chemical oxidation	Easy operation, large scale production, no elaborate equipment	Non-uniform size distribution
	Ultrasonic treatment	Easy operation	Instrumental wastage, high energy cost

" cont. on the next page"

“cont. Table 1.1”

Bottom-up	Microwave synthesis	Short reaction time, uniform size distribution, easy size control	High energy cost
	Thermal decomposition	Easy operation, solvent-free, low cost, large scale production	Non-uniform size distribution
	Hydrothermal treatment	High quantum efficiency, low cost, nontoxic	Low yield

1.4. Synthesis Methods of Carbon Dots

1.4.1. Top-down Methods

1.4.1.1. Laser Ablation

To remove layers from solid metals and industrial compounds using the laser beam, it breaks the chemical bonds and absorbs the laser directed to it. This process is called laser ablation. At 900 ºC and 75 kPa, Sun and colleagues created CQDs by laser-ablation of carbon material in the presence of water vapor with argon as a carrier gas. [4] [5] [6] [7] [8] The acid-treated CQDs generated bright luminescence emission after using in HNO_3 for 12 hours and surface modification the surface with simple organic substances such PEG1500N (amine-terminated polyethylene glycol) and poly(propionylethyleneimine-coethyleneimine) (PPEI-EI) 1,3.

Also, The synthesis of fluorescent CQDs by laser irradiation of a suspension of carbon compounds in an organic solvent was reported by Du et al (Figure 1.3). 1 The surface states of CQDs could be changed to generate adjustable light emissions by using organic solvents.

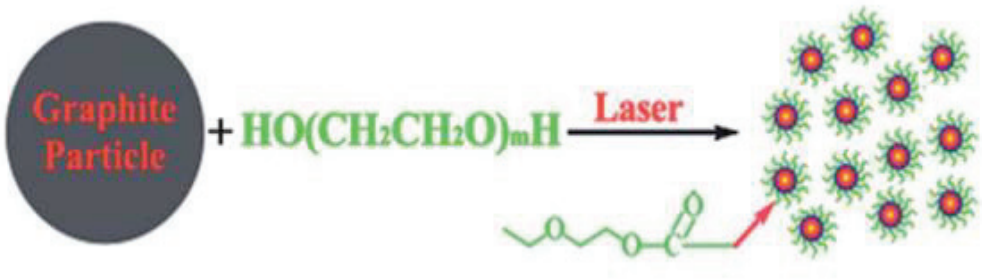

Figure 1.3. Synthesis of CQDs in PEG200N solvent by using laser irradiation. [9]

1.4.1.2. Electrochemical Oxidation

Electrochemical soaking[10] is a successful approach for synthesizing CQDs from a variety of bulk carbon sources. These CQDs methodologies, on the other hand, are on the decline. Zhang et al.[11] developed the electrochemical carbonization of low-molecular-weight alcohols to produce CQDs.

The most common method for producing CQDs is electrochemical oxidation, which has the advantages of high purity, low cost, high yield, easy size modification, and good reproducibility. [12] [13][14][15][16][17] The electrochemical production of CQDs from multiwalled carbon nanotubes was initially demonstrated by Zhou et al (MWCNTs).

1.4.1.3. Chemical Oxidation

Chemical oxidation is a useful technique for large-scale production that requires no specialized technology. [18] [19] [20] [21] Qiao et al. provided a convenient method for producing CQDs with excitation-wavelength-dependent PL that can be scaled up.[21] The preparation of CQDs is shown in Figure 1.4 a). The absence of detectable lattice structures in the TEM images indicates that the as-prepared CQDs are amorphous as shown in Figure 1.4 b)-d).

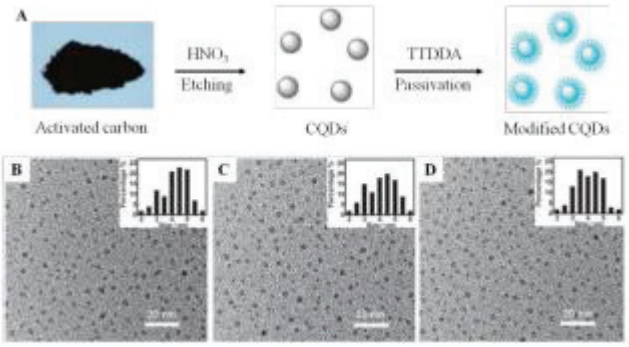

Figure 1.4. a) Preparation procedure of CQDs. TEM images for b) coal activated carbon (CAC) c)coconut activated carbon (CNAC) d)The inset histograms are the size distributions of the CQDs measured by TEM. [21]

1.4.1.4. Ultrasonic Synthesis

Ultrasound has been shown to generate alternate low-pressure and high-pressure waves in liquid, causing miniature vacuum bubbles to develop and disintegrate. High-speed impinging liquid jets, deagglomeration, and intense hydrodynamic shear forces are all caused by these cavitations. [21] [22] [23] As a result, the energy of an ultrasonic pulse can be used to break macroscopic carbon materials into nanoscale carbon quantum dots (CQDs).

1.4.2. Bottom-up Methods

1.4.2.1. Microwave Synthesis

Microwave irradiation is a technique of using organic compounds like sucrose diethylene glycol (DEG), citric acid, and ethylenediamine (EDA) is a quick and inexpensive way to synthesize highly luminescent carbon quantum dots. Microwave irradiation was utilized to synthesis carbon dots with oxygen-containing groups, such as EDA, from various carbon sources. All of the reactions were combined to form a

transparent solution that was heated in a microwave oven. After that, after dissolving, sonication, and dialysis process, pure amino coated carbon dots were collected was shown in Figure 1.5 [24].

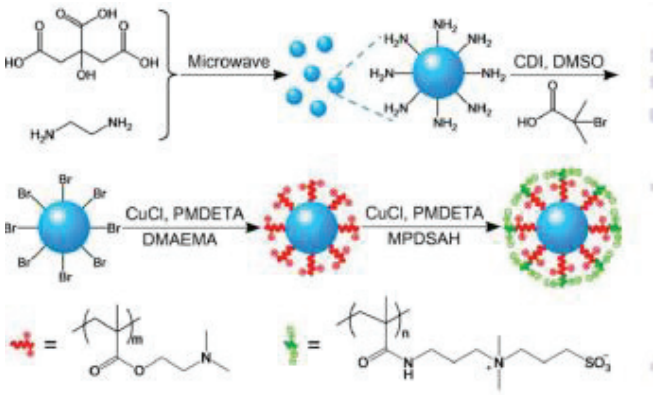

Figure 1.5. Synthetic route of amine coated C-dots, Br coated C-dots, and Polymers functionalized C-dot [24]

Liu et al., demonstrated that synthesized highly luminescent carbon quantum dots produced with citric acid and 1,2- ethylenediamine increased as the N level of content in the reaction.[2526] The amine molecules, particularly the major amine molecules, were used as a starting material for N-doping as well as a surface passivating agent for the CQDs, which improved PL quality. All reaction mechanisms as illustrated in Figure 1.6.

Figure 1.6. Synthesis of CDs in the presence of various ethylenediamine [2526]

According to Zue et al,[27] was reported for the first time that it formed a transparent solution, different amounts of poly(ethylene glycol)(PEG200) and saccharide were added to distilled water. When the reaction time was increased, the solution color changes from colorless to yellow. After a while, a dark-brown solution was obtained which indicated the production of CNPs as shown in Figure 1.7.

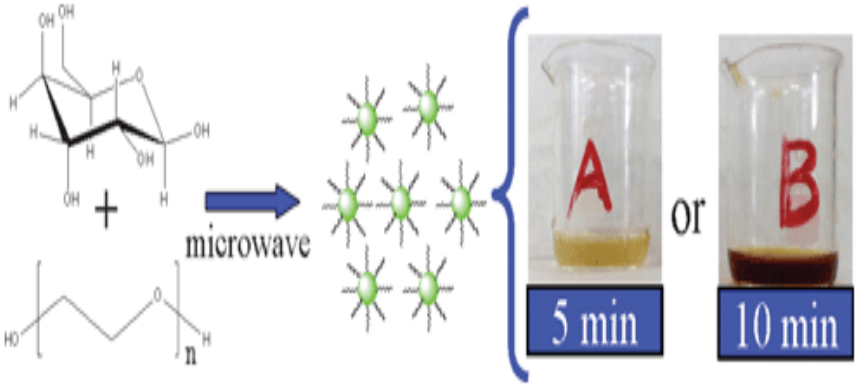

Figure 1.7. Microwave pyrolysis approach to CNPs[27]

1.4.2.2. Thermal Decomposition

In the past, different semiconductor and magnetic nanomaterials have been synthesized by using the thermal decomposition method. External heat was contributed to the dehydration and carbonization process of organics materials and these have been proven to transform into carbon quantum dots.

Ma et al. [28] succeeded in synthesizing nitrogen-doped graphene quantum dot-like graphene structure on the carbonization process formed by heating ethylene diamine tetraacetic acid (EDTA) in a sand bath at 260-280 ºC. The reaction process for GQDs was illustrated in Figure 1.8.

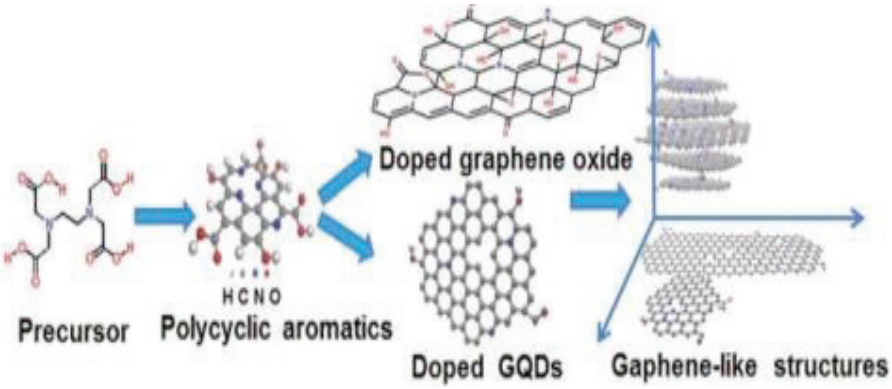

Figure 1.8. Schematic illustration of the reaction process for the preparation of GQDs derived from EDTA (E-GQDs) and their graphene-like structures [28]

1.4.2.3. Hydrothermal Treatment

Hydrothermal carbonization process is a technique of low cost, environmentally friendly, and non-toxic materials that can be used to produce carbon-based products from glucose[29], citric acid[30], chitosan[31], protein[32], organic acids, and some vegetable products. Using a hydrothermal reactor, the carbon dot technique was reacted at high temperatures and pressures.

According to Zhu et al.,[30] a hydrothermal approach using citric acid and ethylenediamine molecule can be used to synthesis polymers such as C-dots with a high quantum yield of 54%. These CDs can be utilized to create printing inks that protect multicolor designs against counterfeiting, as well as a biosensor reagent capable of detecting Fe^{+3} production. All chemical reactions were shown in Figure 1.9.

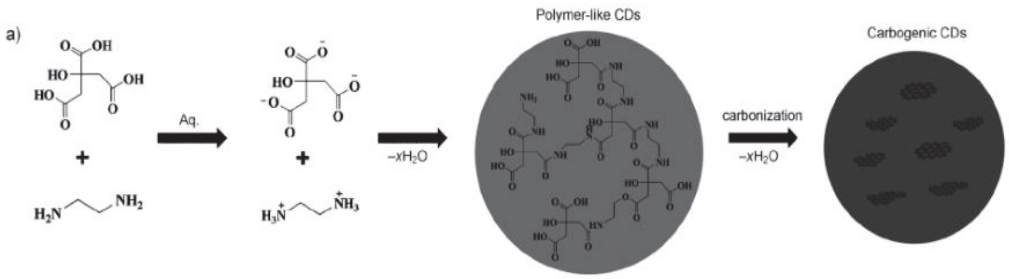

Figure 1.9. A synthetic route using citric acid and ethylenediamine: from ionization to condensation, polymerization, and carbonization[30]

Zeng et al. [33] reported that urea and citric acid was used to synthesize amine-coated C-dots by using hydrothermal synthesis at different temperature. The structure of their surface coating with amino groups and the composite were both affected by the reaction temperature. It provided surface amino groups while simultaneously deactivating the product's surface traps, allowing urea to be used as a very good carbon source. The reaction was synthesized by changing the temperature of carbon dot synthesis, which resulted in varied luminescence ranges in blue and green as shown in Figure 1.10.

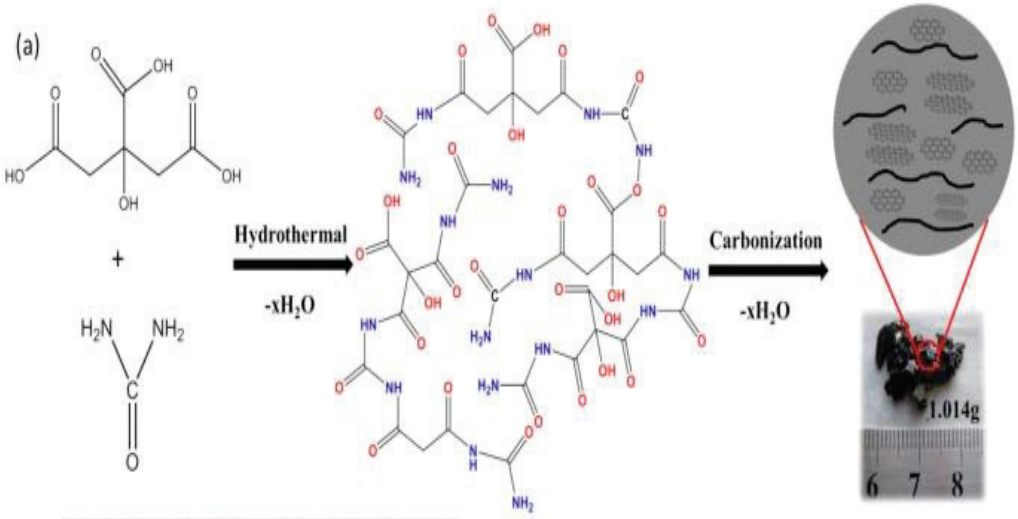

Figure 1.10. The schematic approach preparing for carbon dots [33]

Bhunia et al.[34] It has been reported that the synthesized hydrophobic and hydrophilic fluorescent nanoparticles (FCN) were synthesized with a quantum yield ranging from 6% to 30%. This 1 - 10 nm FCNs were used for biological staining and diagnostics due to their imaging probe and non-toxic properties. FCN-based nanoprobes are stable and have emissions in the visible region. In this way, it exhibits properties similar to those of semiconductor nanoparticle-based nanoprobes. However, another advantage is the small hydrodynamic size and low toxicity. Smaller in size allows easier subcellular access, while low toxicity allows applications for nanoprobes. Producing a fluorescent nanoparticle process was shown in Figure 1.11.

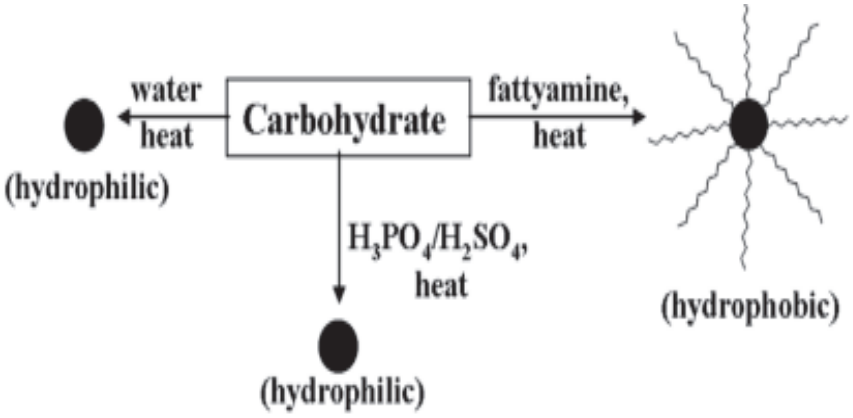

Figure 1.11. Synthesis of fluorescent carbon nanoparticle

1.5. Structural and Optical Characterization of Carbon Dots

1.5.1. Spectrophotometric Analysis

Carbon dots have some characteristic shapes consisting of amorphs and crystalline parts with surface functional groups. Even though the crystalline sp^2 carbon section has been demonstrated by several studies. [35] [14]. The following are some structural models of the CQDs core that have been proposed: amorphous carbon structure, graphite/graphite oxide structure,diamond-like structure.

The UV-visible spectrometer was used to discover the types of structures found in carbon dots, as well as their unsaturated structure and appearance. Two types of absorption peaks are observed in the UV-vis spectrum, resulting from the π-π* transition of the C=C bond and the n-π* transition of heteroatoms to the carbon atom via multiple bonds. The surface groups and a changeable value for synthetic parameters were associated with the absorption position peak. [36]

The ratio of the number of emitted photons to the number of absorbed photons is known as photoluminescence quantum efficiency (PL QE). It is feasible to compute PL QE in two distinct methods experimentally. Comparing the fluorescence and absorption spectra of an unknown material with a dye with a known quantum yield is one of them. When making this calculation, it is important to measure the dye with the appropriate

photoluminescence and absorbance range. Absorption and PL spectra of the appropriate dye should overlap with the unknown sample. The following formula is used to determine the PL QE:

$$QY = Q_{ref} \frac{I}{I_{ref}} \frac{OD_{ref}}{OD} \frac{\eta^2}{\eta_{ref}^2}$$

This phoneme that quantum yields are referred QY, Intensity or area of the emission peak in the emission spectrum is referred I, excitation wavelength for absorbance spectrum is referred OD, and refractive index of the solvent as shown as η. Also, ref means is referred to as reference dye.

As indicated in the equation below, quantum yield can alternatively be defined as the ratio of radiative and non-radiative processes. The rate constants of the sample's radiative and non-radiative processes are k_r and k_{nr}, respectively.

$$QY = \frac{k_r}{k_r + \sum k_{nr}}$$

Fluorescence spectroscopy relies heavily on time-resolved observations. Time-resolved observations give more information than steady-state measurements in many circumstances, such as the overlap of emission and absorption spectra. Exciting the synthesized quantum dot sample with a light pulse at a certain wavelength and then measuring the photon count over time is called time-correlated single-photon counting measurement (TCSPC). This photodynamic information was obtained from fluorescent decay traces of the synthesized quantum dots. FS5, Edinburgh Instrument was used to analyze this information.

1.5.1.1. Absorbance

In general, CDs have high optical absorption in the UV–visible range. The peaks are commonly attributed to n-π* transitions in the C═O, C—N, or C–S groups, as well as π-π* transitions in the conjugated C═C system. Various surface passivation/functionalization approaches could be used to alter the absorption band.[37]

Lin et al, were synthesized multiple-emissive CDs with two distinct absorption peaks, at 247 and 355 nm using phenylenediamine[38] (PD) and poly(vinyl alcohol) (PVA). These peaks correspond to π-π*transition of C═C bonds and n-π* transition of C—N/C═N bonds, respectively.

1.5.1.2. Fluorescence UV-visible and NIR region

Experimental procedures of synthesis CDs are developing in recent years and carbon dots were obtained from different processes. Also, another method for the understanding of carbon dots formation is the photoluminescence (PL) mechanism of the materials.

Ding et al[38] reported that the solvents formamide, dimethylformamide, ethanol, and aqueous H_2SO_4 solution were utilized to manufacture CDs from L-glutamic acid and o-phenylenediamine, and all combinations of reactions produced PL emission from blue to NIR. When the solvent of the material is changed during the synthesis, the photoluminescence spectrum was shifted from blue to red. Also, when the emission range is 600 nm to 700 nm, the material emits in the red region. B-CDs, G-CDs, Y-CDs, and R-CDs are four common CD samples with blue, green, yellow, and red fluorescence emission maxima are at 443 nm, 544 nm, 571 nm, 594 nm, 640 nm, 715 nm, and 745 nm. Their photoluminescence spectra was shown in Figure 1.12. [38]

Also, surface energy level and energy gap can be affected by surface functional groups of the CDs. Sun et al. was reported that increasing the quantum yield of CDs, PEG-1500N was used to enhance and passivate the fluorescence of CDs. As a result, nitrogen-containing particles were used to demonstrate the importance of surface passivation of CDs.[39]

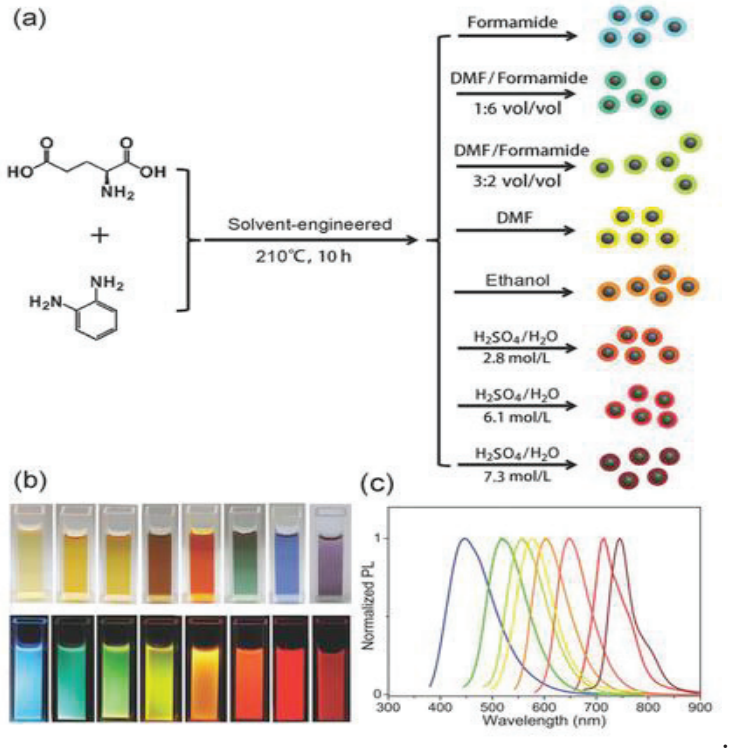

Figure 1.12. a) Multicolor fluorescent CDs synthesized by using L-glutamic acid and *o*-phenylenediamine b)CDs imaged under in daylight (upper) and UV light (bottom), respectively. c) Normalized PL emission spectra showed under excitation of 365 nm.[2]

1.5.2. FTIR Analysis

FTIR spectroscopy was used to determine if a surface functional group on the CDs. For instance, a distinguishing link between the surface of the Carbon points and amine-terminated molecules in amine-bonded carbon dots, materials having carboxyl and amine groups, was amide (-CONH-). A high absorption at 1680-1630 cm^{-1} in the FT-IR spectra of amide (-CONH-) is attributed to the stretching vibration of C=O. N-H bending vibrations will be 1570-1510 cm^{-1}, whereas C-N stretching vibrations will be 1335-1200 cm^{-1}. All organic functional groups in FT-IR spectra was shown in Table 1.2.[40]

Table 1.2. FTIR Absorption Bands of Typical Organic Functional Group

Bond type	Stretching Frequencies (cm^{-1})	Intensity
C≡N	2260–2220	medium
C≡C	2260–2100	medium to weak
C═N	1650–1550	medium
C═C	1800–1600	medium
C═C (aromatic)	1600, 1500–1430	strong
C═O	1780–1650	strong
C—O	1250–1050	strong
C—N	1230–1020	medium
O—H (alcoholic)	3650–3200	strong and broad
O—H (carboxylic)	3300–2500	strong and broad
N—H	3500–3300	medium, broad

According to Sun et al citric acid (CA) and polyene polyamine (PEPA) was used to synthesize new theranostic nanomedicine (CD-Oxa) CDs. Broad absorption bands at 3000- 3500 cm^{-1} were attributed to O-H and N-H stretching vibrations, whereas bands at 1557 and 1352 cm^{-1} were attributed to N-H and C-N bending vibrations, respectively. It has been proven that amino fragments are formed in the carbon dots synthesized.[41]

Zhang et al employed to synthesize amine-coated C-dots by using 4,7,10-Trioxa-1,13-tridecanediamine (TTDDA) and citric acid. According to the article; The bands at 3430 cm^{-1} and 1100 cm^{-1} represent N–H and C–N vibrations, proving the presence of NH_2.[42] According to Zang et al, was synthesized amine-capped C-dot by using citric acid and urea in an autoclave at different temperature ranges. In addition, the FT-IR spectra give the stretching vibrations of the -OH and -NH_2 groups assigned to the absorption

bands at 3000-3500 cm^{-1}. The absorption intensity of the N-H peak was observed at 1549 cm^{-1}. Also, the absorption band for C=O at 1648 cm^{-1} at low temperature, the intense peak is less at low temperature in contrast to a higher temperature.[33]

1.5.3. X-ray Photoelectron Spectroscopy (XPS)

XPS can be used to characterize the composition and chemical bonds of the C-dots and the structural basic properties of the prepared C-dots. According to Shi et al. reported that using citric acid and 2,2'-(Ethylenedioxy) bis(ethylamine) to synthesize C-dots by microwave method. In the high-resolution C 1s and N 1s spectra, there were two peaks centered at 286.1 and 400.05 eV, indicating the presence of C-N bonds in the amine capped C-dots. [43]

In addition to this Li et al, reported that synthesizing Luminescent carbon dots by using citric acid and urea, hydrothermal method. XPS spectroscopy of L-CDs characterized by Li et al. proved different types of chemical components are graphitic or aliphatic (283.87 eV), oxygenated (286.13 eV) and nitrous (287.75 eV). Also, the same L-CDS result of aromatic N and surface H_2N- groups were centered at 399.25 eV and 400.49 eV.

1.6. Synthesis of different color emitting Carbon Dots

They have some structural properties that alter the fluorescence effect when producing carbon dot synthesis. They may contribute indirectly to higher QY of C-dots from bandgap transitions of conjugated π domains, related to energy levels of functional groups, electron donor abilities, or bonding of nitrogen, sulfur, and different atomic groups. All literature summaries have been given in Table1.3.

The functional groups want to donate electrons, the more energy they produce, and when the functional groups on the surface of these carbon dots are changed, the emission wavelengths can also be changed.

The color shift of carbon dots from blue to red varies depending on the mole ratios of the reacting materials and the reaction temperature. Miao et al, [44] using different molar

ratios of citric acid, and urea were able to synthesize carbon dot that emit in the blue, green, and red region at different temperatures between 430 nm and 630 nm. All reactions were shown in Figure 1.13[45]

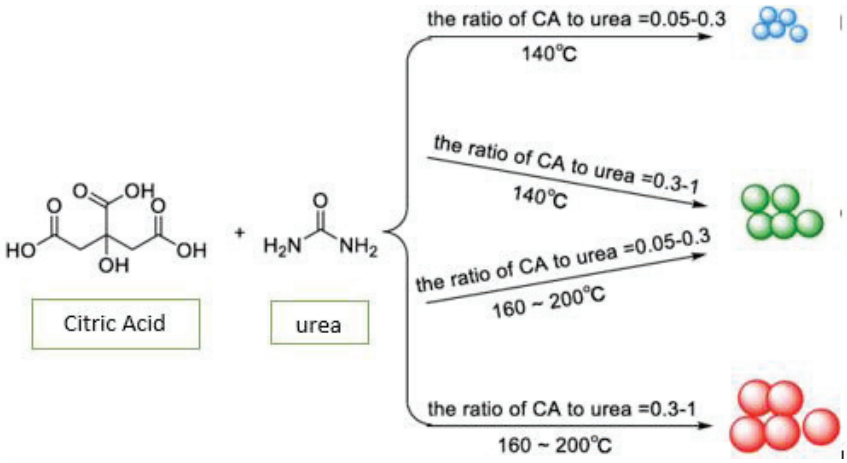

Figure 1.13. C-Dots synthesized by using CA and urea at different reaction conditions[45]

Ding et al.[2] reported that a gradual color change from blue to red to different fluorescence properties using p-phenylenediamine and urea was obtained using silica column chromatography. It is thought to emit radiation due to the oxygen atoms and conjugated carbon atoms attached to the carbon dot surfaces. The bandgap between HOMO and LUMO decreases, resulting in a redshift of the PL emission as it also increases surface oxidation due to the increased oxygen atom.

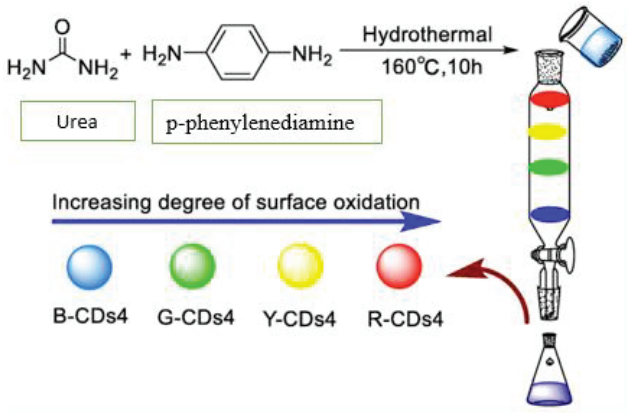

Figure 1.14. Different emission of C-Dots prepared from urea and p-phenylenediamine by using column chromatography[45]

Carbon dots are usually emitted in the blue region and most of these carbon dots containing carbon, oxygen element have low quantum efficiency. To increase this quantum efficiency, the light efficiency can be increased by improving the carbon dots by contributing to the surface modification. By binding other elements to the carbon dot surface, it can correct structural defects, increase surface functional groups and interactions between carbon atoms and neighboring atoms. Thanks to the doped elements, the energy band gaps can be changed as the energy levels change. In addition, these doping elements can be modulated into the core structure of carbon dots and contribute to the change of the fluorescence mechanism.

Quantum yield defines the ratio of emitted photons to absorbed photons. This quantum yield can well control the bandgap and electron local density of C-dots due to nitrogen sulfur and other heteroatoms, metal ions and precursor, surface passivation, and elemental doping. As a result, the quantum yield increases, giving us the effect of a longer Pl degradation life in, which passivation defects on the surface are removed.

Nitrogen atom can easily be incorporated into the carbon material skeleton, its radius is similar to that of a carbon atom. Thanks to the nitrogen atom, it increases the quantum efficiency by red-shifting the emission wavelength of the material and producing a new surface state energy level. Pan et al.[46] succeeded in synthesizing F-CDs by using citric acid and formamide by microwave method at 160 degrees, which emits from blue to red due to the presence of functional groups related to C=N/C=O and C-N. All reaction mechanisms was shown in Figure 1.15.

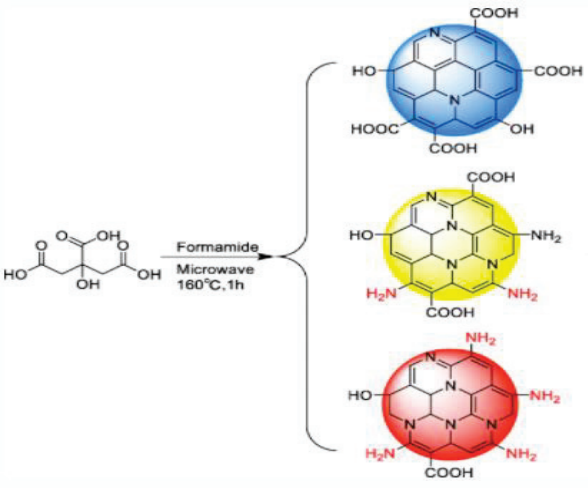

Figure 1.15. A schematic illustration of the preparation of the full-color emission CDs[45]

Jian et al. succeeded in synthesizing photoluminescent (PL) carbon dots that emit red, green, and blue fluorescence in different regions using three different isomers of phenylenediamine and ethanol in a 180 °C hydrothermal pathway. (Figure 1.16)

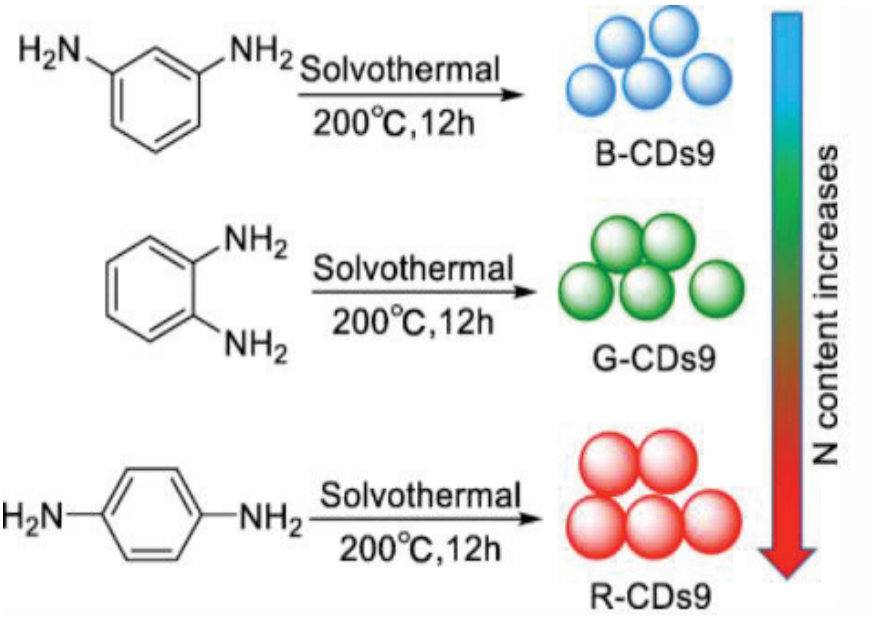

Figure 1.16. Preparation of the RGB PL CDs from three different phenylenediamine isomers[45]

Another element that affects carbon dots is the addition of sulfur elements. Although sulfur alone does not have a significant effect on the fluorescence emission wavelength, N and S doped elements significantly affect carbon dot synthesis. Since the last valence atom of nitrogen and sulfur is six, it makes it easier to bond with carbon and can increase the possibility of electronic transition from the ground state. Thus, it causes a change in the bandgap energy and increases the quantum efficiency. Bao et al.[47] using L-cysteine and citric acid, synthesized N, S-CD at 70 °C by hydrothermal route as a result of recombination of electrons and holes caused by surface doped nitrogen and/or sulfur atoms as shown in Figure 1.17.

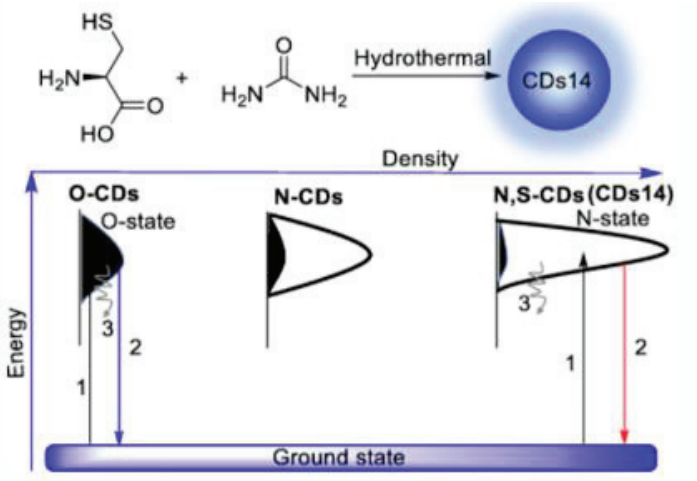

Figure 1.17. Preparation of N,S-CDs from using L-cysteine and Citric acid[45]

All reaction techniques and ingredients was summarized in Table 1.3.

1.6.1. Blue light-emitting Carbon Dots

Blue emitting carbon dots are the most widely used and have the most diversity due to the highest quantum efficiency. They have a strong fluorescence emission for synthesizing process. Liu et al.,[48] reported that using the hydrothermal method with different concentrations using citric acid and ethylenediamine, they succeeded in synthesizing blue emissions carbon dots with a maximum emission peak from 480 and 440 nm at 150 °C and 5 hours. All reactions were illustrated in Figure 1.18.

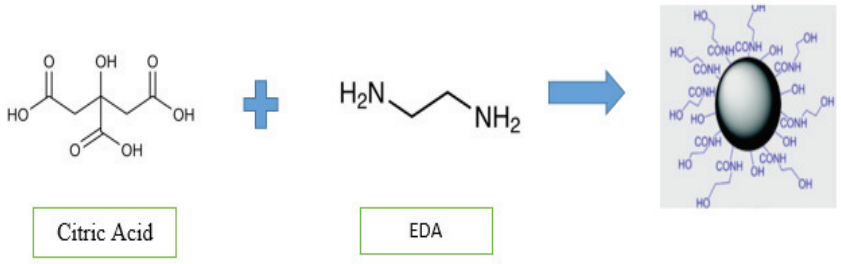

Figure 1.18. A schematic illustration of the preparation of the CDs[48]

Another method is to synthesize nitrogen-doped CDs, Liu et al.[49] synthesized N-CDs with 75% efficiency by hydrothermal carbonization with citric acid and tris(hydroxymethyl)methyl aminomethane. These carbon dots have imparted an invisible property in the ink. In addition, these carbon dots, the maximum emission peak at 408 nm when excited at 330 nm and had a blue emission under the UV lamp was shown in Figure 1.19.

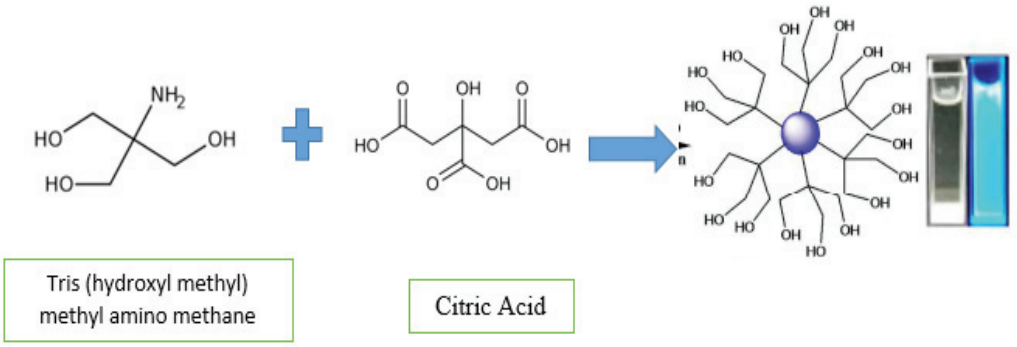

Figure 1.19. A schematic illustration of the preparation of the N-CDs[48]

According to Yang et al.[50] reported that for the synthesis of nitrogen-doped carbon dots with high fluorescence lifetime, they succeeded in synthesizing them for 6 hours at 160 °C using ammonium citrate and deionized water. These carbon dots give absorbance peaks at 235 and 327 nm, and these peaks p–p* transition C=C bond and n–p* transition band C=O bond peaks.

Lu et al. [50] succeeded in synthesizing water-soluble carbon dots simply and easily using oxalic acid as a carbon source and urea as another material, using a one-step microwave method with a quantum efficiency of 28.7%. All reaction mechanisms as illustrated in Figure 1.20.

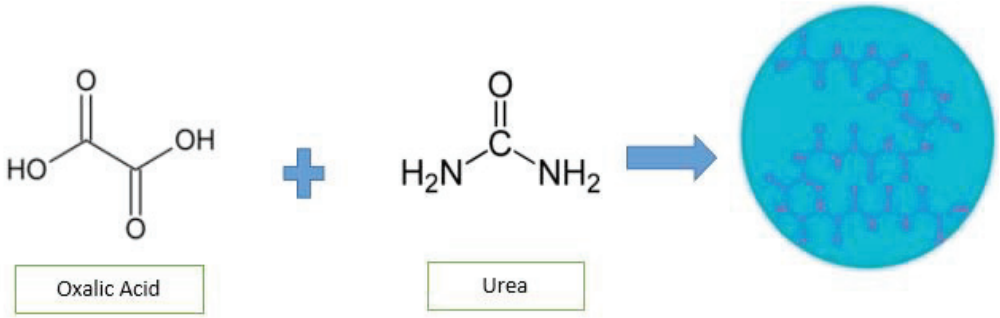

Figure 1.20. A schematic illustration of the preparation of the Blue luminescent carbon dots[50]

Qgi et al.[51] succeeded in synthesizing stable nanocrystalline CDs with 35.5% high QY at varying temperature parameters using a custom-made autoclave apparatus thanks to citric acid and urea hydrothermal reaction to synthesize blue luminescent nitrogen-doped carbon dot. In the synthesis of colloidal solution, N-CD has an emission peak at 461 nm, whereas N-CD-PVA (polyvinyl alcohol) nanofibers composite nanofiber mat has an emission peak at 449 nm with a higher intensity than N-CDs. All reaction mechanisms was shown in Figure 1.21.

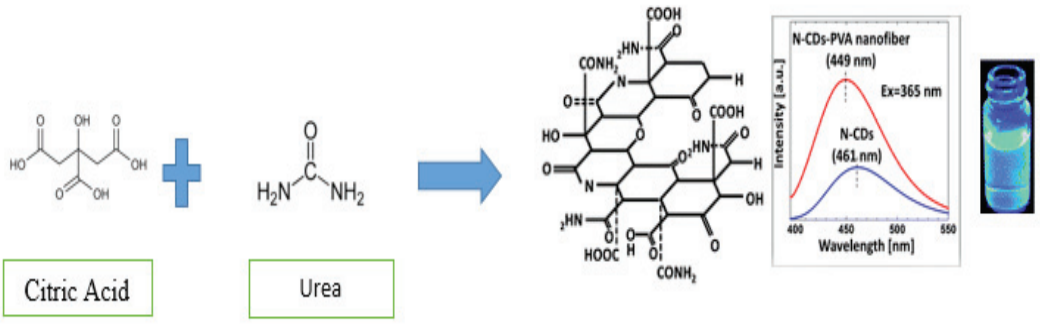

Figure 1.21. Proposed mechanism of the formation of N-CDs *via* hydrothermal reaction of citric acid and urea [51]

Xu et al.[52] succeeded in synthesizing S-doped C-dots at varying temperatures using an autoclave with 67% quantum efficiency using sodium citrate and sodium thiosulfate. While spherical S doped C dots give an emission peak at 440 nm, it was able to be synthesized for the first time by the hydrothermal way, using it in biological applications thanks to its high fluorescence feature at 4.6 nm as illustrated in Figure 1.22.

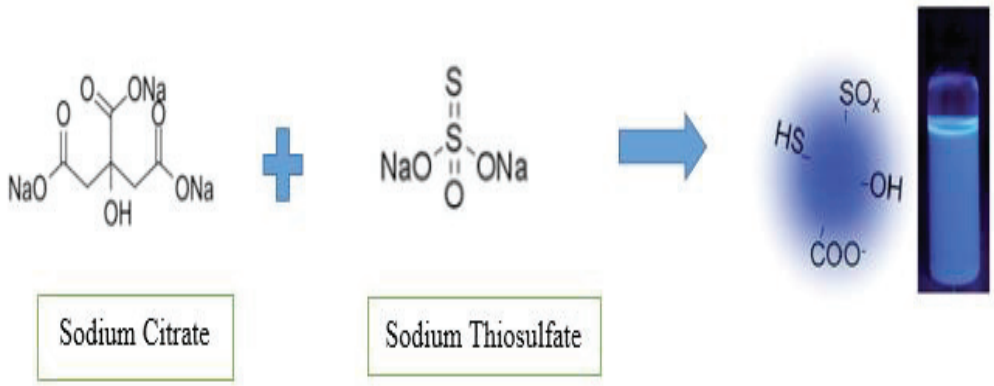

Figure 1.22. Proposed mechanism of the formation of S-CDs *via* hydrothermal reaction of sodium citrate and sodium thiosulfate[52]

1.6.2. Green light-emitting Carbon Dots

The synthesis of green carbon dots by modulating different surface functional groups, which are stable, water-soluble, green fluorescent carbon dots that emit at 450 and 550 nm, have become more common in recent years.

Li et al.[53] using 2,3-diaminophenazine and folic acid, after 24 hours at 80 ^{o}C, carbon dots that give green photoluminescence (PL) emission for application on tumor cells with 93.40% quantum efficiency by binding to the modified N-doped carbon on the folic acid (FA) surface by a hydrothermal way succeeded in synthesizing. All reactions as illustrated in Figure 1.23.

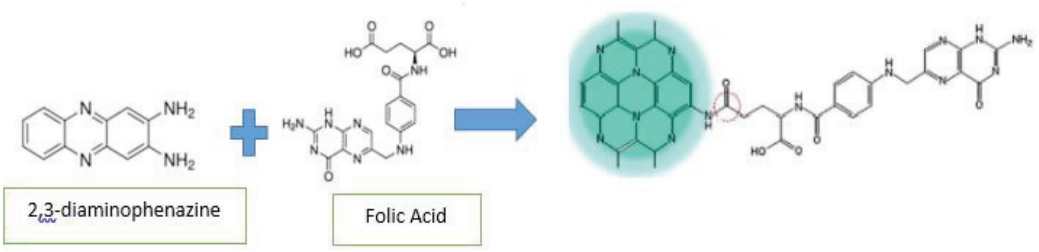

Figure 1.23. Proposed mechanism of the formation of FN-CDs *via* hydrothermal reaction of 2,3-diaminophenazine and folic acid[53]

Mohan et al.[54] using ascorbic acid and ethylene glycol, succeeded in synthesizing carbon dots that emit green fluorescence, showing double band emission at 382 nm and 538 nm by hydrothermal route for 1 hour at 160 °C in deionized water. These carbon dots were used in cell imaging applications because of their strong and changeable fluorescence properties. All reactions as illustrated in Figure 1.24.

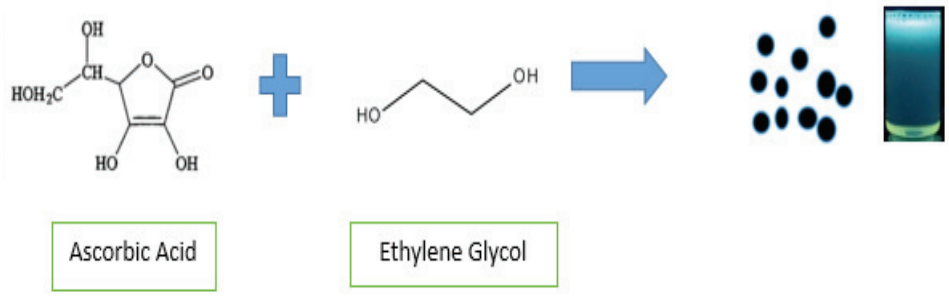

Figure 1.24. A schematic illustration of the preparation of the CDs *via* hydrothermal reaction of ascorbic acid and ethyleneglcol[54]

Xu et al.[55] were synthesized by hydrothermal route in an autoclave for 8 hours at 150°C using tartaric acid and brain as the carbon source and DMF as the nitrogen source as the organic solvent. This carbon dot was synthesized with 46% efficiency, green fluorescence

emitting at 539 nm, and probes commonly used in detection fields were also used. All reactions was shown in Figure 1.25.

Figure 1.25. A schematic illustration of the preparation of CDs *via* hydrothermal reaction of tartaric acid and brain[55]

Using RhB-doped and citric acid, Dong et al.[56] synthesized high quantum yield green-emitting carbon dots with a hydrothermal pathway at 280 °C emitting isolated sp^2 clusters at 534 nm. Also, these carbon dots were applied to potential bio-applications of the CDs for cell imaging. All reactions are shown in Figure 1.26.

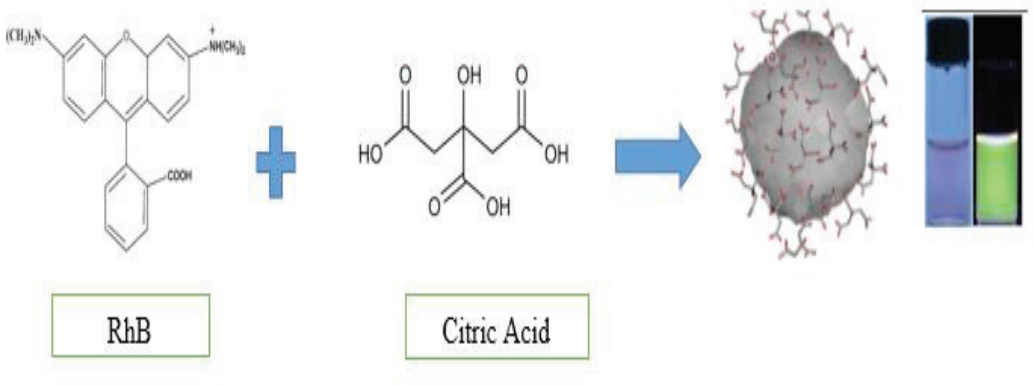

Figure 1.26. A schematic illustration of the preparation of CDs *via* hydrothermal reaction of RhB-doped and citric acid[56]

As shown in Figure 1.27, Yang et al.[57] using citric acid monohydrate, methylamine hydrochloride, and lanthanum chloride heptahydrate were able to synthesize La-doped CDs (La-CDs) with 35% quantum efficiency, emitting in the green fluorescence at 445 nm, by microwave method. And these CDs were used to detect Fe^{+3} in living cells.

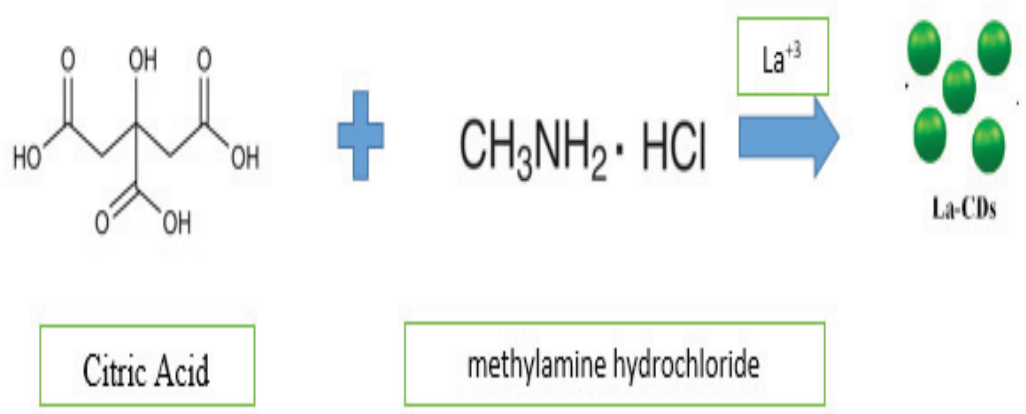

Figure 1.27. A diagram depicting the hydrothermal reaction of citric acid, methylamine hydrochloride, and lanthanum chloride heptahydrate to produce CDs. [57]

Also, Yang et al.,[58] succeeded in synthesizing green-emitting CDs by hydrothermal route using phenol and ethylenediamine at 180 °C for 10 hours for cartap detection.

Qu et al.[59] using citric acid as a carbon source and thiourea, urea as an S and N source, succeeded in synthesizing S, N co-doped carbon dots that green-emitting fluorescence at 360 and 435 nm by hydrothermal route for 4 hours at 160 °C in deionized water. Also, S,N:GQD/TiO_2 composites have a good photocatalytic effect thanks to these carbon dots, it has been used for energy conversion in the solar energy system. It was seen in Figure 1.28.

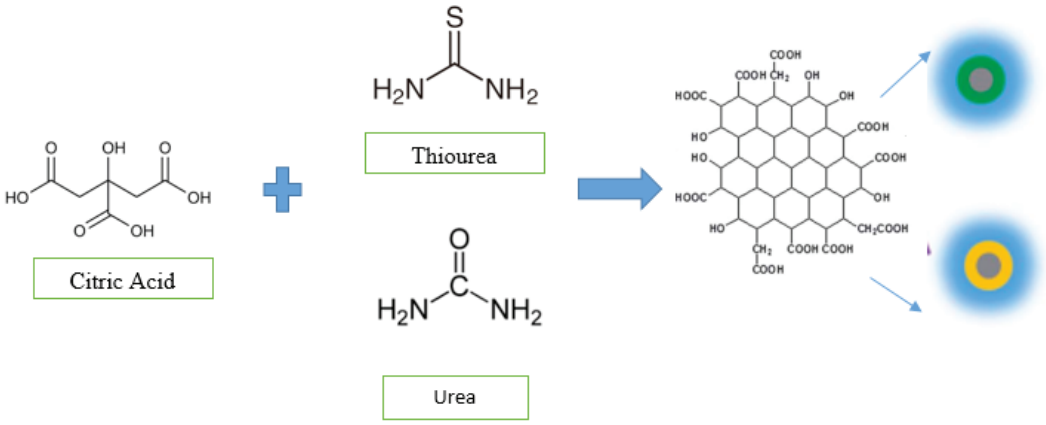

Figure 1.28. A procedure for making CDs is presented based on the hydrothermal reaction of thiourea and urea [59]

While Liu et al.[60] used sucrose as a carbon source and diethylene glycol as the reaction medium, it was synthesized in 10 minutes by microwave method with green luminescent DEG-CDs in 540 nm, with 54% quantum efficiency. (Figure 1.29) While these DEG-CDs are easily soluble in water, these dots, which emit green fluorescence under UV-lamp, are thought to originate from surface oxygen-containing groups, and thus the carbon dots applied to the C6 cells show that these carbon dots can be taken into the cell efficiently. This proves that DEG-CDs can be used as bioimaging and nanosensor.

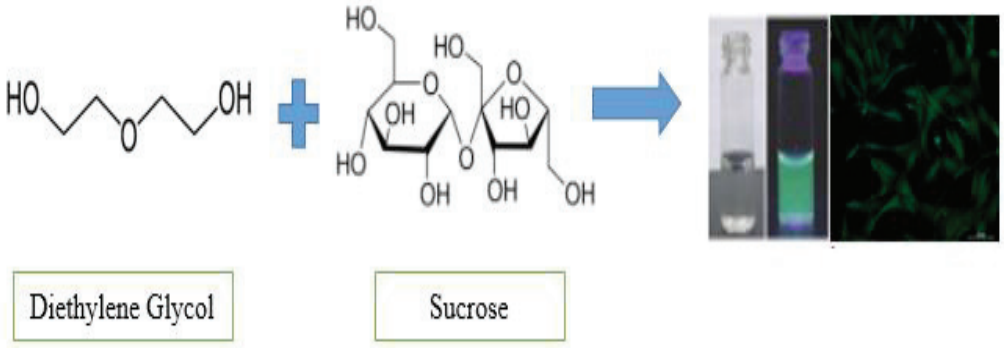

Figure 1.29. A schematic illustration of the preparation of CDs *via* microwave reaction of diethylene glycol and sucrose

Liu et al.[61] succeeded in synthesizing CD-PEIs with a high QY of 54% in a very short time using the microwave method, thanks to the reaction of polyethyleneimine, glycerol, and phosphate to synthesize the passivated photoluminescent C-dots with green route branched PEI. This CD-PEI was used to demonstrate bioimaging and bio labeling.

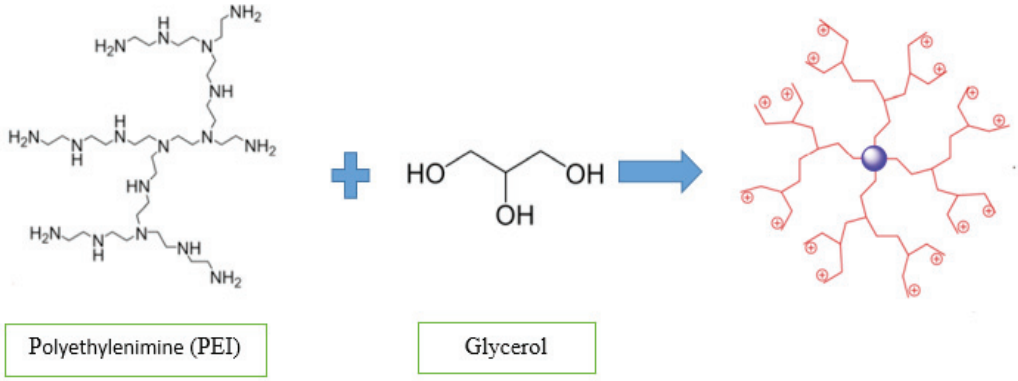

Figure 1.30. A schematic illustration of the preparation of CDs *via* microwave reaction of polyethyleneimine, glycerol, and phosphate

Zhang et al.,[62] in Figure 1.31, using p-benzoquinone and ethylenediamine, produced a dark brown product with a maximum emission peak at 530 nm by exothermally for 16 hours, while the green fluorescent route of CDs containing abundant amino groups allowed it to actively target lysosomes and was sensitive to lysosomal pH visualized in vitro.

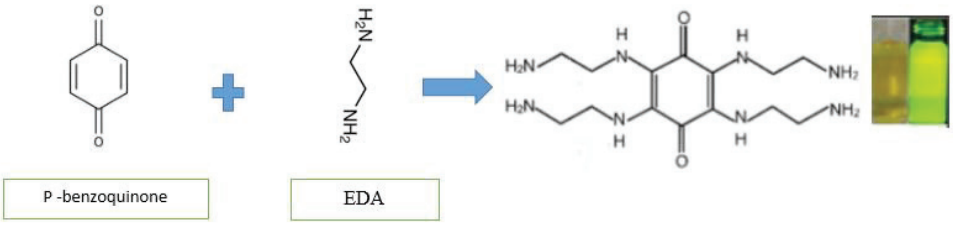

Figure 1.31. Proposed mechanism of the formation of CDs *via* hydrothermal reaction of p-benzoquinone and ethanediamine.[62]

1.6.3. Yellow and orange light-emitting Carbon Dots

The synthesis of the blue carbon dots gives strong emission in the blue emission region, but its long wavelength emissions are very low, so the synthesis of carbon dots that emit from yellow to red is very important. Yellow CDs have the large Stokes shift however, quantum yields are relatively, low. But if obtained high-quality yellow fluorescence CDs, they can be used for biological applications. Liu et al.,[63] dissolved a solution of citric acid, urea, and manganese acetate in toluene, transferred to an autoclave, and heated at 180°C for 12 hours, successfully synthesizing carbon dots with 46% quantum efficiency, emitting at 550 nm and showing yellow fluorescence as shown in Figure.1.32.

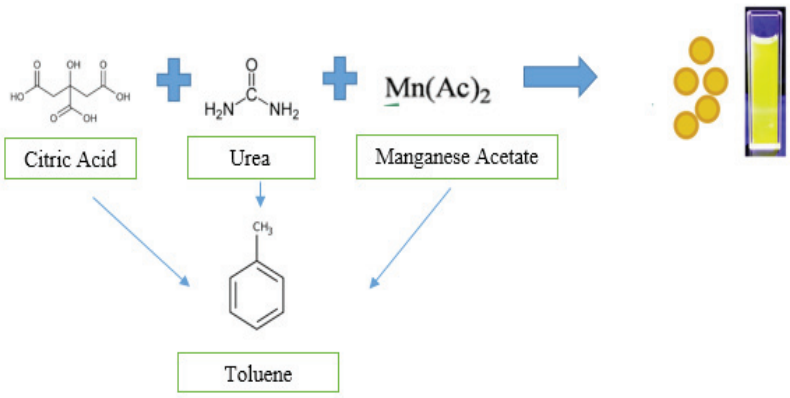

Figure 1.32. A schematic illustration of the preparation of CDs *via* hydrothermal reaction of citric acid, urea, and manganese acetate

Jiang et al.[64] succeeded in synthesizing yellow carbon dots, a rare example of N-doped CDs, using 1,2,4-triaminobenzene, and formamide by a hydrothermal pathway in Figure 1.33, which gave an emission peak of 568 nm for 12 hours at 120 °C**.** It also shows that as a result, of the gradual addition of Ag+ and Cys to the synthesized yellow carbon dots, it emits three states called ON-OFF-ON, and these are practical, applied for the detection of Cystine in human plasma samples.

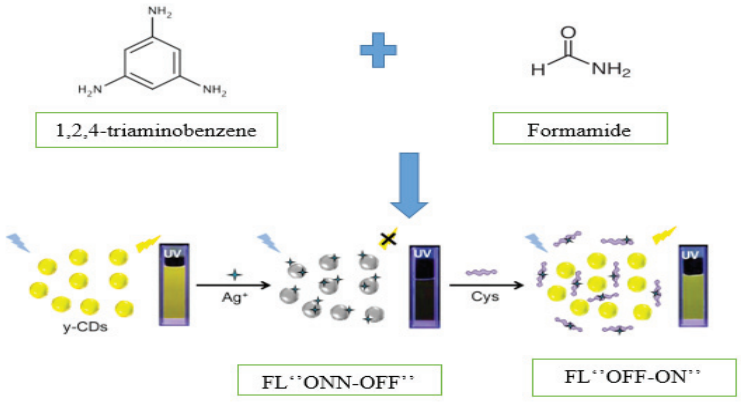

Figure 1.33. A schematic illustration of the preparation of CDs *via* hydrothermal reaction of 1,2,4-triaminobenzene and formamide

Using citric acid and dicyandiamide, Hou et al.[65] succeeded in synthesizing N-CDs with a maximum emission peak of 528 nm at 90 minutes, 170°C with a high quantum yield of 73.2% without solvent. All reactions as illustrated in Figure.1.34.

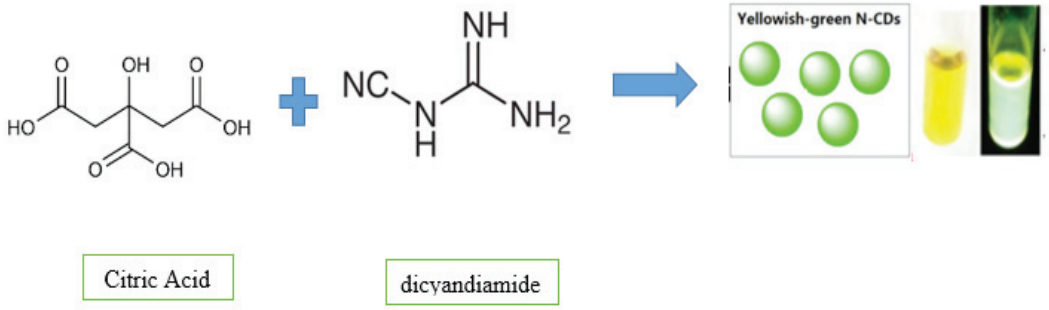

Figure 1.34. A schematic illustration of the preparation of CDs *via* hydrothermal reaction of citric acid and dicyandiamide

Using o-phenylenediamine and water as solvents, Song et al.[66] succeeded in synthesizing it in 20 minutes by microwave with 38.5% quantum efficiency, giving a high emission peak in the 573 nm yellow region. In addition, it was predicted that these synthesized o-CDs could be detected efficiently in SW480 cells and used as fluorescence probes for cell imaging.

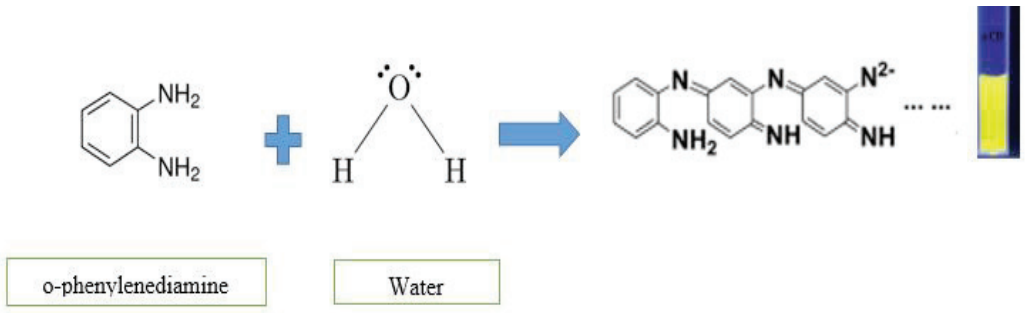

Figure 1.35. Proposed mechanism of the formation of CDs *via* microwave reaction of o-phenylenediamine and water

Using citric acid and 2,3-phenazinediamine, Yan et al.,[67] succeeded in synthesizing carbon dot with 24% quantum efficiency, maximum emission point at 568 nm, good fluorescence stability with large Stokes shift (188 nm), and fluorescence emission in the yellow region. These types of carbon dots can be applied for the detection of Ag(I) and GSH for using H1299 cells. (Figure 1.36)

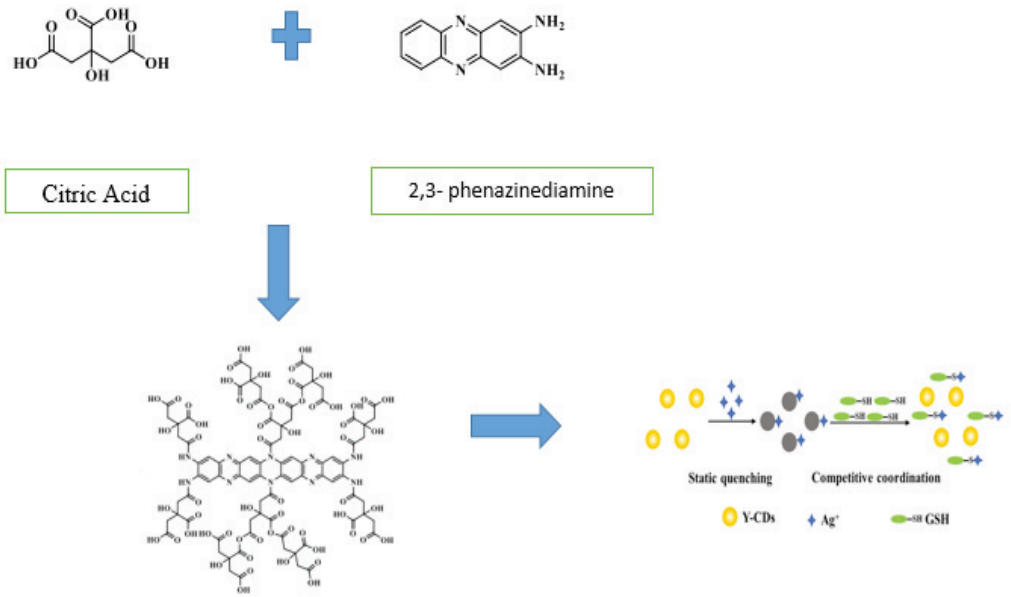

Figure 1.36. Proposed mechanism of the formation of CDs *via* hydrothermal reaction of citric acid and 2,3-phenazinediamine

Wang et al.[68] succeeded in synthesizing P,Cl-CDs using maltose, phosphoric acid, and hydrochloric acid using an autoclave with a maximum emission peak at 590 nm for 6 hours at 180 °C. P and Cl atoms were replaced by C and H atoms by applying high temperatures, and these structures showed a good fluorescence quenching effect in the presence of Fe(III) while improving surface reactivity. (Figure 1.37)

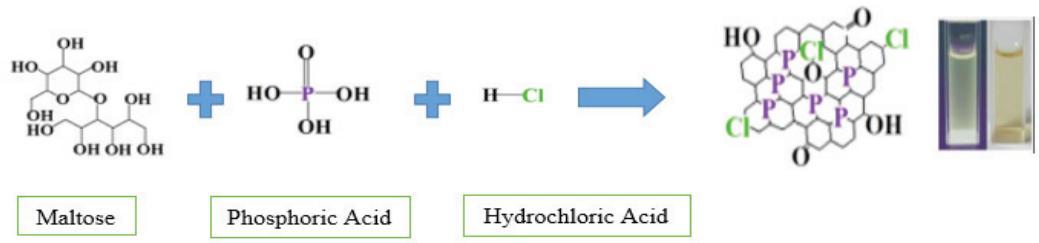

Figure 1.37. Proposed mechanism of the formation of CDs *via* hydrothermal reaction of maltose, phosphoric acid, and hydrochloric acid

Geng et al,[69] using citric acid, triethylenetetramine, rhodamine 6G, and ethanol, were able to synthesize yellow carbon dots with a 130-degree microwave method, emitting between 500-800 nm in 15 minutes, with 43% efficiency. Thanks to this carbon dot, a new sensor system has been developed that opens after the acidic one enters the lysosome and binds with ATP.

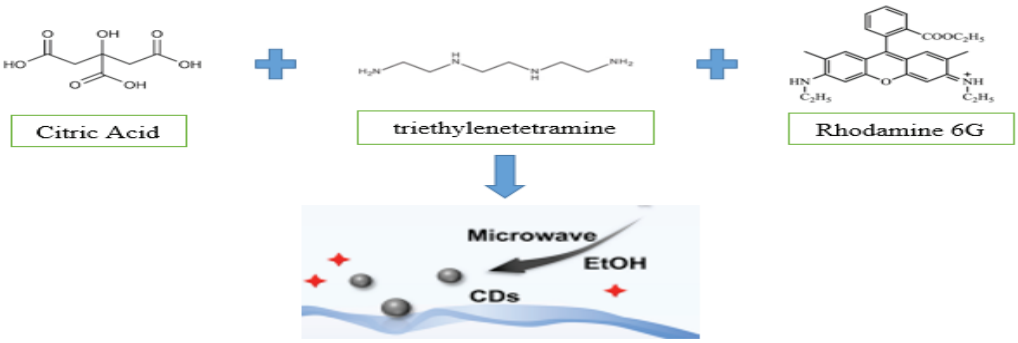

Figure 1.38. A schematic illustration of the preparation of CDs *via* hydrothermal reaction of citric acid, triethylenetetramine, rhodamine 6G

N doped carbon dots were synthesized in a short time by using the microwave method at 535 nm, which gives high emission in the orange region, using p-phenylenediamine and ethylenediamine by Ding et al.[70] as shown in Figure 1.39. As a result, it has a 65.93% quantum efficiency, is easily dispersed in water, and has a detection feature in cells thanks to its low toxicity and biocompatibility.

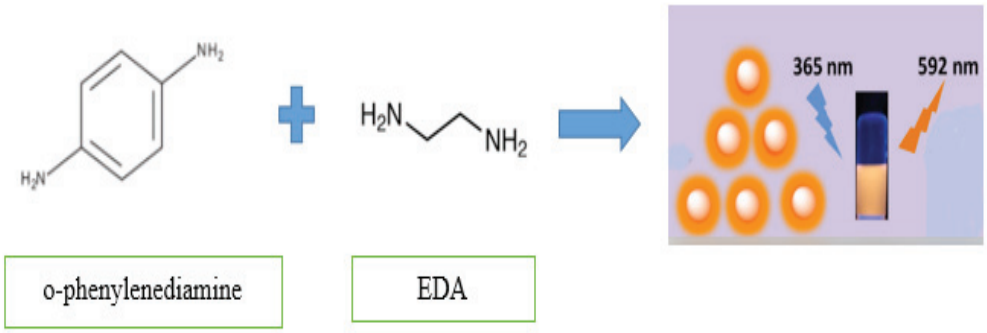

Figure 1.39. A schematic illustration of the preparation of CDs *via* microwave reaction of p-phenylenediamine and ethylenediamine

Wu et al.[71] succeeded in synthesizing organic soluble CQDs (o-CQDs) using TNP and toluene at 180 °C for 12 h with a hydrothermal method with ~90% quantum efficiency. By using this carbon dot different solvent, it was ensured to reach a high emission peak of 715 nm and shifted to the red region, and this was used to make a photoelectronic device.

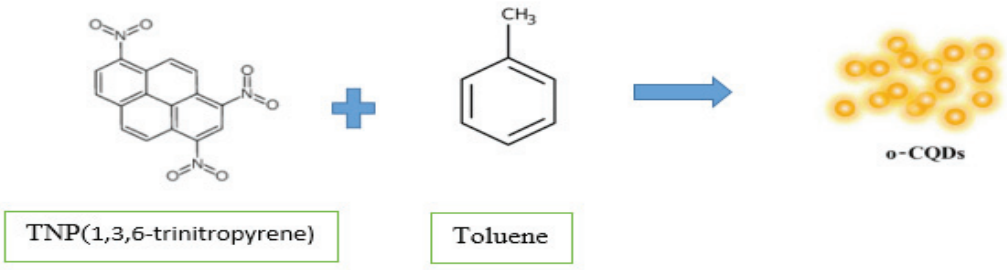

Figure 1.40. A schematic illustration of the preparation of CDs *via* hydrothermal reaction of TNP and toluene

Vedamalai et al.,[72] using OPD (o-phenylenediamine) were dissolved in ultrapure water, was synthesized at 567 nm by the water-dispersible simple hydrothermal method with photoluminescence at 300 °C for 2 hours. Thanks to the Cu^{+2} ion added to these carbon atoms, it gives an orange emission with the formation of $Cu(OPD)_2$ complexes on the surfaces of the C points. Also, A549 has been used in the cell as it has great selectivity and biocompatibility by mapping Cu^{2+} ions.

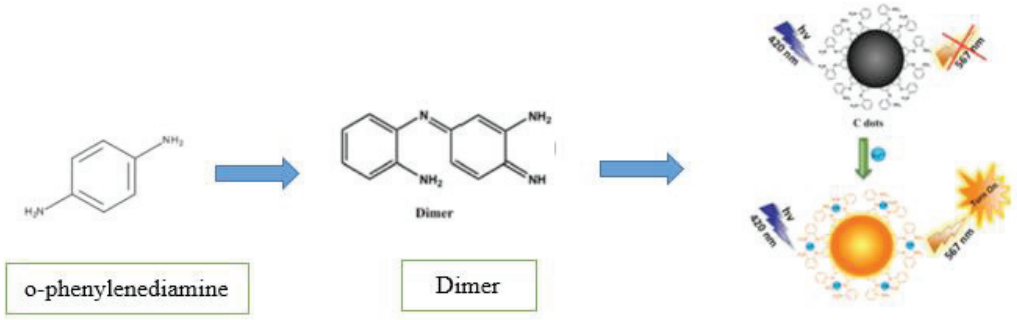

Figure 1.41. A schematic illustration of the preparation of CDs *via* hydrothermal reaction of o-phenylenediamine and water

1.6.4. Red Light-Emitting Carbon Dots

Since carbon dots emitting red light show minimal damage to biological samples and are applied in the lighting and biomedical field, numerous studies involving the development of emitting CDs with this long-wavelength are given priority.

Liu et al.[73] synthesized o-PD by hydrothermal route after 10 hours at 200 degrees using HNO_3 with 31% yield. Looking at the absorption peak, optimum emission peaks exhibit at 282 nm, 630 nm and give a shoulder peak at 677 nm. And these peaks give the π–π* transition C=C band, while the n–π* transition gives C=N, C-N-C bands on the imine and phenazine band. Thanks to this carbon dot synthesis, a new and highly efficient red-emitting carbon dot in vivo biodistribution imaging system have been reported for the first time. These carbon dots with good biocompatibility are also used in biomedical and clinical analysis. The reaction mechanisms was shown in Figure 1.42.

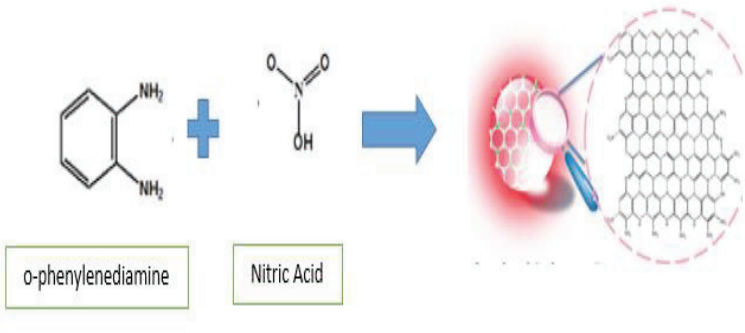

Figure 1.42. A schematic illustration of the preparation of CDs *via* hydrothermal reaction of o-phenylenediamine and nitric acid

Huang et al.,[74] using 3-aminobenzene boronic acid and 2,5-diaminobenzene sulfonic, were able to synthesize NBS-CDs in 11% efficiency with nitrogen, boron, sulfur co-doped hydrothermal at 180°C for 8 hours maintaining the emission peak at 605 nm. Thanks to the light quenching feature of Ag^{+} ions on NBS-CDs, it enabled the determination of L-Cys in human cells after Ag^{+} and L-cystine interaction. In addition, these ions have been detected in cancer cells and used as biosensors in clinical applications.

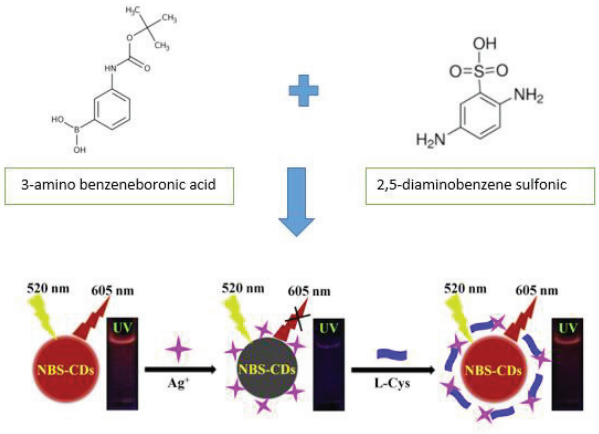

Figure 1.43. A schematic illustration of the preparation of CDs *via* hydrothermal reaction of 3-aminobenzene boronic acid and 2,5-diaminobenzene sulfonic (bottom of these imaged copied taken by [74])

Li et al.,[75] using citric acid and thiourea, acetone was chosen as the solvent and the hydrothermal reaction was at 160 degrees for 8 hours, and they were able to synthesize S, N-CDs with sulfur and nitrogen co-doped carbon points emitting 593 nm as showed in Figure 2.26. In addition, the carbon dot S synthesized after conjugation to these carbon dots using phenylboronic acid is called N-CDs-PBA and this dot was quickly taken into the PC12 cell. As a result, it was used in biomedical optical imaging and detection to detect Fe^{3+} ions.

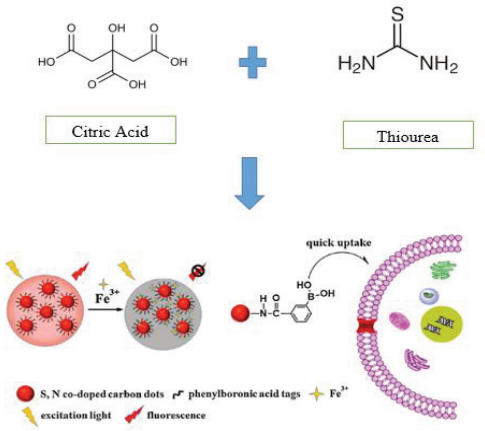

Figure 1.44. A schematic illustration of the preparation of CDs *via* hydrothermal reaction of citric acid and thiourea (bottom of these imaged copied taken by [75])

Sun et al.[76] provided the synthesis of red carbon dots with high emission at 640 nm using the microwave method with 22.9% efficiency using citric acid and formamide. In addition to synthesizing in a short time with high efficiency, it also offers use in biomedicine and emission emitting devices.

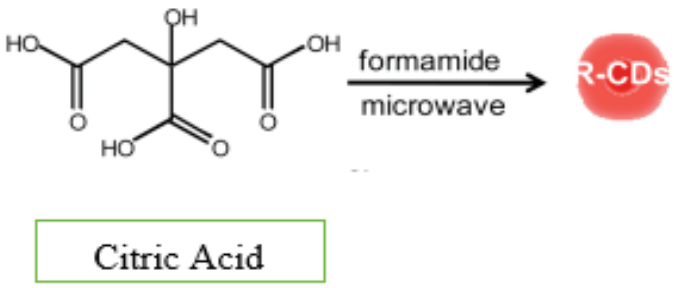

Figure 1.45. A schematic illustration of the preparation of CDs *via* microwave reaction of citric acid and formamide

Another area of use of red carbon dots is the use of LEDs. Wang et al.[77] succeeded in synthesizing 1,3-Dihydroxynaphthalene using KIO_4 and ethanol as a solvent, using a 180 degree 1-hour autoclave reactor with 53% quantum efficiency and emission at 628 nm. Subsequently, a UV-pumped CQD phosphor-based hot WLED was reported by magnifying the π-conjugated structure in carbon dots showing red fluorescence.

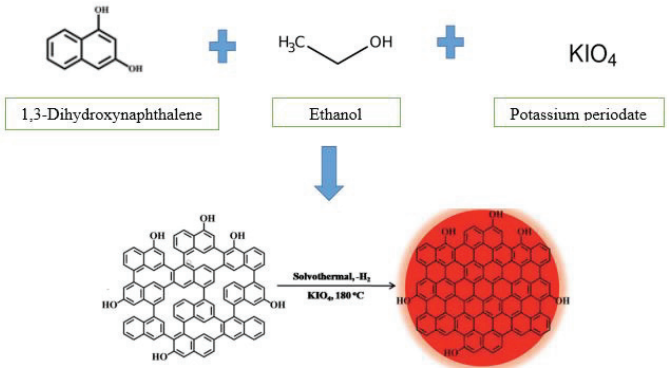

Figure 1.46. Proposed mechanism of the formation of CDs *via* hydrothermal reaction of 1,3-Dihydroxynaphthalene using KIO_4 and ethanol

By using 2,5-diaminobenzenesulfonic acid 4-aminophenylboronic acid hydrochloride, Liu et al.[78] succeeded in synthesizing BSN-CDs with an emission peak of 600 nm at 180°C with a yield of 5.44% after 8 hours. Thanks to this carbon dot, they used colorimetric and fluorescent dual-mode detection methods to detect Fe^{+3} in the cell for its effective and intracellular imaging.

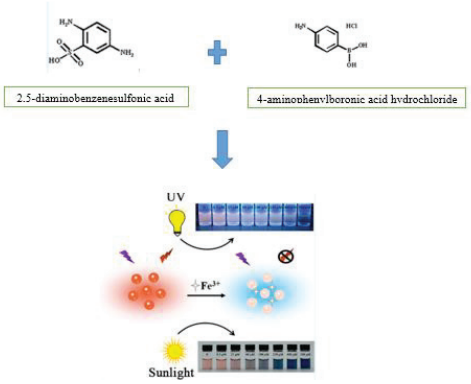

Figure 1.47. A schematic illustration of the preparation of CDs *via* hydrothermal reaction of 2,5-diaminobenzenesulfonic acid 4-aminophenylboronic acid hydrochloride

Ali etc al.[79] succeeded in synthesizing a red fluorescent functional FCN emitting 550 nm with a method different from the others, using a three-necked round-bottomed flask at 280 °C for 4 hours using ascorbic acid and oleylamine. Thanks to these dots, it is converted into the desired nano bioconjugate thanks to the existing reagents and it is possible to use it as nanoprobes.

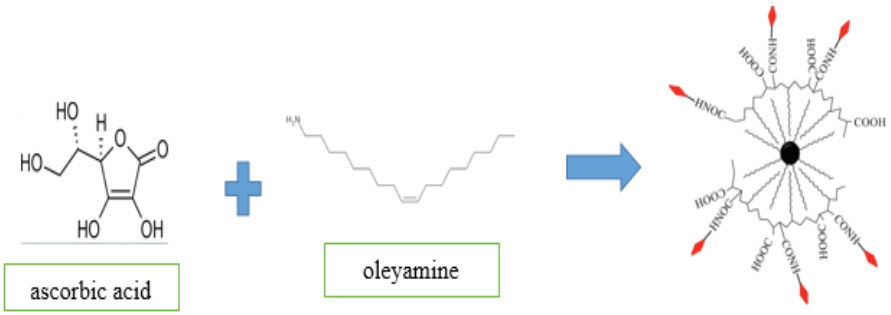

Figure 1.48. Proposed mechanism of the formation of CDs *via* hydrothermal reaction of ascorbic acid and oleylamine

Su et al. succeed in synthesizing cancer-stem-cell-nucleus-penetrable R-CQDs with 20.1% quantum yield at 195 ºC 1 hours using an autoclave thanks to 4-aminophenol and potassium periodate in an ethanol solution hydrothermal reaction to synthesize these types of red CDs. In addition, CSCNP-R-CQDs show photoluminescence emission at 620 nm and nitrogen functional groups are bound on the surface of this carbon dot, and the destruction of cancer cells shows a new way to design nano-drug.

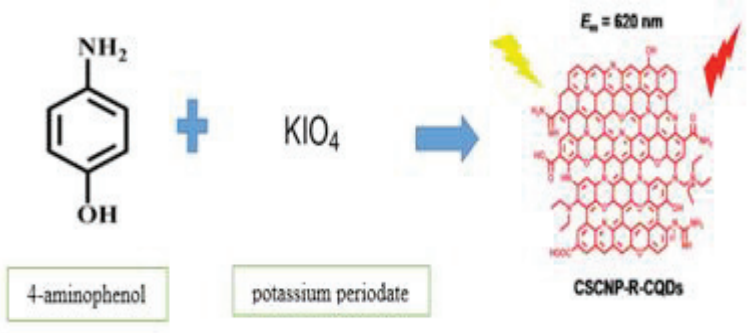

Figure 1.49. Proposed mechanism of the formation of CDs *via* hydrothermal reaction of 4-aminophenol and potassium periodate

Another method for creating red carbon dots is nitrogen-doped carbon dots. Ju et al.[80] succeeded in synthesizing o-phenylenediamine as a carbon and nitrogen source by hydrothermal route using HCL and water as solvents, emitting at 620 nm at 150 °C for 8 hours in 12% yield quantum. These N-CDs allowed the rapid and reliable determination of hematin in human red cells.

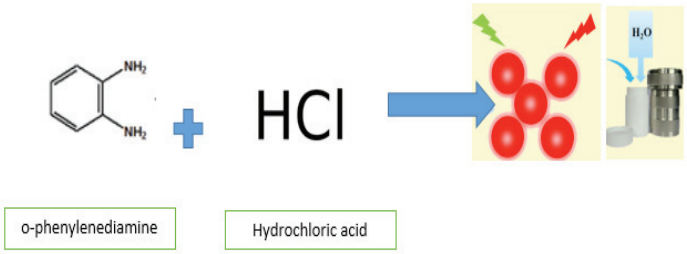

Figure 1.50. A schematic illustration of the preparation of CDs *via* hydrothermal reaction of o-phenylenediamine and HCl

Zhao et al.[81] succeeded in synthesizing N and P co-doped red emissive carbon dots using o-phenylenediamine and phosphoric acid with emission at 622 nm with 15% quantum efficiency at 160 degrees after 5 hours. These long-wavelength emitting CDs have been successfully applied in biological and medical applications and in vitro cell imaging.

Zuo et al.[82] dissolved phenylenediamine in ethanol and tartaric acid dissolved in deionized water, the resulting carbon dot has an emission at 600 nm with 39.3% quantum efficiency. This carbon dot can be used as a sensor or fluorescent label while contributing to the design of lipophilic red emission materials.

Ding et al.[83] synthesized high-efficiency carbon dots with 53% efficiency and red emission at 627 nm by heating a solution of citric acid and ethylenediamine and formamide by hydrothermal way to 180 degrees for 4 hours. The nitrogen-derived structures in the dot cores show us an intense red emission. Due to its low toxicity and good dispersibility in water, it has been successfully used for both in vitro and in vivo bioimaging.

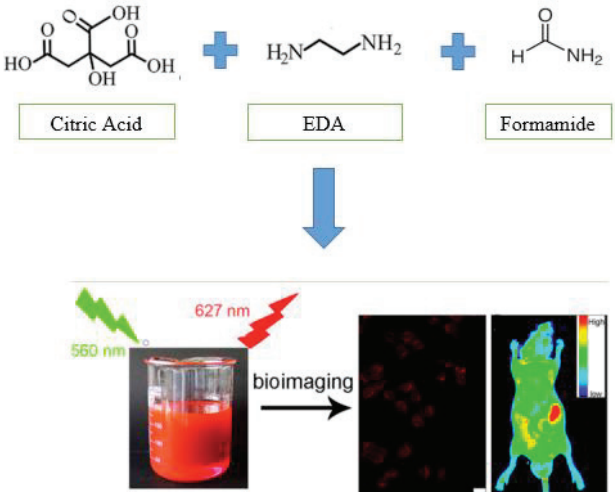

Figure 1.51. A schematic illustration of the preparation of CDs *via* hydrothermal reaction of citric acid and ethylenediamine and formamide

Ghosh et al [84] synthesized 25% efficiency of CDs and red emission at 600 nm by heating a solution of resorcinol, ethylene glycol, and Na_3PO_4 by hydrothermal way to 160 degrees for 6 hours. With the reaction of glycol and resorcinol in Na_3PO_4 under an oxygen atmosphere, the formation of a graphitic structure between adjacent H/OH functional groups with the formation of oligomeric products as a result of the phenol binding reaction. It can be used as a bioimaging probe by converting to different colloidal nanoconjugates.

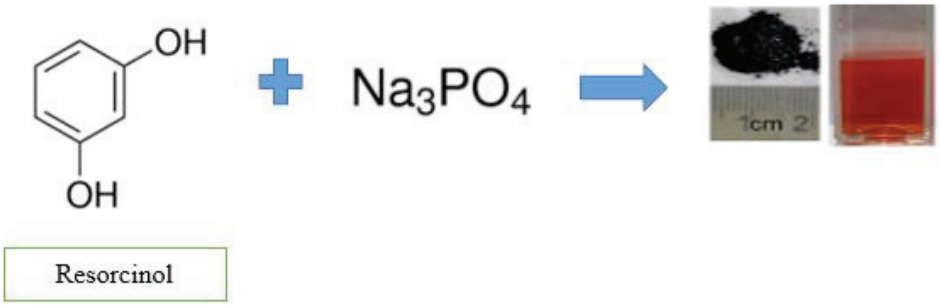

Figure 1.52. A schematic illustration of the preparation of CDs *via* hydrothermal reaction of resorcinol, ethylene glycol, and Na_3PO_4

Yuan et al.[85] succeeded in synthesizing 1,2,4-triaminobenzene as carbon source and PEG- 200 at 100 °C in 15% yield, emitting 650 nm red after 3 hours. Thanks to the solvent effect on the formed carbon dots, it exhibited emissions in different regions. As a result, warm white light is effective in emitting diodes.

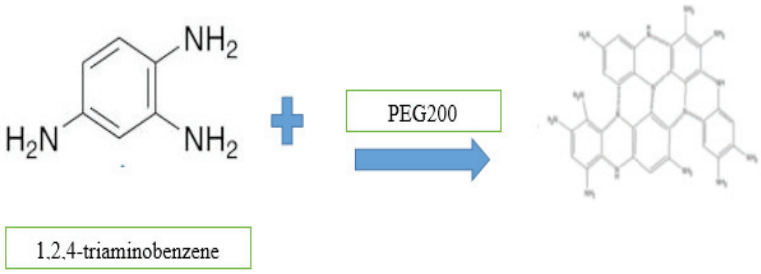

Figure 1.53. Proposed mechanism of the formation of CDs *via* hydrothermal reaction of 1,2,4-triaminobenzene and PEG200

Another synthesis of red carbon dots is the synthesis of S and Se doped carbon dots. Lan et al.,[86] used PT2 polythiophene and diphenyl diselenide to produce red fluorescent carbon dots. They succeeded in synthesizing S,Se-encoded CDs by a hydrothermal method at 180° C with ~17.5% quantum efficiency, which emits two peaks at 731 nm 821 nm, as a result of the reaction for 24 hours. These carbon dots have a TPA cross-section at 880 nm, which resulted in NIR to NIR photoluminescence. This carbon do was used to screen cancer cells in vivo and in vitro.

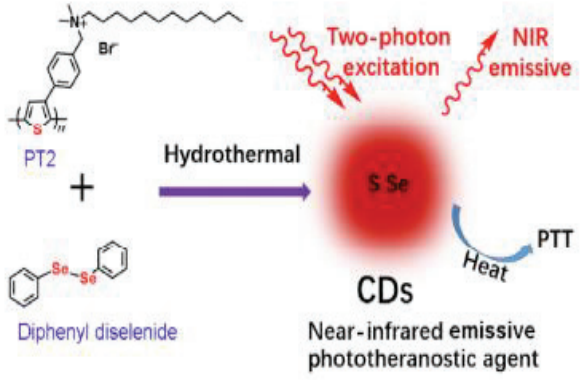

Figure 1.54. Proposed mechanism of the formation of CDs *via* hydrothermal reaction of PT2 polythiophene and diphenyl diselenide (bottom of these imaged copied taken by [86])

1.7. Application of Carbon Dots

Carbon dots have some application areas like bioimaging, sensing, drug delivery, and catalysis. Synthesis of carbon dots emitting PL in the NIR region is used in bionanotechnology and bioimaging due to the transparency of body tissues.[87] Therefore, NIR PL emission was significantly observed in vivo images for carbon dot injected mice as shown in Figure 1.55.

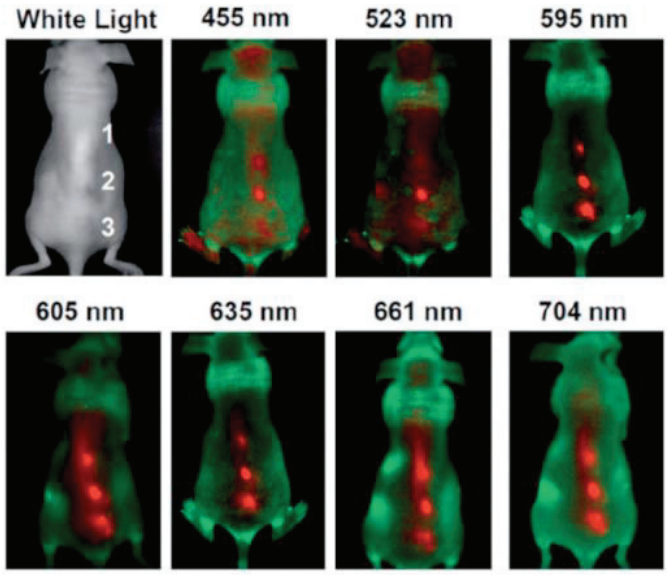

Figure 1.55. A digital picture of in vivo fluorescence images of CQDs-injected mice taken at different excitation wavelengths. (Image adapted from [39])

According to Du et al, a carbon dot-based multifunctional FRET sensor for detecting and visualizing mitochondrial H2O2 levels in L929 and Raw 264.7 cells has been developed. Also, all fluorescence images for living cell lines co-stained by the nanoprobe and rhodamine 123 were shown in Figure 1.56. [88] As a result of this study, the fluorescence signals from L929 and Raw 264.7 cells overlap with the fluorescent signals from rhodamine 123, showing that the probe is primarily localized in the mitochondria.

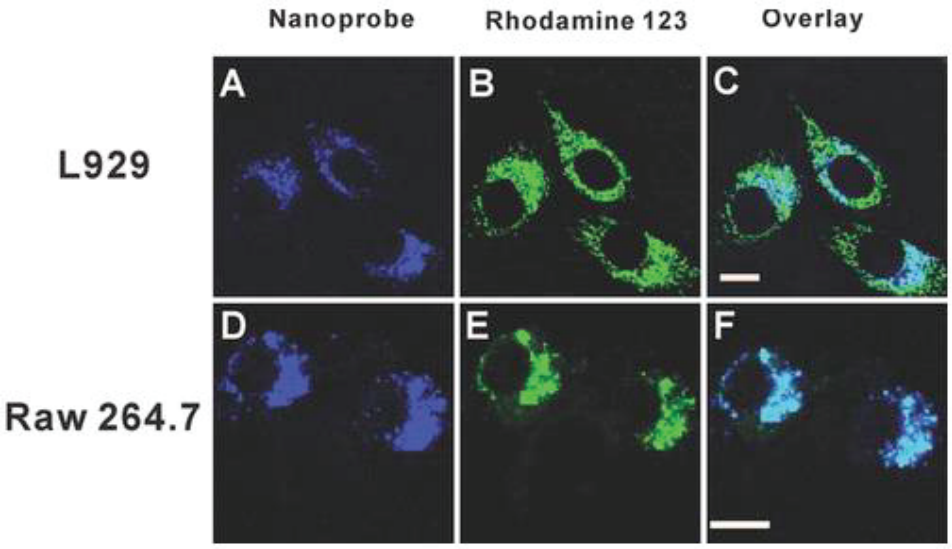

Figure 1.56. Images of a-c) L929 live and d-e) raw 264.7 cells by using Confocal fluorescence with Mito-CD-PF1 (0.3 mg mL^{-1}) and rhodamine 123 (2 μM). (Image adapted from [88])

Table 1.3. Table of all Reaction Techniques and Ingredients Summary

Color	TYPES	Measerement type	Precursor A	Precursor B	Solvent	T (^oC)	Time (h)	QY (%)	Absorbance wavelength (nm)	PL wavelength (nm)	Particle size (nm)
Blue 1	N,S-CDs	hydrothermal	citric acid	L-cysteine	water	70	12		242 and 345	345 and 415	8
2	NCDs	hydrothermal	citric acid	$(HOCH_2)_3CNH_2$	water	200	6	60	328	408	3.45
3	NCDs	hydrothermal	ammonium citrate		water	160	6	54	235 and 327	437	2.14
4	CDs	microwave	oxalic acid	urea	water	700 W	0.16		350	352 and 426	
5	N-CDs	hydrothermal	streptomycin		water	200	12	7.6	275	410	3
6	CDs	hydrothermal	citric acid	ethylenediamine				60	360	443	3
7	S-C-dot	hydrothermal	sodium citrate	sodium thiosulfate		240	6	67	350	450	4
8	Blue CDs	hydrothermal	citric acid	ethylenediamine		150	5	74.8	243 and 345	480 to 443	2.5-5
9	N-CDs	hydrothermal	citric acid	urea		180		35.5		449	1

“cont. on the next page”

“cont. Table 1.3”

Color	Types	Measurement type	Precursor A	Precursor B	Solvent	T (ºC)	Time (h)	QY (%)	Absorbance wavelength (nm)	PL wavelength(nm)	Particle size (nm)
Green 1	FN-CDs	hydrothermal	2,3-diaminophenazine	folic acid	water	80	24	0.91		525	4.6
2	N-CDs	hydrothermal	shiitake mushroom powder			200	12	54.0	330	410	2–6
3	phenyl-CDs	solvothermal	N-Phenyl-o-phenylenediamine	ethanol		180	12	10.50	420	530	2.2
4	CNDs	solvothermal	citric acid	Urea	DMF	160	6	46.0	540	580	10 to 30 μm
5	FCDs	hydrothermal	ascorbic acid	ethylene glycol	water	160	1		335 to 420	435 - 538	4.5
6	N-CQDs	hydrothermal	tartaric acid	bran	DMF	150	8	46.0	350	539	4.85
7	CDs	hydrothermal	citric acid	RhB	water	80	24		450	500–650	3.3
8	La-CDs	microwave	Citric acid	CH_6CIN	water	700 W	4 min		360-420	300 to 480	
9	G-CDs	hydrothermal	phenol	ethylene diamine	water	180	10	29.00	519	513	

“cont. on the next page”

“cont. Table 1.3”

10	G-CDs	solvothermal	PEG-200	NaOH		160	24	0.69	262	410	1
11	S, NGQDs	hydrothermal	Citric acid	urea	water	160	4	78.00	234 -337	360 and 435	2.69
12	F- CDs	hydrothermal	o-phenylenediamine	4,5-difluoro-1,2-benzenediamine	ethanol	180	8		360	550	5.18
13	raw-Cdots	hydrothermal	citric acid	EDA	water	200	4	69.30	420–460	460	4.2- 3.1
14	G-CDs	microwave	DEG	sucrose		750W		54.00	320	540	
15	G-CDs	microwave	glycerol	phosphate		700W		54.00	350	470	
16	G-CDs	solvothermal	p-benzequonine	EDA	water		25	15	400	450	

“cont. on the next page”

“cont. Table 1.3”

Color	Types	Measerement type	Precursor A	Precursor B	Solvent	T (°C)	Time (h)	QY (%)	Absorbance wavelength (nm)	PL wavelength (nm)	Particle size (nm)
yellow 1	Y- CDs	hydrothermal	citric acid	urea	toluene	180	12	46	435 and 450	550	2.68
2	N-CDs	hydrothermal	1,2,4-Triaminobenzene		Formamide	120			270 and 400	568	14.3
3	N-CDs	hydrothermal	citric acid	dicyandiamide		170	1.5	73.2	232 and 405	525 to 555	2.7
4	Y-CDs	microwave	o-PDs		water	750 W	20 min	38.5	300	573	8–11
5	Y-CDs	solvothermal	citric acid	2,3-phenazinediamine	ethanol	170	4	24	263 and 387	575	7.2
6	P,Cl-CDs	hydrothermal	maltose	phosphoric acid	HCL	180	6	15	220 and 280	590	4.83
7	Y-CDs	microwave	citric acid	triethylenetetramine	ethanol	130	15 min	43	400 to 700	500-800	4.6

“cont. on the next page”

"cont. Table 1.3"

Color	Types	Measerement type	Precursor A	Precursor B	Solvent	T (oC)	Time (h)	QY (%)	Absorbance wavelength (nm)	PL wavelength (nm)	Particle size (nm)
red 1	R- CDs	microwave	p-PD	Ethanol	water	800 W	1	15	365 and 470	620	3.8
2	NBS-CDs	hydrothermal	3-amino benzeneboronic acid	2,5-diamino benzenesulfonic	water	180	8	11.6	234 and 286	605	2.84
3	S,N-CDs-P	hydrothermal	citric acid	Thiourea	acetone	160	8	23	250 350 550	593	3.27
4	R-CDs	microwave	citric acid	Formamide		160-120		22.9	340 and 580	640	4
5	R-CDs	hydrothermal	1,3-Dihydroxynaphthalene	KIO	ethanol	180	1	53	530	628	5
6	R-C-dots	hydrothermal	PPA	alkaline solution		240	36				10 ± 4
7	BNS-CDs	hydrothermal	2,5-Diamino benzenesulfonic acid		water	180	8	5.44	233, 281 and 520	600	2.4 ± 0.6

"cont. on the next page"

cont. Table 1.3”

8	R-FCN	TN-bottomed flask	ascorbic acid	oleylamine	&	280	4	14	no bond	550	3 and 8
10	N-CDs	hydrothermal	o-PD	HNO3	water	200	10	10.83	282 and 535–621	630 nm	5.74
11	R-CQD	solvothermal	4-Aminophenol	KIO	ethanol	195	1	20.1	227 -274 and 537	620nm	3.3
12	N,P-R-CDs	hydrothermal	o-PD	H3PO4	water	160	5	15	234-286 and 428	622 nm	2.99
13	R-CDs	hydrothermal	thiourea	citric acid	DMF	160	6	24	540	610 nm	4−7
14	R-L-ODs	solvothermal	o-phenylenediamine and	L-tartaric acid	water	170	5	39.3	300 and 450	540 nm	21.6 ± 3.4
15	N,S-CDs	hydrothermal	CA monohydrate	L-cysteine	water	200	3		245 and 345	415 to 540	7

“cont. on the next page”

“cont. Table 1.3”

16	R-CDs	hydrothermal	citric acid	EDA	&	180	4	24	564	627	4.1
17	R-CDs	solvothermal	urea	citric acid	DMF	160	4	18	340-400 and 550	380 440 and 540	5.6
18	red CDs	hydrothermal	PT2	diphenyl diselenide	NaOH	180	24	17.5	526	731 821	4
19	N-CDs	hydrothermal	citric acid	urea	formamide	180	12	4	430 and 550	630	2.3
20	R-CDs	hydrothermal	1,2,4-triaminobenzene		PEG 200	100	3	15	225 and 325	650	4.5
21	N,F,PCDs	hydrothermal	p-PD	HNO3, H3PO4 and HF		200	2	15.8	290 and 510	600 and 680	3.46

CHAPTER 2

SYNTHESIS AND CHARACTERIZATION OF CARBON DOTS, AND GOLD NANOPARTICLE

2.1. Introduction

The emission of carbon dots in different regions depends on chemical structure, size, and crystalline degree. The PL feature varies according to the size of the material. If the synthesized cd is 1.2 nm in size (small), the UV region is located at 350 nm. It has a medium-size between 1.5-3 nm (medium) and exhibits 400-700 nm emission in the visible region. The 3.8 nm (large) carbon dot exhibits absorption spectra at 800 nm in the near-infrared region. These particle sizes are related to the quantum confinement effect. Two factors affect that the surface state of carbon dots, originating from surface configurations and doping atoms. [89] Polymers with different degrees of oxidation can vary as a large-area structural type where functional groups, defects, and edge states are important. Changes in the surface design of CDs can affect electron energy levels or light-emitting regions. Redox processes, amino modification, and molecular modification all modify the surface configuration. To control the electrode potential and current density for manufacturing carbon dots, electrochemical techniques can be employed initially. Bao et al.[89] electrochemically synthesized CDs, which increased the surface defect density with higher potential leading to smaller CDs and whose recombination yielded a red-shifted emission band, enhanced surface oxidation. In addition, Liu et al.[90] investigated the effect of pH on carbon dots. Carbon dots formed under alkaline conditions, PL emission is quenched under an acidic environment. The hydroxyl or carboxyl groups electrons and holes on carbon dots radiatively recombine under illumination with excitation light, resulting in PL. While these hydroxyl groups donate electrons and raise PL, electron-withdrawing groups such as carboxyl groups absorb some of the radiation signals, weakening the PL. We can provide the surface configuration of CDs by amino modification. A single radiative transition mode of the sp^2 carbon occurs if all surface states are passivated by the amino, independently of the excitation wavelength. Functional groups for C-O, C=O, and O=C-OH emit fluorescence emission depending on the

excitation energy if the surface groups are not passivated by amino groups. Heteroatom doping can be achieved by using heavy atoms for example phosphorus, selenium, sulfur, fluorine, and nitrogen since it changes the electronic structure of CDs. Nitrogen and sulfur are similar to carbon atoms in terms of atomic radius and electronegative properties and are therefore widely used as dopant atoms. Dong et al. [47] succeeded in synthesizing o-doped O-CDs, N-doped N-CDs, and nitrogen- and sulfur-doped N,S-CDs using citric acid and L-cystine. It expands the nitrogen band and shows excitation-independent PL emission by eliminating the oxygen state with the addition of sulfur. In addition to this, Song et al.[91] syntheses of N-S co-doped carbon dots using citric acid, urea, and thiourea, red-shifted photoluminescence peaks were observed independent of excitation points. Fluorine and sulfur or selenium, which are more electronegative, are other doping elements. It has been demonstrated that these elements cause PL spectra to shift to the red region more effectively than nitrogen doping and that this shift is dependent on heteroatom electronegativity. The surface state is mostly dependent on the carbon core due to surface modification and heteroatoms, and the PL mechanism controls the electronic structure and energy levels of CDs.

In this study, carbon dots with high photoluminescence wavelength, which can be easily synthesized in one step, a cheap, reproducible, and high quantum yield that will not cause toxic effects in the cell. Carbon dots were tried to be synthesized with high efficiency by using different carbon and nitrogen sources, but while it gave high emission in the blue region, the desired result could not be obtained in the green and red regions. In the light of literature information, studies have been carried out for the synthesis of N-S doped carbon dots by increasing the amine and sulfur source.

2.2. Various Synthesis Method for CDs

2.2.1. Experimental

2.2.1.1. Reagents

The Citric acid (99.9%), urea (99.9%), were purchased from Sigma –Aldrich. Thiourea (99.9%) were purchased from Alfa Easer. Ethylenediamine was purchased from MERCK.

2.2.1.2. Synthesis of Blue Luminescent Carbon Dots

Some experimental supplies are mentioned in this section. Using different types of starting materials and experimental procedures, carbon dots exhibiting different types of emission wavelengths were obtained.

Firstly, 0.005 mol of citric acid and 335 μL of ethylenediamine were added into 10 mL and 300 mL deionized water. Then the solution was well-stirred and transferred to Teflon-autoclave and heated at 150 ^{o}C for 5 hours. After the reaction was cooled at room temperature.

Secondly, in this study citric acid and urea were used to synthesize of N-CDs. Carbon dot solutions with different molecular concentrations are prepared as 0.025M, 0.0763M, 0.25M, 1.27M. After 2 mixing compound was transferred to the Teflon-autoclave and heated at 150 ^{o}C for 33 minutes. After heating, the reaction waited at room temperature, and then the colorless solution was observed.

The third method is 0.009 mol of citric acid and 0.005 mol of L-cysteine was added into 5 mL deionized water. Then the solution was well-stirred at 70 ^{o}C approximately 4 hours and thick syrup was obtained. Then transferred solution to the Teflon-autoclave and the solution was heated at 200 ^{o}C for 3 hours. After the reaction was cooled at room temperature.

2.2.2. Experimental

2.2.2.1. Reagents

The P-benzoquinone (99.9%), o-phenylenediamine (99.9%), were purchased from Sigma –Aldrich. Ethylenediamine was purchased from MERCK. Tartaric acid was purchased from Sigma –Aldrich.

2.2.2.2. Synthesis of Green Luminescent Carbon Dots

0.05 g of p-benzoquinone was dissolved in 5 mL, 10 mL, 15 mL ultrapure water, followed by the addition of 150 µL and 100 µL ethylenediamine and mixed for 8 and 16 hours and after a dark-brown component occurred. The mixtures were mixed completely at ambient air, temperature, and pressure. After methanol was added to the reactions and centrifuged at 6000 rpm, 20 minutes. Finally, the reaction was filtered by using a syringe filter.

Table 2.1. Reaction parameters for Green-emitting Carbon-Dot synthesis

Sample	P-benzoquinone (mmol)	Ethylenediamine (mmol)	Water (L)	M (mol/L)	Reaction time (h)
1	0.5	22.4	0.015	1.52	8
2	0.5	22.4	0.01	2.28	8
3	0.5	22.4	0.005	4.57	8
4	0.5	22.4	0.015	1.02	8
5	0.5	22.4	0.01	1.53	8
6	0.5	22.4	0.005	3.07	8
7	0.5	22.4	0.015	1.52	16
8	0.5	22.4	0.01	2.28	16
9	0.5	22.4	0.005	4.57	16
10	0.5	22.4	0.015	1.02	16
11	0.5	22.4	0.01	1.53	16
12	0.5	22.4	0.005	3.07	16

.

2.2.3. Experimental

2.2.3.1. Reagents

The p-phenylenediamine (p-PD) (99.9%), o-phenylenediamine (o-PD) (99.9%), were purchased from Sigma –Aldrich. HCL(30-32%) and HNO 3 were purchased from TEKKİM. Deionized water supply by IYTE.

2.2.3.2. Synthesis of Red Luminescent Carbon Dots

In this part, we tried to synthesize Red fluorescent emission carbon dots using o-phenylenediamine, p-phenylenediamine with different kinds of solvents which are HCL and HNO_3.

Firstly, 0.25 mmol of o-PD and p-PD was mixed with different microliters of HCL and HNO_3 compounds which were added to 5 mL of ultrapure water. Then the compound waited in the sonicator for obtaining a pure solution. And the solution was heated at 150 °C for 8 h in a Teflon-autoclave (20 mL). After the reaction waited at room temperature. Deep red products were centrifuged at 6.000 rpm for 30 minutes and, then the solid precipitate was removed by using a syringe filter.

Table 2.2. Reaction parameters for Red-emitting Carbon Dots synthesis

number	o-PD (mmol)	HCL (mol)	water (L)	M (mol/L)	Reaction Time (h)	pH
1	0.25	0.05	0.005	0.0299	8	1.1
2	0.25	0.03	0.005	0.0279	8	1.31
	o-PD (mmol)	HNO_3 (mol)	water (L)	M (mol/L)	Reaction Time (h)	pH
3	0.25	0.05	0.005	0.0299	8	0.12
4	0.25	0.03	0.005	0.0279	8	0.74
	p-PD (mmol)	HCL (mol)	water (L)	M (mol/L)	Reaction Time (h)	pH
5	0.25	0.05	0.005	0.0299	8	0.96
6	0.25	0.03	0.005	0.0279	8	1.32
	p-PD (mmol)	HNO_3 (mol)	water (L)	M (mol/L)	Reaction Time (h)	pH
7	0.25	0.05	0.005	0.0299	8	0.81
8	0.25	0.03	0.005	0.0279	8	1.03

2.2.4. Result and Discussion

2.2.4.1. Blue Luminescent Carbon Dots Experimental Results

In this study, the synthesis of the carbon dot, which varies depending on the solution concentration and emits in the blue region, has been successfully carried out. At the end of the reaction, the carbon dots prepared with 10 mL of water were yellowish, and the carbon point prepared using 300 mL of water was obtained as colorless as shown in Figure 2.1a). All reaction colors were shown in Figure 2.1b) under UV-Lamp.

a) **b)**

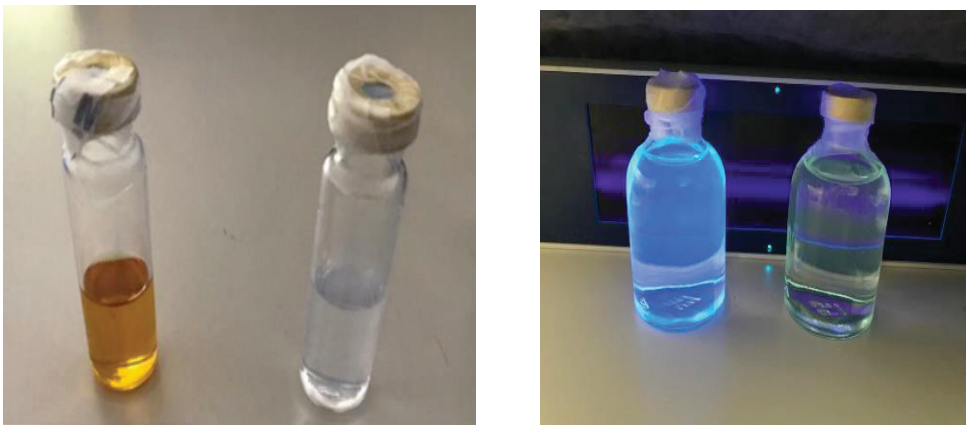

Figure 2.1. Reaction solution for 10 mL (left) an solution for 300 mL (right) under a)day-light and b)UV-light

According to the article, The absorption peak at 243 nm is assigned to the CD solution of C=C refers to π→π*, while the absorption peak at 346 nm is due to the C=O refer to n→ π * transition. Here, the absorption peak at 248 nm is assigned to the CD solution of C=C refers to π→π*, while the absorption peak at 349 nm corresponds to the n→ π * transition was shown in Figure 2.2.

a) b)

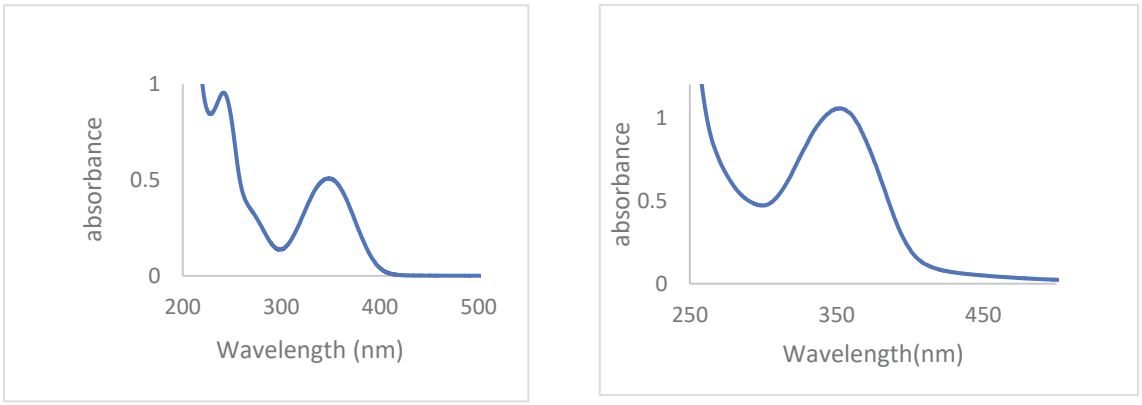

Figure 2.2. The UV visible absorption spectrum of CDs for a)10 ml and b) 300 ml(right)

The emission spectra of the carbon dots prepared with 10 mL and 300 mL of water are shown in Fig. 2.3. It exhibited emission from 480 to 450 nm at the same excitation wavelength of 350 nm, and the pl intensity increases as the concentration decrease.

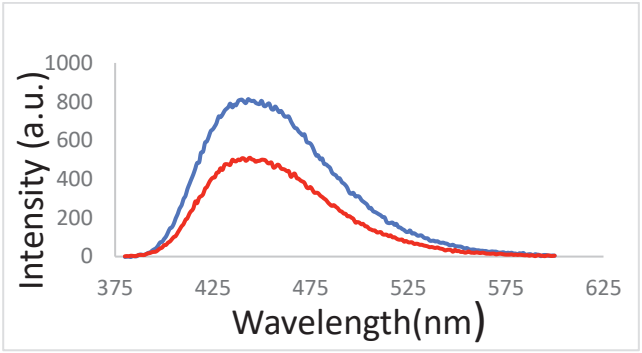

Figure 2.3. PL emission spectra of CDs in different volumes of water with an excitation wavelength of 350 nm for preparing with 300 mL(red) and 10 mL(blue) of water

According to the results of the second experiment, carbon dots emitting in the blue region were successfully synthesized after 33 minutes using citric acid and urea. When the concentration was increased, the pl emissions of carbon dots emitting in the blue region decreased, and this was shown under the UV lamp in Figure 2.4b)

a) b)

Figure 2.4. Reaction solution for citric acid and urea for preparing different concentration 0.025M, 0.076M, 0.25M, 1.27M under a)visible and b)UV-light

As a result of the experiment prepared with citric acid and urea, PL density increased at low concentrations, but no PL emission was obtained at high concentrations. This is because reaction rates are quite slow when CA and urea concentrations are low. As the precursor concentration is increased, the reaction time should be longer.

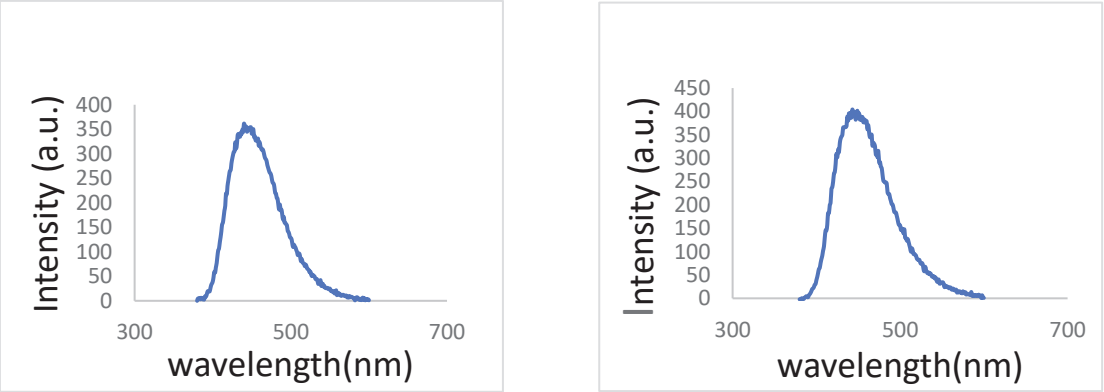

Figure 2.5. Effect of 0.025M and 0.076M concentration of the solution on PL spectra of N-CDs under excitation at 350 nm

As a result of the third experimental procedure, the reaction was neutralized with 1 $molL^{-1}$ NaOH solution and then diluted with 30 mL deionized water, blue emission was observed under the UV lamp as shown in Figure 2.6 b).

a) b)

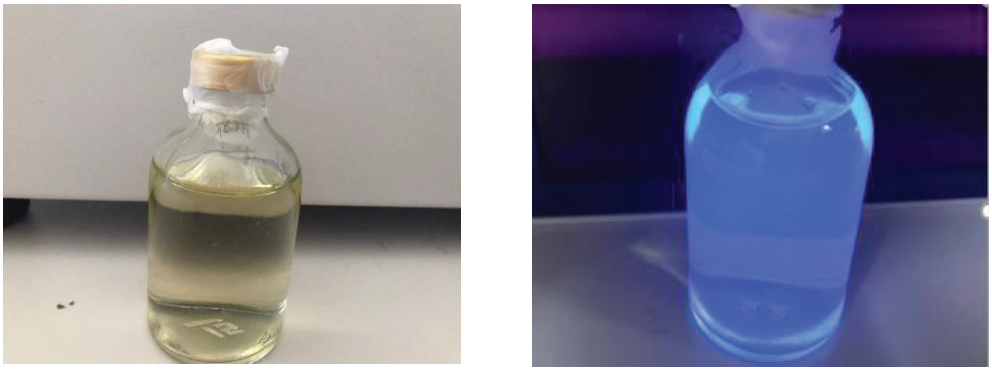

Figure 2.6. Bright yellow solution of the N,S-CDs under daylight and Blue emission under UV irradiation of the N,S-CDs

According to Dong etc al. reported that N,S-CDs in an aqueous solution was synthesized by using citric acid and L-cysteine. Only one absorption peak was seen at 345 nm as shown in Figure 2.7.

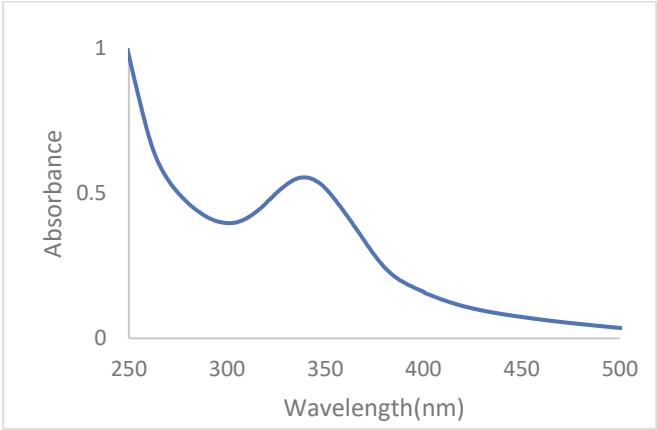

Figure 2.7. The UV visible absorption spectrum of main N-CDs solution

The emission spectrum of N,S-CDs of an aqueous solution was shown in Figure 2.8. According to the article; the maximum excitation and emission wavelength of N,S-CDs aqueous solutions are 345 and 415 nm, respectively.

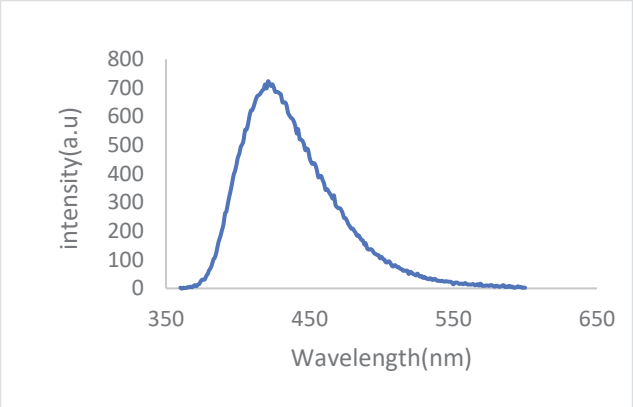

Figure 2.8. PL spectra of the aqueous solution of the obtained N-CDs under excitation at 350 nm

2.2.4.2. Green Luminescent Experimental Results

At ambient air, temperature, and pressure, the mixes were well mixed. Because the change in Gibbs energy (G) was less than zero, the reaction between p-benzoquinone and ethylenediamine was determined to be spontaneously exothermal. Before the characterization process, The color of the CD solution changed from dark brown to red after each sample was collected 8 and 16 hours later as shown in Figure 2.9 and Figure 2.10.

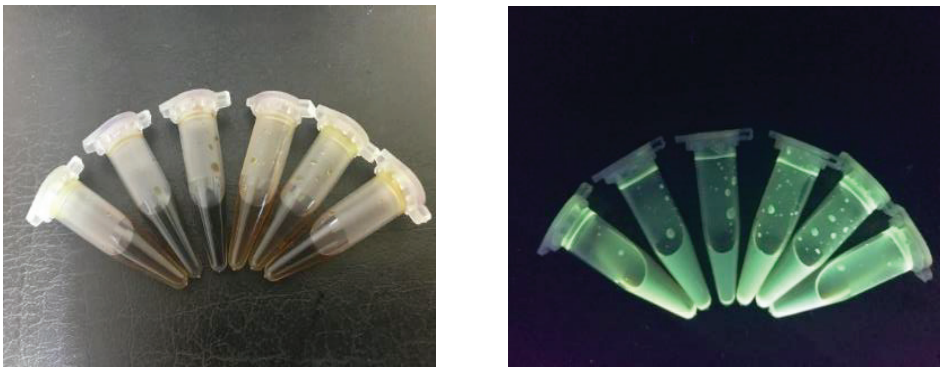

Figure 2.9. The color of the CD solution after 8 hours under daylight and UV-lamp (from left to right 1,2,3,4,5,6)

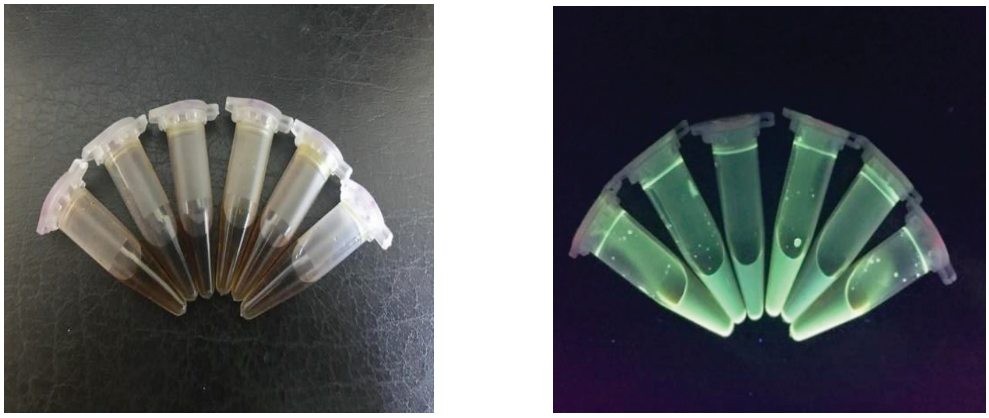

Figure 2.10. The color of the CD solution after 16 hours under daylight and UV-lamp (from left to right 7,8,9,10,11,12)

Also after characterization of the process, all samples were shown in Figure 2.11 and Figure 2.12

Figure 2.11. The color of the CD solution after 8 hours under daylight and UV-lamp (from left to right 1,2,3,4,5,6)

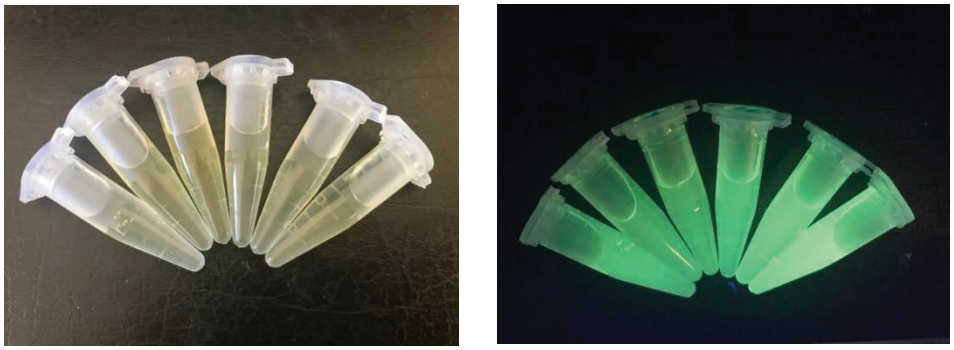

Figure 2.12. The color of the CD solution after 16 hours under daylight and UV-lamp (from left to right 7,8,9,10,11,12)

Zhang et al succeed the synthesizing green-emitting CDs by using p-benzoquinone and ethylenediamine. According to the article; the CD solution of the absorption peak at 234 nm is attributed to π→π* of C=C, and the absorption peak at 410 nm corresponds to n→ π * transition of the C=O and C=N bond. Also, CDs solution of PL spectra was shown in Figures 2.13.c) and 2.13.d) which is changeable of emission wavelength when the sample is prepared by exciting different wavelength. In addition to this, absorption spectra of CDs diluted by different volumes of deionized water show an absorption peak at 400 nm for every different volume of water was shown as Figure 2.13.a) and Figure 2.13.b).

a) **b)**

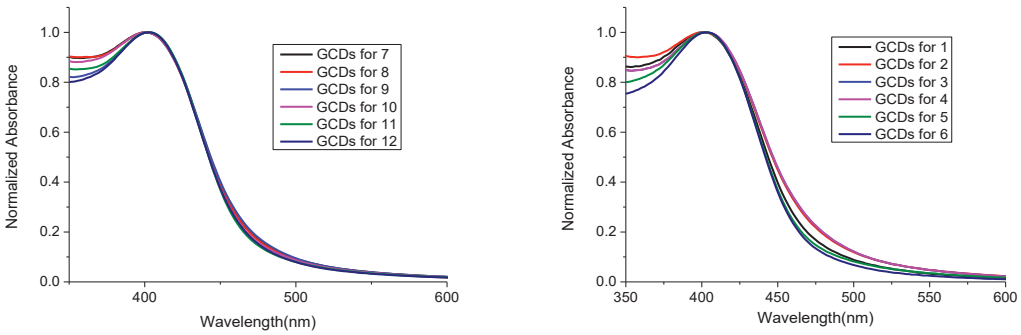

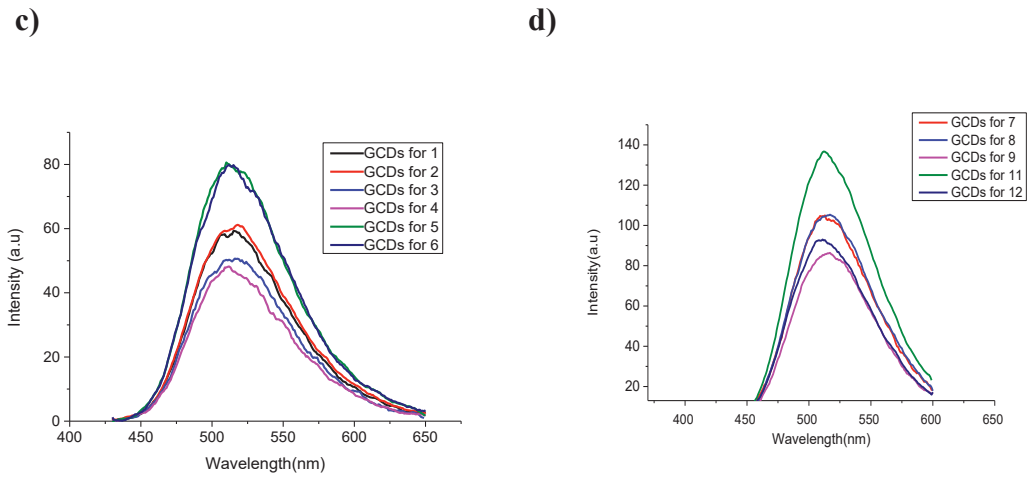

Figure 2.13. The absorption spectra of Green CDs synthesis a)8 hours b)16 hours and

The PL emission spectra of Green CDs for c) 8 hours, d)16 hours under excited at 400 nm

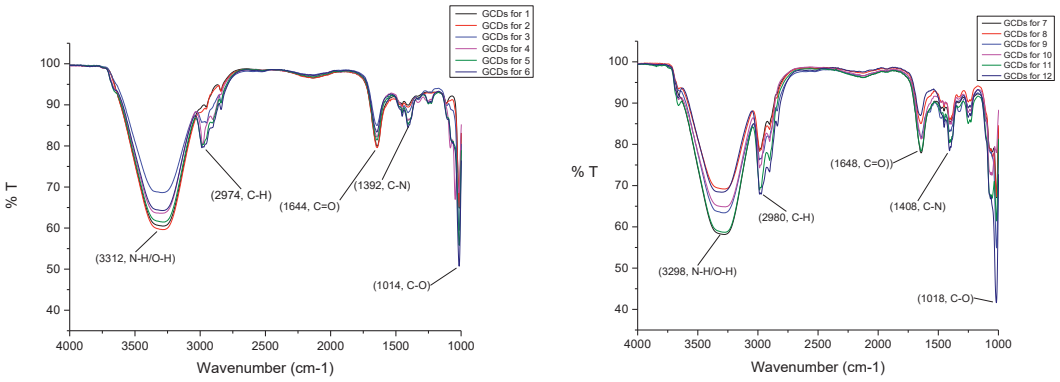

Figure 2.14. FT-IR Spectra of green emission CDs

The second trial is that, before the characterization process, The color of the CD solution changed from colorless to bright yellow after each sample was collected from the reaction at the beginning of each hour. Also, blue emission was observed for samples collected each hour as shown in Figure 2.15, under UV irradiation.

Also, this reaction was controlled 2 weeks later and we observed the green emission under UV light. After checking the PL emission characterization process.

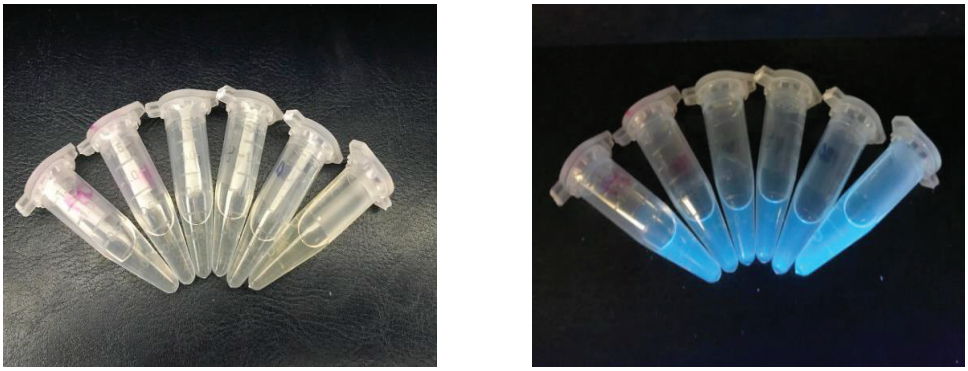

Figure 2.15. The color of the CD solution after 10 hours later under daylight (left) and UV-light (right) from left to right (5h,6h,7h,8h,9h,10h)

After 2 weeks later we observed green fluorescent emission under UV-Lamp. Also, look at the absorbance and PL emission was mentioned about the characterization part.

Figure 2.16. The color of the CD diluted solution after 10 hours later under daylight (left) and UV-light (right) from left to right (5h,6h,7h,8h,9h,10h)

Zuo et al reported that red-emitting oligomeric carbon dots synthesis by using o-phenylenediamine and tartaric acid. However, while the red emission carbon points were desired to be synthesized, the green emission carbon point was obtained. And all rection images was shown in Figure 2.17.

Figure 2.17. After the reaction, every hour was be taken (2,4,5,6 hours from left to right)

Figure 2.18. After reaction every hour solid particle was diluted with ethanol under daylight (left) and UV-Lamp (right) (2,4,5,6 hours from left to right)

Zuo et al succeed in synthesizing green-emitting CDs by using o-phenylenediamine and tartaric acid. According to the article, they want to synthesize red emissive organic oligomeric carbon dots but we do not obtain red fluorescence emission CDs. The UV-vis absorption spectra of L-ODs reveal two absorption bands at 250-300 and 450-600 nm, which correspond to the π–π* transition of C=N or C=C and n–π* of C=O or intermolecular hyperconjugation, respectively, according to the paper. On most CDs with fluorophores, you'll see wavelength-dependent fluorescence. But the end of the experiment, only one absorption peak was observed at 450 nm as shown in Figure 2.19. Also, a PL emission peak was observed at 525 nm when excited at 430 nm as shown in Figure 2.20.

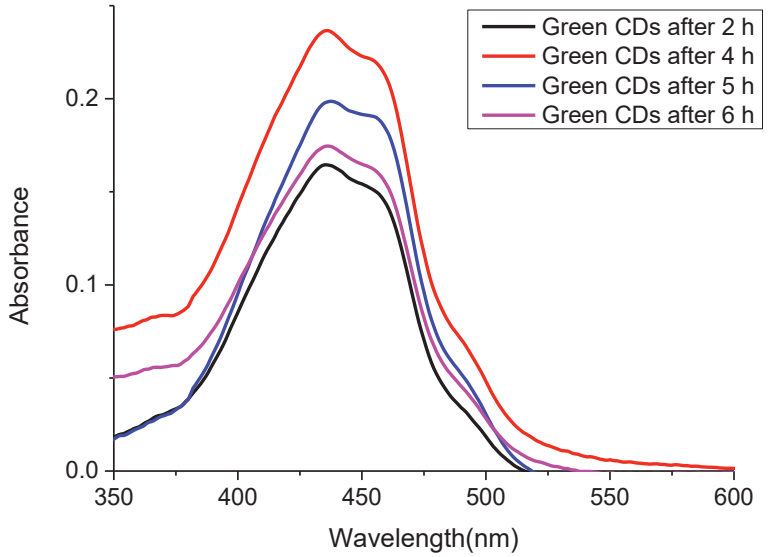

Figure 2.19. The UV-vis absorption spectrum of CDs at 6 hours

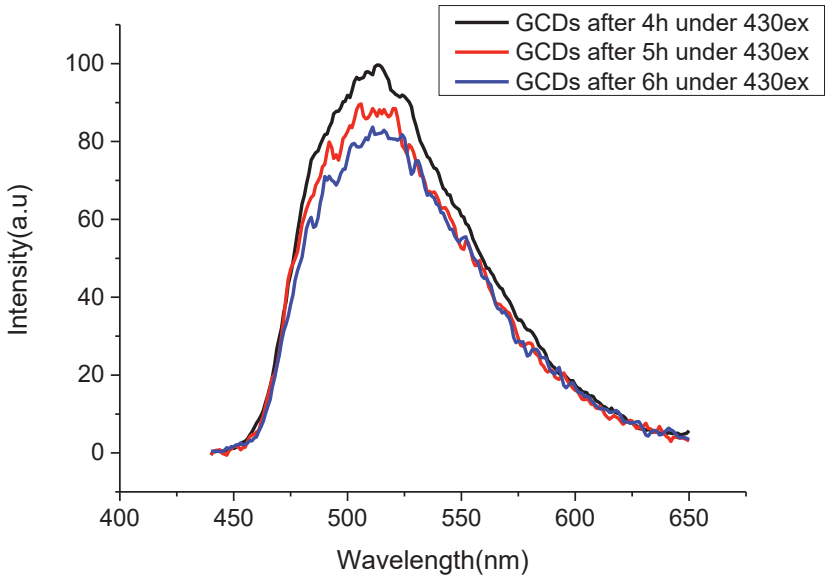

Figure 2.20. Emission spectra of prepared CDs under excited at 430 nm

2.2.4.3. Red Luminescent Experimental Results

First experimental procedure results, products of these 8 different synthesis experiments gave different pH values (Table 2.2), whose color varied from purple to red. Then each sample was diluted with water and all samples results were shown under UV-lamp in Figure 2.21. As a result, solvent effects on the reaction were observed.

a) b)

Figure 2.21. a) o-PD with HCL for 1,2 and o-PD with HNO_3 for 3,4 and b) p-PD with HCL for 5,6 and P-PD with HNO_3 for 7,8 samples, respectively under UV-Lamp

According to the article; HCL(50 µL) plays a vital role in the formation of red fluorescent CDs. And also, HNO_3 plays an important role in synthesizing red CDs. The UV-vis absorption spectrum of nitrogen-doped carbon dots (N-CDs) exhibits a characteristic band centered at 277 nm and two weak absorption peaks at 413 and 475 nm in the range of 410-630 nm because of π-π* transition of C=C bond, and n-π* transitions of C=N and C=O bonds. The UV-vis absorption spectrum of red emissive CDs exhibits at 400 nm and 500 nm but the PL intensity of these types of CDs has not the high quality of red emission was shown in Figure 2.22.

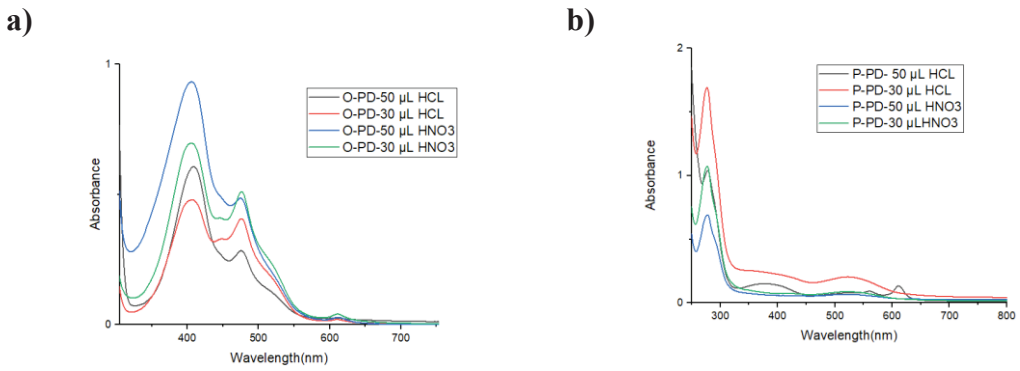

Figure 2.22. All UV- vis absorption spectrum of N-CDs for a)o-PDs and b)p-PDs

2.2.5. Conclusion

In this study, blue, green, and red emission and high-quality carbon dot nanoparticles were synthesized by using a hydrothermal method in an autoclave and two-necked bottom flask. Different kinds of carbon sources like citric acid, p-benzoquinone and o-PDs, p-PDs, and amine sources which names are ethylenediamine, urea, L-cystine, tartaric acid create a different color of CDs under UV-lamp. We want to synthesize high-quality blue luminescent carbon dots because it was easy to synthesize by using the hydrothermal method. Firstly, it was desired to achieve the best result by trying 2 synthesis methods for the synthesis of blue and green carbon dots, which are easy to synthesize. Using autoclave, materials are synthesized at a certain pressure and under a certain temperature, but when the pressure and temperature of the gas inside cannot be followed, this method is not given high-quality CDs. Therefore, the test results could not be optimized because the autoclave method used was not controllable for synthesizing process. After increasing only the amino modification for the synthesis of carbon dots, we had difficulty synthesizing the material in the green and red regions. Also, adding some functional groups, polymers, defects and state of edges was important for surface configuration. And solvent effects were important to act synthesizing high quality of CDs. After all, procedures choosing the best method and compounds to synthesize highly fluorescent CDs will mention in below side(2.3)

2.3. Synthesis of N,S-Carbon Dots, and Gold Nanoparticles

2.3.1. Experimental

2.3.1.1. Reagents

The Citric acid (99.9%), Dimethylformamide(99.9%), ethanol (99.8) %were purchased from Sigma –Aldrich. Thiourea (99.9%) were purchased from Alfa Easer.

2.3.1.2. Characterization of Carbon Dots

Firstly, Absorbance and Photoluminescence and quantum yields measurement by Edinburg FS5 Spectrophotometer (IYTE-MAM), Particle size measurement was measured by DLS (Malvern ZS-Zetasizer) (İYTE) SEM analysis SEM-EDS and High-Resolution SEM images analysis was measured by using FEI, QUANTA 250 FEG (İYTE MAM). XRD pattern was measured by Philips X'Pert Pro (IYTE MAM). The ultracentrifuged method was measured by OPTIMA MAX-XP (IYTE MAM). Lyophilization was used to obtain powder by using LABCONCO (IYTE). Also, Fourier Transforms Infrared Spectroscopy(FT-IR/PERKIN ELMER FRONTIER) was used.

2.3.1.3. Synthesis Method of N,S-Carbon Dots

Here, highly luminescent carbon dots in the visible region was synthesized. Two different types of methods were mentioned in this chapter. Firstly, all reaction was tried to synthesize by using autoclave, after reaction type was changed by using a two-nacked bottom flask.

2.3.1.4. Using Autoclave

All reaction was synthesized in a Teflon-lined autoclave at 160 ºC for 6h. This system was developed for an experimental procedure for hydrothermal reaction under constant pressure and heating the reaction by using an oil bath. But this system is not controllable for the synthesizing process. After the end of the reaction, a carbon dot can be obtained by using Teflon-autoclave. All reaction mechanisms were illustrated in Figure 2.23. and shows the reaction experimental apparatus Figure in 2.24.

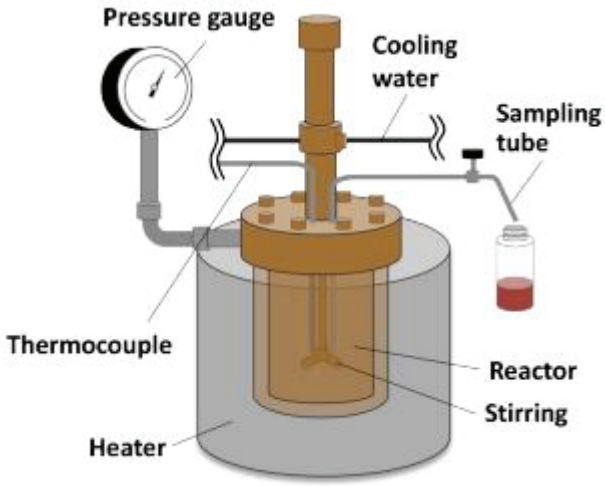

Figure 2.23. A schematic illustration of the reaction apparatus for Teflon-lined Autoclave

Figure 2.24. Images of a reaction mechanism

2.3.1.5. Two-Necked Round-Bottomed Flask

Firstly, thiourea and citric acid were mixed in DMF (20 mL) solution. And then, the mixture was transferred into a two-necked round-bottomed flask and heated at 160 °C. After 5 hours, 1 mL of sample was taken from the reaction. End of the 6 hours, the reaction was completed. After cooling room temperature, samples were imaged under UV-Lamp.

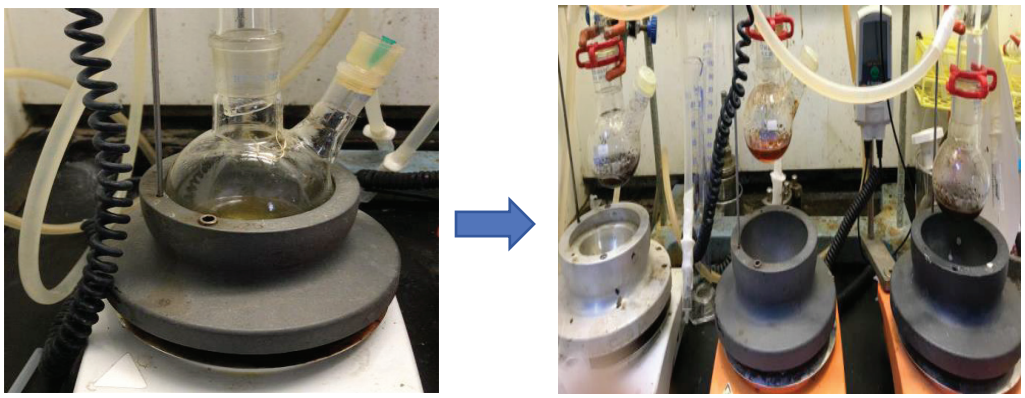

Figure 2.25. Reaction mechanism images of Two-Necked Round-Bottomed Flask

The second method is to synthesize carbon dot synthesis by using different parameters with another method which name is a two-nacked bottom flask. The weight of the 1:2 mixture is citric acid and thiourea. Then, 15 mL of DMF solvent was added to the solution and the reaction was stirred until a white solution was obtained. After all processes, the reaction was put into two nacked bottom flasks and heated under nitrogen gas and all mechanism was illustrated in Figure 2.26.a). And 4 hours of reaction, the reaction was allowed to cool. DMF was used in the synthesis of the reaction and we had difficulty in obtaining the material in powder form because the DMF boiling point was very high. First of all, we tried to remove the solvent as much as possible by attaching it to the rotary evaporator, then an oil vacuum was applied. The second method, the lyophilizer was applied after waiting for -80 °C in the freezer. However, solid material could not be obtained. This lyophilizer method was not suitable for solidifying high boiling point materials such as DMF DMSO, because the small amount of DMF remaining in it affects the strength of the vacuum. We tried to separate the carbon dot

points in the material by establishing the Colon Chromatography, but it was not preferred due to the use of too much solvent and the long process. As a result of all these, it has been contributed to the literature by applying the ultracentrifuge method to obtain the powder part from the solvent in high milliliters for half an hour at 40,000 rpm by diluting it with ethanol solvent. All reaction procedures was shown in Figure 2.26.b).

a)

b)

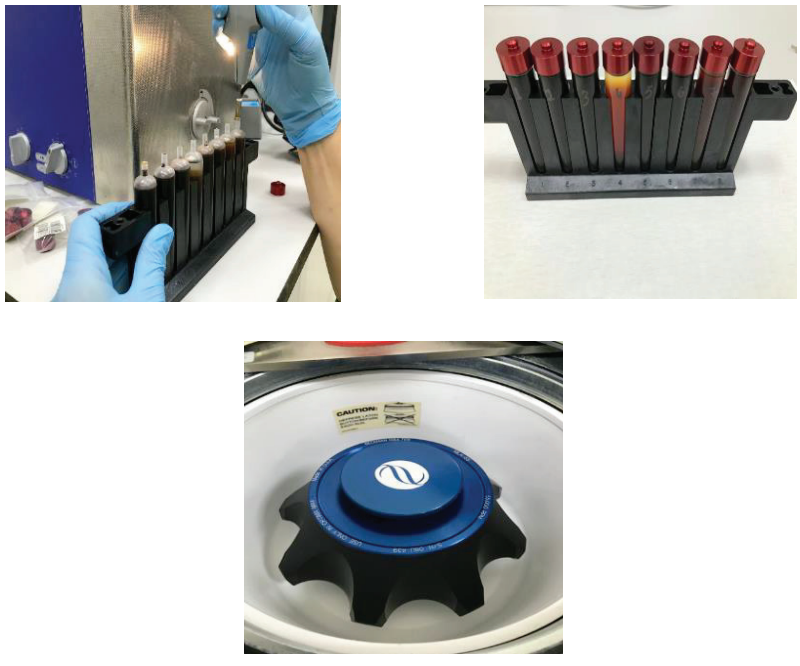

Figure 2.26. a) Systematic illustration for synthesizing N,S-CDs b) İmages of the reaction characterization set-up by using Ultra Centrifuged Method

2.4. Synthesis of Gold Nanoparticles (AuNPs)

2.4.1. Experimental

2.4.1.1. Reagents

Hydrogen tetrachloroaute (III) trihydrate HAuCl4.3H2O, 99%, sodium borohydride (NaBH4, 99%) used for synthesizing gold nanoparticles supplies by Sigma Aldrich. Ultrapure water was obtained from Millipore instrumentation.

2.4.1.2. Characterization for Gold Nanoparticles (AuNPs) Synthesis

Optical and Structural techniques were used to synthesize AuNPs. The spectrum of UV-Visible absorption was measured by using Varian Cary 50 UV-Visible Spectrometer and Edinburg FS5 Spectrophotometer. Dynamic Light Scattering (DLS, Malvern Zetasizer-ZS) was used to measure size distribution and zeta potential. Also, structural characterization of a particle was measured by using a field emission scanning electron microscope (FEI, QUANTA 250 FEG) for scanning electron microscopy (SEM) analysis.

2.4.1.3. Synthesis of 40 nm Gold Nanoparticles (AuNPs)

Turkevich's method was used to synthesize gold nanoparticles.[92] Also, trisodium citrate ($Na_3C_6H_5O_7$) is a reducing agent in an aqueous solution. 50 mL of water and 0.25 mM $HAuCl_4$ (Chloroauric Acid) were mixed into 100 mL of ballon and heated the temperature to approximately 120 ^oC on a hot plate by using a condenser system. 0.3 mL of trisodium citrate was added to the reaction after sea the boiling of water. And waiting 15 minutes, the reaction color was turned to a bright red solution. And the reaction was waited in the stirrer at 90 ^oC for 30 minutes to remain stable. AuNPs were obtained after centrifuging process (4000 rpm 10 minutes).

2.5. Result and Discussion

In this study, green to red emission carbon dot was preferred to synthesize because these types of carbon dots can be applicable for imaging. Citric acid, thiourea, and DMF solvent were used to synthesize high luminescent emission CDs. Firstly, N,S-CDs was synthesized by trying different reaction temperature rising from 160 ºC to 200 ºC and different method using an autoclave, and a two-nacked bottom flask.

2.5.1. Results of Autoclave Method

After obtaining results, the absorbance spectrum of the N,S-CDs was diluted in different solvents as shown in Figure 2.27. According to the absorption peak, optimum emission peaks exhibit at 350 nm, 500 nm and give a shoulder peak at 550 nm. And these peaks give the π–π* transition C=C band, while the n–π* transition gives the C=N band.

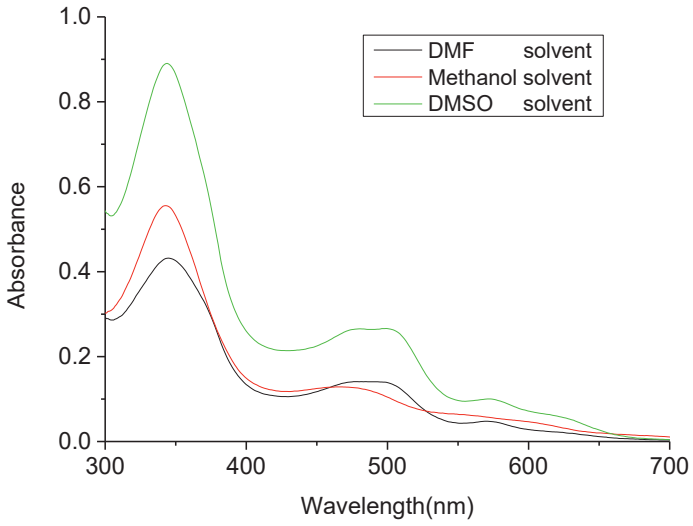

Figure 2.27. UV–vis absorption spectra of N,S-CDs in different solvent

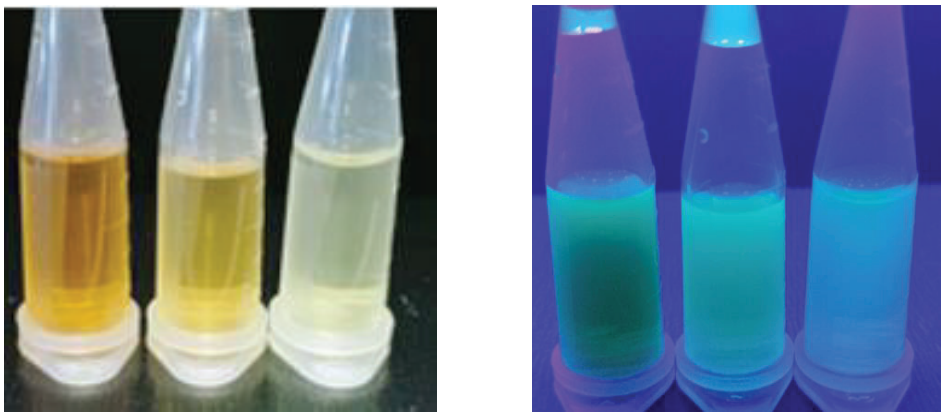

Figure 2.28. Reaction images of N,S-CDs in DMSO, DMF, and Methanol, respectively under daylight (left) and UV-Lamp (right)

According to Figure 2.29, when the solvent of the reaction was changed, the photoluminescent of spectra was shifted green to red emission of the spectrum. DMSO DMF and ethanol solvent were used to measure PL spectra. If the solvents are more polar, PL emission was shifted to the red emission range. Because spectrally, we can divide the shift in two ways as general solvation effect and specific solvation effect. The general solvation effect is the polarity change of the solvents, the specific solvation effect is due to the hydrogen bonds, internal charge transfer, probe-probe interactions between the probe and the solvents.

Hydrogen bonding in protic solvents is stronger than in aprotic solvents, thus giving larger spectral shifts and resulting in shorter fluorescence lifetimes. It is known that the photoluminescence (PL) property of carbon dots is dependent on the H bond effect. Carbon dots exhibit different emission ranges in protic and polar aprotic solvents and are known to form strong H bonds in these solvents. When DMSO solvent is added to the solution, nitrogen atoms on carbon dots form strong Hydrogen bonds with DMSO, shifting the emission energy level and spectral shift to red.

a)

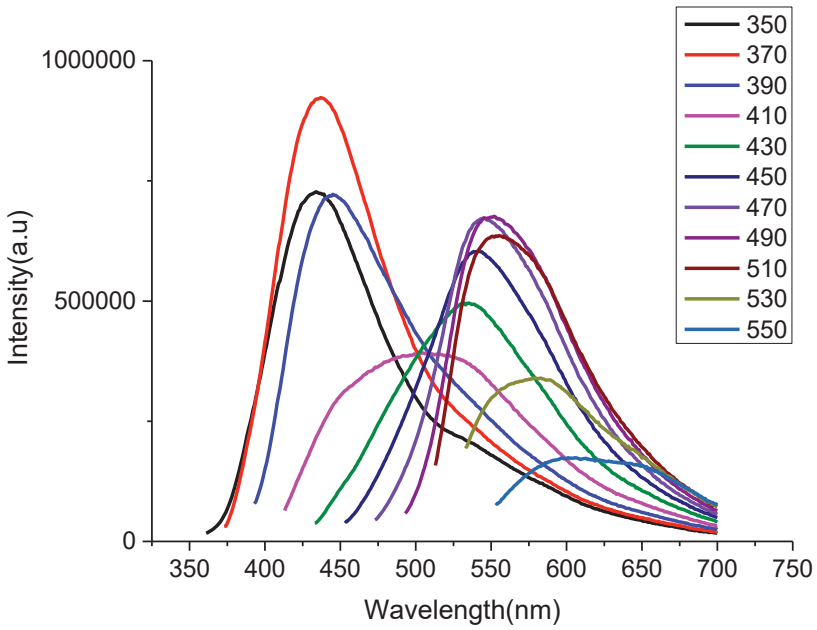

b)

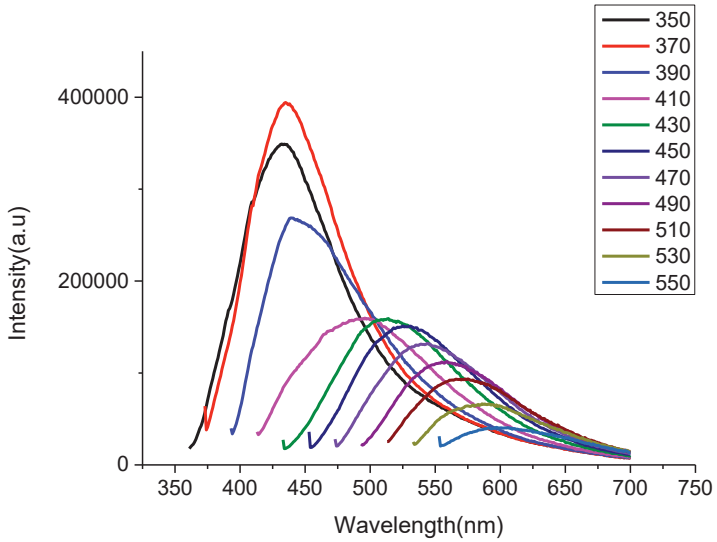

Figure 2.29. Photoluminescence Spectra of N,S-CDs in a)DMSO b)DMF with an excitation wavelength of 350 to 550 nm

Photoluminescence lifetime is another optical parameter for CD synthesizing were measured by using Time-correlated single-photon counting (TCSPC) system in different

solvents. These obtaining CDs decay curve excitation with 450 nm laser is shown in Figure 2.30. It is known that in excited states, 3 different photophysical processes occur and these carbon dots have 3 different decay times. These findings show that at the excited states, three separate photophysical processes take place. The fastest decay time is 11 ns with 50% contribution, the slowest decay is 1 ns with 11% contribution in DMSO solution. Another is the fastest decay time is 10 ns with 60% contribution, the slowest decay is 0.7 ns with 4.7% contribution in DMF solution as shown in Table 2.3. In particular, the proportion of τ1 declined from 1.05 to 0.76 percent, while the proportion of τ3 grew from 50.05 to 60.93 percent, showing that the carbon core's contribution to N-Cdot emission reduced with time, whereas surface states such as function groups became increasingly.

Table 2.3. The lifetime values and relative percentages of each process for carbon dot synthesized

Sample	**τ_1 (ns)**	**% Rel_1**	**τ_2 (ns)**	**% Rel_2**	**τ_3 (ns)**	**% Rel_3**	**$\tau_{average}$ (ns)**	**χ^2**
DMSO	1.05	11.72	3.36	38.23	11.32	50.05	8.25	0.949
DMF	0.76	4.75	3.95	34.32	10.62	60.93	9.42	1.049

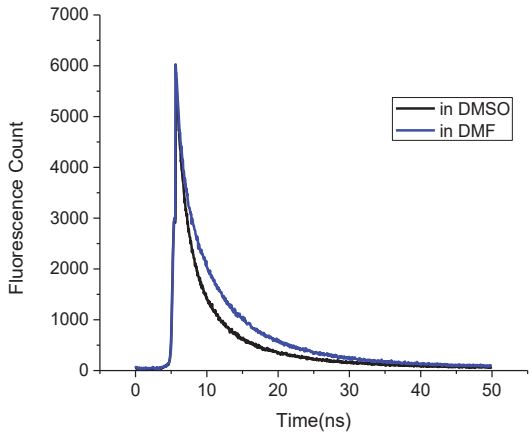

Figure 2.30. A lifetime of N, S-CDs in DMSO and DMF

2.5.2. Results of Two-necked Bottom Flask

And all solution was diluted with DMF and the UV absorption spectrum was shown in Figure 2.31. In here, best timing analyzed for synthesizing process.

a)

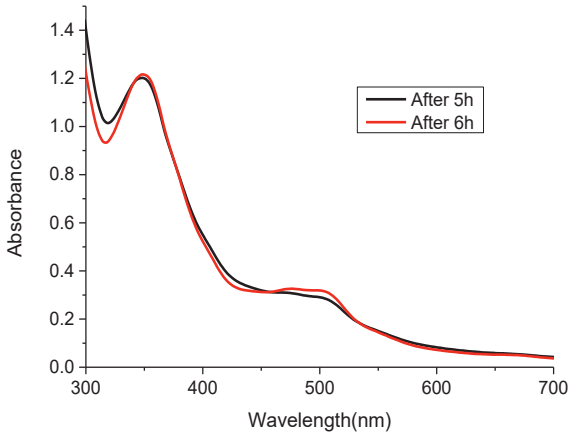

b)

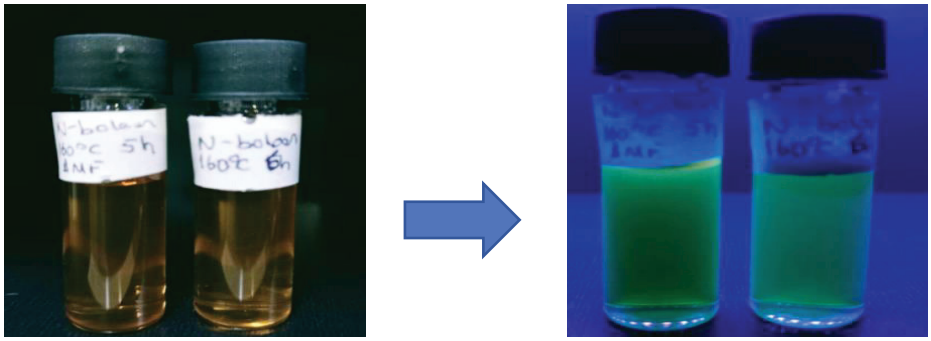

Figure 2.31. UV–vis absorption spectra of N, S-CDs in different time at 5h and 6h and reaction images under daylight(left) and UV-Lamp(right) for 5h(left) and 6h(right)

As a result of carbon dot synthesis prepared at different time intervals, it was observed that the emission wavelength of the sample shifted to the right when the excitation wavelengths between 350 and 520 nm were changed as shown in Figure 2.32 and Figure 2. 33. When the excitation is at 400 nm, the maximum emission peak is at 500 nm.

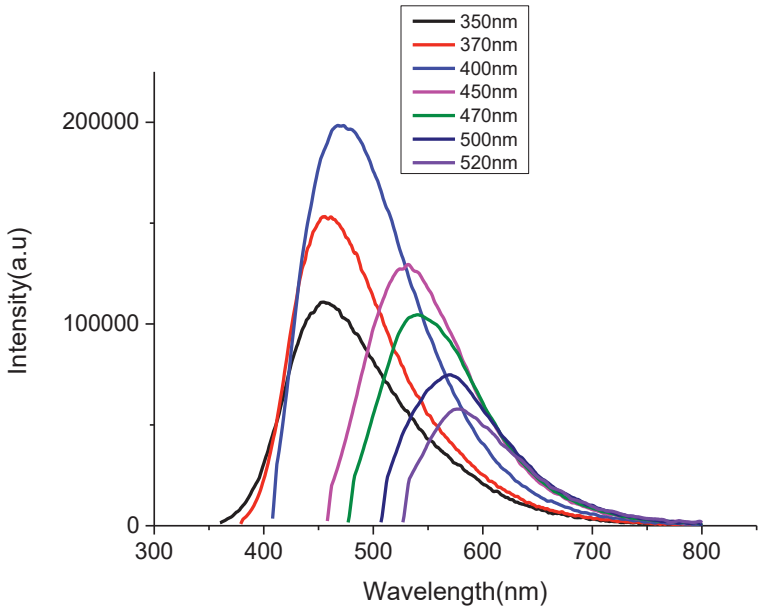

Figure 2.32. Fluorescence emission spectra of N,S-CDs for 5h with the excitation wavelength of 350 to 520 nm

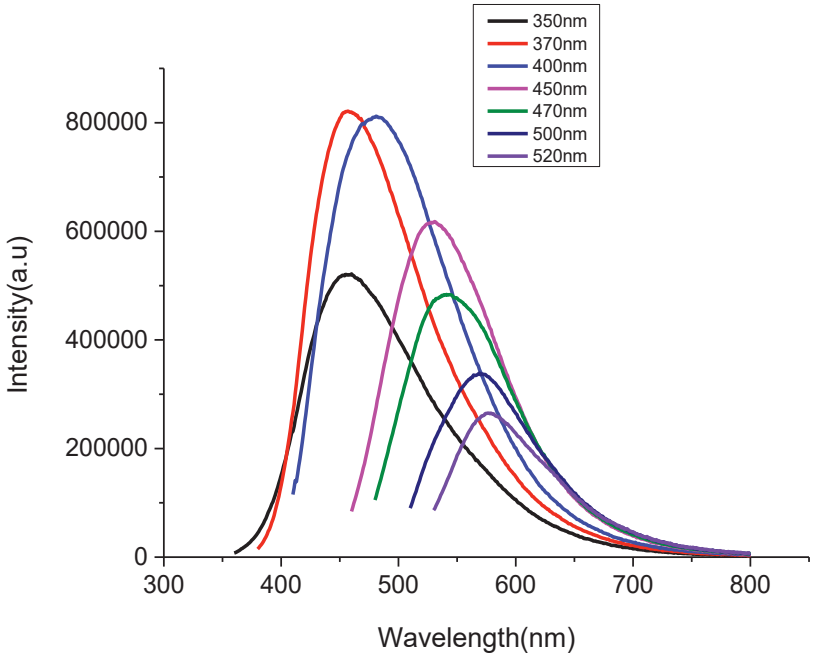

Figure 2.33. Fluorescence emission spectra of N,S-CDs for 6h with the excitation wavelength of 350 to 520 nm

The emission spectrum of CDs of a DMF solution was shown top-side for 5 and 6 hours. According to the article[93] ; At 300 nm to 500 nm as excitation wavelength, the CDs show maximum emission gradually increases from 375 nm to 590 nm. Here, when exciting the CDs with 350, 370, 400, 450, 470, 500, and 520 nm, the emission peak was shifted from 450 to 600 nm as shown in Figure 2.32 and Figure 2.33. Also, all excitation-emission and quantum yield was shown in Table 2.4 and Table 2.5. According to these results, 20 mL solvent was used and time was stable at 160 ºC. As a result of the time-dependent increase, the quantum yield increased slightly. İncreasing the excitation wavelength from 350 to 520 nm, the emission peak red shifted from 450 to 600 nm

Table 2.4. All Quantum yields of CDs in different excitation, emission wavelength for 5h

CDs	Quantum Yield (%)	Excitation Wavelength (nm)	PL Emission Peak(nm)	Time (hours)
1	2.83	350	455	5
2	4.76	370	458	5
3	10.2	400	473	5
4	16.7	450	531	5
5	19.3	470	540	5
6	10.5	500	571	5
7	9.1	520	578	5

Table 2.5. All Quantum yields of CDs in different excitation, emission wavelength for 6h

CDs	Quantum Yield (%)	Excitation Wavelength (nm)	PL Emission Peak(nm)	Time(h)
1	3.57	350	456	6
2	5.77	370	459	6
3	12.2	400	478	6
4	21.5	450	530	6
5	23.6	470	540	6
6	11.4	500	571	6
7	9.12	520	581	6

Figure 2.34 shows time-resolved PL decay curves to further investigate the impacts of surface states and intrinsic states. The recombination activity in the carbon core after 5 h expression is attributed to a short-lived τ1 component with a lifetime of about 1.17 ns, while the recombination process at the surface is attributed to a long-lived τ3 component with a lifetime of about 12.58 ns. Another recombination activity in the carbon core at the end of the 6 h synthesis process is attributed to a short-lived τ1 component with a lifetime of about 0.76 ns, further the recombination process at the surface is attributed to a long-lived τ3 component with a lifetime of about 11.79 ns. All results are shown in Table 2.6. The weighted average PL lifetime is estimated to be 10.32 ns for 5h and 9.87 ns for 6h.

Table 2.6. The lifetime values and relative percentages of each process for carbon dot synthesized for 5h and 6h

Sample	**τ_1 (ns)**	**% Rel_1**	**τ_2 (ns)**	**% Rel_2**	**τ_3 (ns)**	**% Rel_3**	**$\tau_{average}$ (ns)**	**χ^2**
5h	1.17	6.65	4.59	48.01	12.58	45.35	10.32	1.093
6h	0.76	3.92	4.15	46.2	11.79	49.88	9.87	1.007

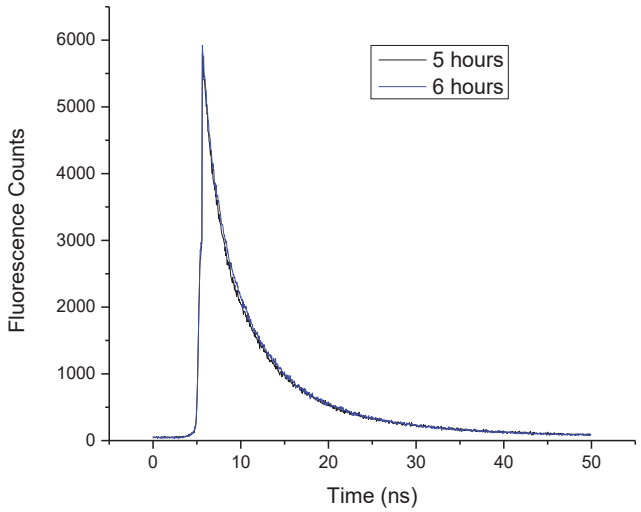

Figure 2.34. The lifetime of N,S-CDs for 5h and 6h in DMF

Also, the same procedure was repeated by using the different volumes of DMF solvent. 4.0 g of thiourea and 2.0 g of citric acid were mixed in 15 mL and 20 mL of DMF solution. And then, the mixture was transferred into a 100 mL two-necked round-bottomed flask and heated at 240°C for 4h under Nitrogen gas. After 4 hours, the reaction was complete and the reaction was left at room temperature until it had cooled. The UV-absorption spectrum of samples exhibited three absorption peaks at 347 nm, 451 nm, and give a shoulder peak at 502 nm for DMF at 240 °C for CDs solution as shown in Figure 2.36. And all reaction images was shown in Figure 2.35.

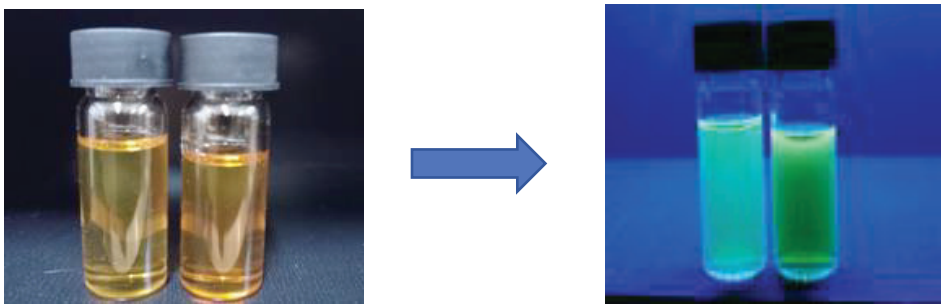

Figure 2.35. Reaction images for CDs sthesis by using 20 mL(left) and 15 mL (right) under UV light

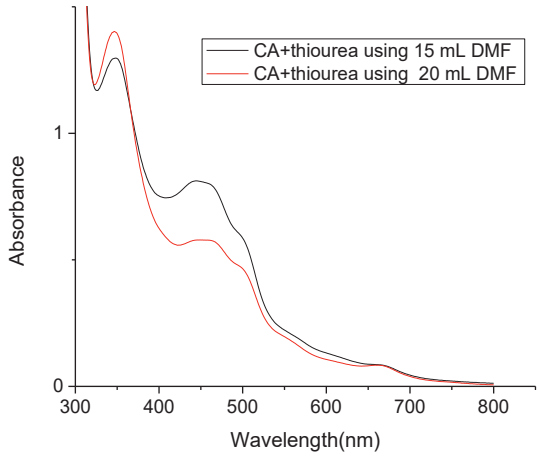

Figure 2.36. The UV-vis absorption spectrum of N,S-CDs for 15 mL and 20 mL DMF solution

CDs solution of PL spectra was shown in Figure 2.37 and Figure 2.38 where is changeable of emission wavelength when changed the exciting wavelength of 350 to 500 nm. The maximum emission wavelength of CDs solution is 540 nm. Its difference from

other carbon dot synthesis is that it takes place at high temperatures. When using high temperature and 15 mL of DMF solution, the photoluminescence emission intensity increased compared to the other procedure. According to these results, the quantum yield was estimated as 17.9% for preparing 15 mL of DMF solution also, the quantum yield was estimated as 18.4% for preparing 20 mL of DMF solution in the same concentration as shown in Table 2.7. There are no big differences in the quantum yield of these results.

Table 2. 7. Table of estimated QY for carbon dots using 15 mL and 20 mL of DMF solvent

CDS	QY (%)	Excitation Wavelength (nm)	PL Emission peak (nm)	Time (h)	Figures
15 mL DMF solvent	17.9	470	550	4	Figure 2.37
20 mL DMF solvent	18.4	470	550	4	Figure 2.38

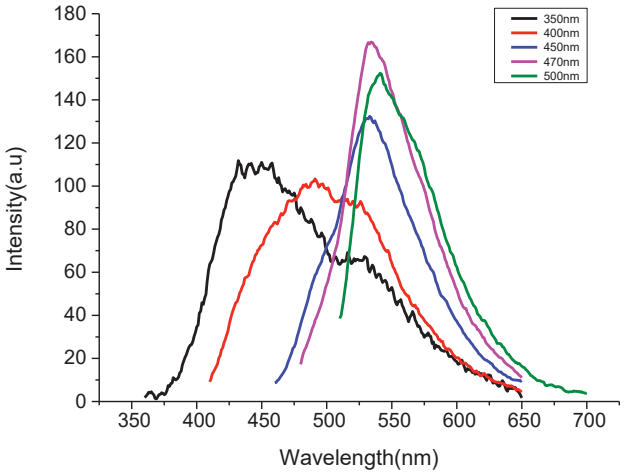

Figure 2.37. Fluorescence emission spectra of N,S-CDs for 4h with the excitation wavelength of 350 to 500 nm in 15 mL DMF at 240 °C

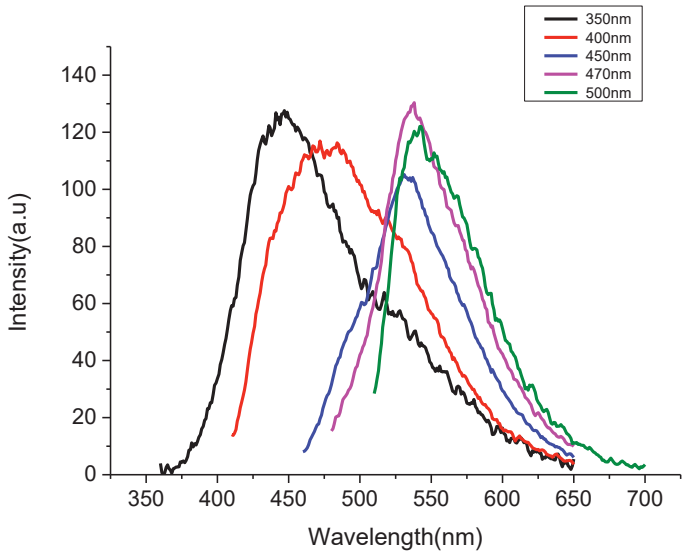

Figure 2.38. Fluorescence emission spectra of N,S-CDs for 4h with the excitation wavelength of 350 to 500 nm in 20 mL DMF at 240 ºC

In the light of all these studies, we were able to synthesize N,S CDs that emit photoluminescence in the blue-green region, but we were able to synthesize these carbon dots with AuNPs to increase the emission intensity.

Second experimental results, the same optical and structural characterization method was applied for observing only N,S-CDs synthesis by using powder after characterization process. Thiourea and citric acid were mixed in DMF (15 mL) solution. After centrifuging process, powder solution was obtained and all solution was diluted with DMF and UV absorption spectrum was shown as Figure 2.39 by using Edinburg FS5 Spectrophotometer. According to the absorption peak, optimum emission peaks exhibit at 350 nm and give a shoulder peak at 470 and 500 nm. And these peaks relevant to the π–π* transition gives the C=C band, while the n–π* transition gives the C=N band. Reaction images were shown in Figure 2.40 demonstrating that green-luminescent was obtained.

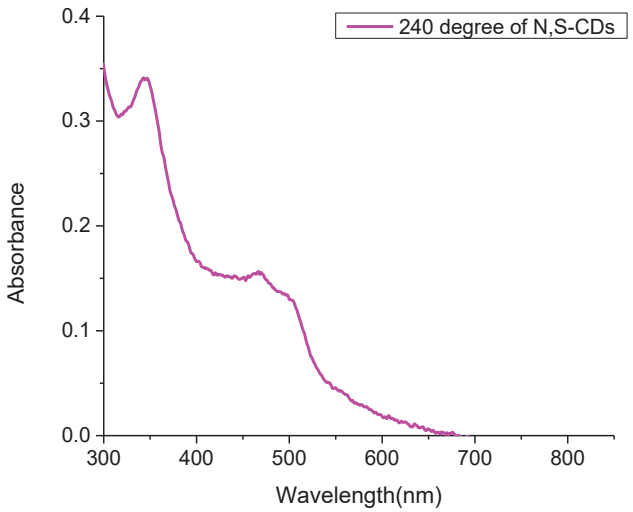

Figure 2.39. UV-visible absorption spectrum for N,S-CDs

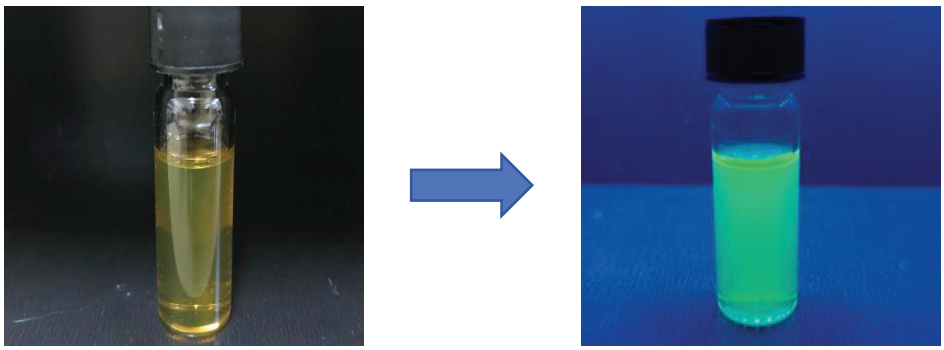

Figure 2.40. Reaction images for N,S-CDs synthesis at 240 °C

CDs solution of PL spectra was shown in Figure 2.41 where is changeable of emission wavelength when changed the exciting wavelength of 300 to 550 nm. The maximum emission wavelength of CDs solution is 530 nm. The QY yield of reaction was estimaed as %14.2.

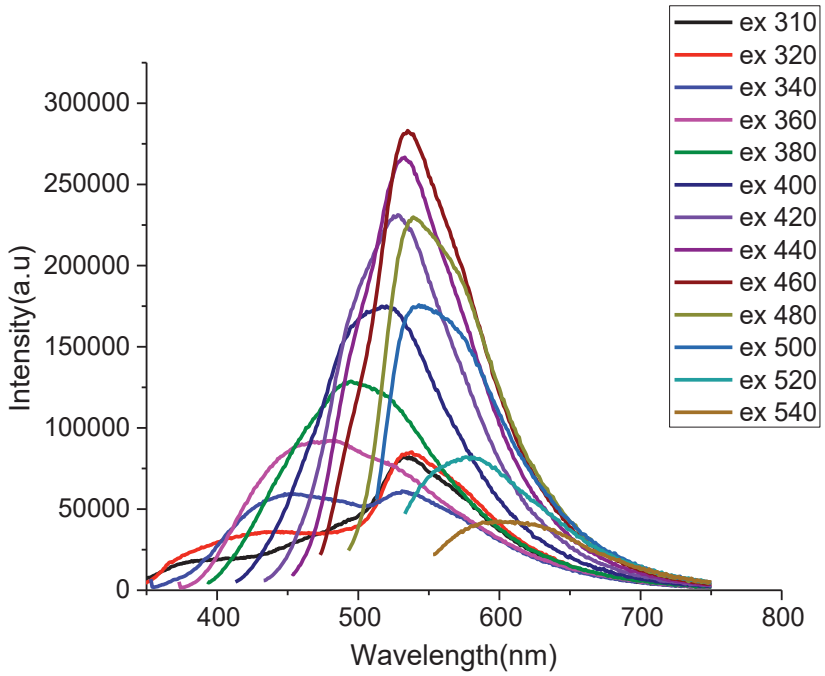

Figure 2.41. Fluorescence emission spectra of N,S-CDs for 4h with the excitation wavelength of 300 to 550 nm in 15 mL DMF at 240 ºC

2.5.3. Gold nanoparticle (AuNPs) Synthesis

In this study, firstly AuNPs were synthesized with the combination of N,S-CDs solution. The reaction was adjusted by trying different concentrations of AuNPs. The formation of the AuNPs was measured by using absorption spectroscopy and DLS measurements. This particle size and surface potential were measured and as found as -40 mV, -30 mV. And all procedure formation of the spherical sphere of particle images was supported by using SEM measurement. Optical characterizations of the synthesized gold nanoparticles were measured using the UV vis spectrophotometer, utilizing its distinctiveness by showing a specific peak centered around 510 nm to 540 nm. Figure 2.42 shows the optical and structural characterization of AuNPs produced by the interaction of $HAuCl_4$ with $NaBH_4$ in water under ambient conditions. According to this graph, The UV-absorption spectrum of samples exhibited at 540 nm. All these conditions were supported by using DLS measurements and a Scanning electrın microscope (SEM).

The surface potential of particles was estimated as -37 mV and -22.0 mV. These results were supported by using SEM measurements as shown in Figure 2.43.

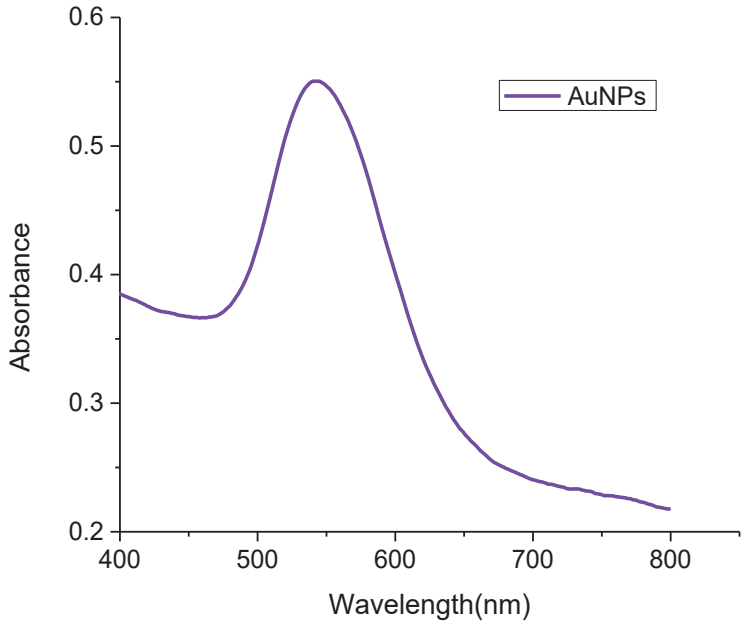

Figure 2.42. UV-visible spectrum for 40 nm of gold nanoparticles

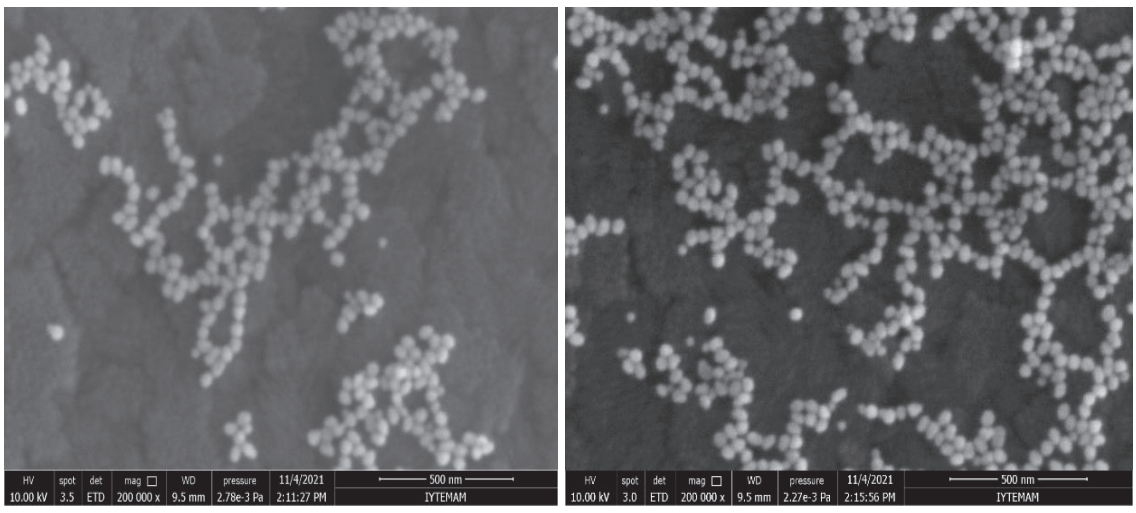

Figure 2.43. SEM images for 40 nm gold nanoparticles (AuNPs)

CHAPTER 3

SYNTHESIS AND CHARACTERIZATION OF CARBON DOTS WITH GOLD NANOPARTICLE

3.1. Introduction

Carbon dots are designed to improve the adsorption capacity and catalytic activity of gold nanoparticles (AuNPs) thanks to some functional groups such as –OH, –COOH, C=O on their surface**.** There are many different ways to synthesize carbon dot reactions with gold nanoparticles. According to Liu et al, [94] using sodium hydroxide and polyethylene glycol (PEG-200) were able to synthesize CDs using the reflux method at 6h for 120 ºC. After producing carbon dot solution, gold nanoparticle was synthesized. When all process was completed, two reactions were mixed under room temperature. According to this article, AuNPs was surrounded by carbon dot.

Zheng et al,[95] succeeded in synthesizing carbon dots at 150 ºC by microwave method by using citric and urea. After this procedure, gold nanoparticles are synthesis when the addition of carbon dot solution. In this synthesis, while the gold nanoparticles were being synthesized, the synthesized carbon dot solution was added to the medium, and AuNPs@CDs nanocomposites were synthesized in sodium polyacrylate-$HAuCl_4$. According to this article, carbon dots were used as conventional reducing agents and acted as both electron donors and acceptors. However, the sem images of the study showed that carbon dots were attached around the gold nanoparticles. Considering the PL emission peak of this article, the emission intensity of AuNPs-CDs at 524 nm is quite low. This is because, during the formation of AuNPs-CDs, electrons are transferred from the shell of the carbon dots to the core of the gold nanoparticle.

Song et al,[96] synthesized carbon quantum dots with emission at 300 nm by heating a solution of chitosan and acetic acid by hydrothermal way to 180 ºC for 12 hours. After gold nanoparticles and CQDs were mixed after synthesizing process was done. In addition, the CQDs/AuNPs combination was employed in a colorimetric technique to detect iodine ions.

Zhu et al,[97] reported that gold-effect catalysts were used to reduce 4-aminophenol (4-NP). According to this article, 4-NP is a p-rich molecule in nature. The catalytic activity of metal nanoparticles for the reduction of 4-NP to 4-AP was effectively enhanced by $NaBH_4$. High decoration of carbon dots by the catalytic activity of AuNPs can be enhanced for 4-NP reduction. The room-temperature in situ carbonization of cetylpyridinium chloride monohydrate (CPC) pre-adsorbed on AuNPs as an organic ligand has been presented as a practical and straightforward approach for synthesizing CD-decorated AuNPs (AuNPs/CDs). A nanocomposite of AuNPs/CDs was synthesized by carbonization at room conditions, while CPC acted as a capping agent for gold nanoparticles.

In all these literature summaries, we want to synthesize gold nanoparticles with carbon dot solution. Firstly AuNPs were synthesized. After carbon dot synthesis was carried out in the presence of gold nanoparticles. Unlike the literature, no addition could be made while synthesizing gold, and carbon dot and gold nanoparticle were synthesized not separately and not reacted again. Because the literature summary showed that materials to act as an linker were used to synthesize gold nanoparticles and carbon together. Our goal is to generate the high photoluminescence emission of carbon dot synthesis in the presence of gold nanoparticles.

3.2. Experimental

3.2.1. Reagents

The Citric acid (99.9%), Dimethylformamide(99.9%) %were purchased from Sigma –Aldrich. Thiourea (99.9%) were purchased from Alfa Easer. Hydrogen tetrachloroaute (III) trihydrate HAuCl4.3H2O, 99%, sodium borohydride (NaBH4, 99%) used for synthesizing gold nanoparticles supplies by Sigma Aldrich. Ultrapure water was obtained from Millipore instrumentation.

3.2.2. Characterization

Optical and Structural techniques were used to synthesize AuNPs. The spectrum of absorption and photoluminescence spectra was measured by using Varian Cary 50 UV-Visible Spectrometer, Varian Cary Eclipse Fluorescence Spectrometer and Edinburg FS5 Spectrophotometer. XRD pattern was measured by Philips X'Pert Pro (IYTE MAM). The ultracentrifuged method was measured by OPTIMA MAX-XP (IYTE MAM). Fourier Transforms Infrared Spectroscopy(FT-IR/PERKIN ELMER FRONTIER) was used. Also, structural characterization of a particle was measured by using a field emission scanning electron microscope (FEI, QUANTA 250 FEG) for scanning electron microscopy (SEM) analysis.

3.2.3. Synthesizing N,S-CDs in the presence of AuNPs

Firstly, By applying the gold nanoparticle precipitation process, the concentration amounts added to the solution from the absorbance value were adjusted. 4.0 g of thiourea and 2.0 g of citric acid were mixed in 15 mL of DMF solution. After number of AuNPs per volumes were added to the solution. And then, the mixture was transferred into a 100 mL two-necked round-bottomed flask and heated at 240°C for 4h under Nitrogen gas.

Table 3.1. Table of Experimental Data for CDs with AuNPs (Number of AuNPs is represented for a given volume of AuNPs)

Number	Citric acid (mmol)	Thiourea (mmol)	DMF (L)	Number of AuNPs/mL	Temperature (°C)
1	10	50	0.015	$2.5x10^{9}$	240
2	10	50	0.015	$5.0x10^{9}$	240
3	10	50	0.015	$1.0x10^{10}$	240

In the second experiment, the concentration amounts were kept constant and different microliters of AuNPs were added to the solution. These AuNPs were observed to bind to carbon dots when the microliter of AuNPs solution was changed.

Table 3.2. Table of Experimental Data for CDs with AuNPs (Number of AuNPs is represented for a given volume of AuNPs)

Number	Citric acid (mmol)	Thiourea (mmol)	DMF (L)	Number of AuNPs/mL	Temperature (°C)
4	10	50	0.015	$3.5x10^{9}$	240
5	10	50	0.015	$5.8x10^{9}$	240
6	10	50	0.015	$1.06x10^{10}$	240
7	10	50	0.015	$1.7x10^{10}$	240

3.3. Result and Discussion

3.3.1. Synthesizing N,S-CDs in the presence of AuNPs with for using Table 3.1

The absorbance graph of the material synthesized using the data Table 3.1, which is the result of the combination of AuNPs and N,S-CDs is given in Figure 3.1. According to the absorption peak, optimum emission peaks exhibit at 350 nm, 470 nm and give a shoulder peak at 500 nm. And these peaks give the π–π* transition C=C band, while the n–π* transition gives the C=N band.

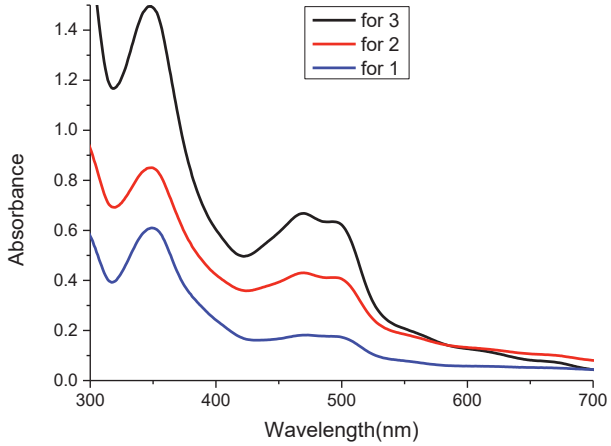

.

Figure 3.1. UV-visible Absorption Spectrum for N,S-CDs synthesizing in the presence of AuNPs

The different concentrations of AuNPs and N,S-CDs were mixed to obtain gold nanoparticles with N,S-CDs while other reaction conditions were kept constant as shown in Table 3.1. As the concentrations increase from 0.05 to 0.1, the photoluminescence intensity increases at the emission peak at 550 nm. The maximum emission wavelength of the CDs solution is changeable from 450 nm to 550 nm when changed the exciting wavelength of 350 to 500 nm. All PL emission peak was observed in Figure 3.2 a)-c) by using Varian Cary Eclipse fluorescence spectrometers. AuNPs with CDs synthesis of quantum yields were estimated and shown in Table 3.3.

Table 3.3. All quantum yields for synthesizing N,S-CDs in the presence of AuNPs for the first synthesis

Number	Number of AuNPs/mL	QY (%)	Excitation Wavelength (nm)	PL Emission wavelength (nm)	Figures
1	$2.5x10^9$	18.7	470	535	Figure 3.2 a)
2	$5.0x10^9$	21.3	470	535	Figure 3.2 b)
3	$1.0x10^{10}$	31.2	470	537	Figure 3.2 c)

a)

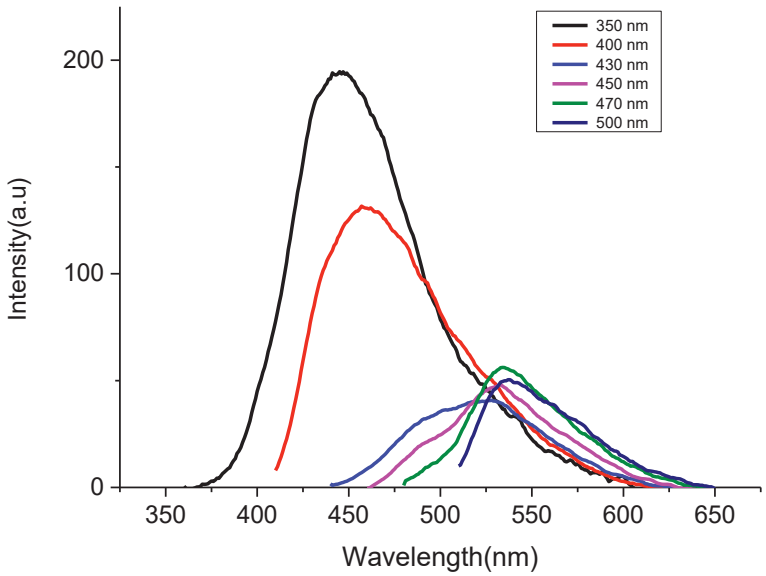
350 nm
400 nm
430 nm
450 nm
470 nm
500 nm
Intensity(a.u)
200
100
0
350
400
450
500
550
600
650
Wavelength(nm)

b)

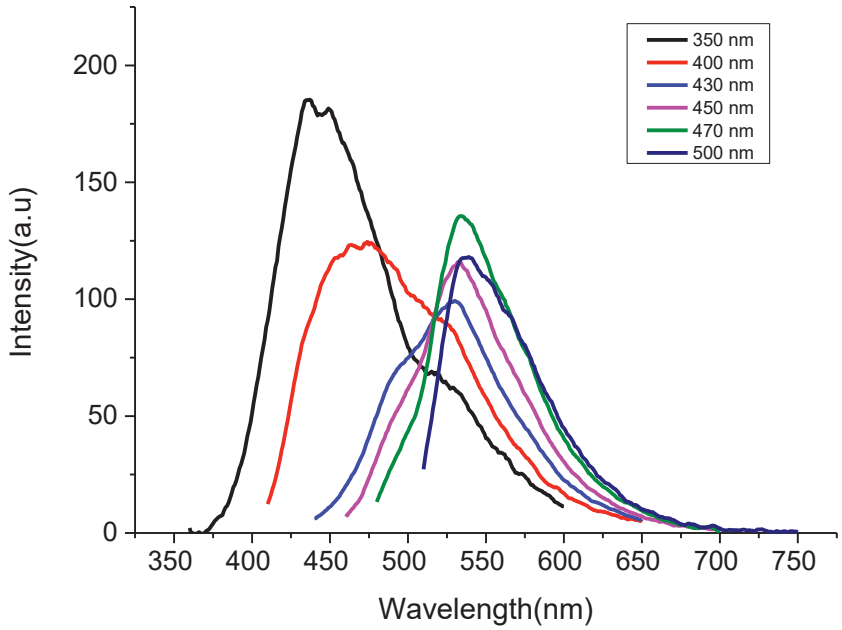
350 nm
400 nm
430 nm
450 nm
470 nm
500 nm
Intensity(a.u)
200
150
100
50
0
350
400
450
500
550
600
650
700
750
Wavelength(nm)

c)

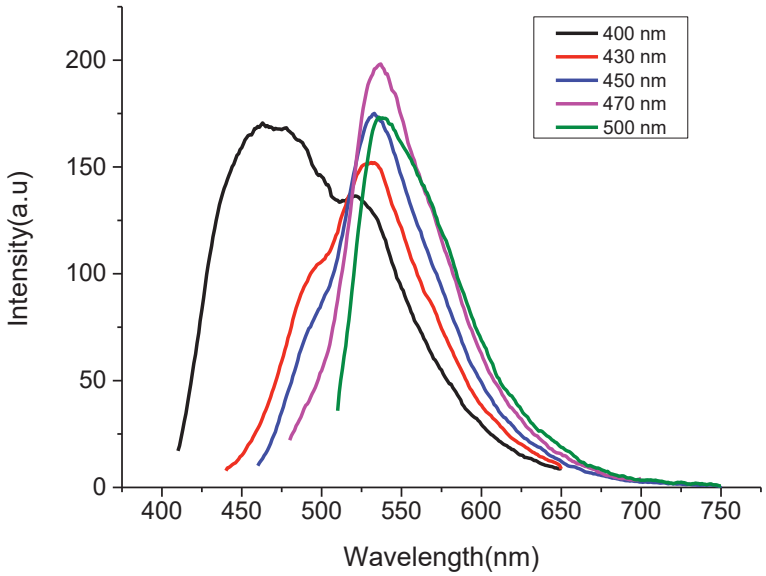

Figure 3.2. Fluorescence emission spectra of CDs for 4h with the excitation wavelength of 300 to 550 nm in 15 mL DMF at 240 °C with different amounts of AuNPs a)1.5x10^{10}AuNPs/mL b)1.9x10^{10}AuNPs/mL c)3.0x10^{10} AuNPs/mL

After all reaction images were shown in Figure 3.3 under day-light (left) and UV-Lamp.

Figure 3.3. AuNPs with CDs solution under day-light (left) and UV-Lamp for 3.0x10^{10} AuNPs/mL, 1.9x10^{10} AuNPs/mL, 1.5x10^{10} AuNPs/mL from left to right

3.3.2. Synthesizing N,S-CDs in the presence of AuNPs for using Table

The absorbance graph of the material synthesized using the data Table 3.2, which is the result of the combination of AuNPs and N,S-CDs is given in Figure 3.4. In the N,S-CDs solution prepared with 250, 330, and 400 microliters of AuNPs, the absorbance points are given at 350 and 400 nm and short shoulder peak at 500 nm. If 970 microliters AuNPs were added and the concentration is kept at 0.1 mol, as a result of increasing concentration, the emission at 350 nm increases, while other peaks were disappeared. Also, The black absorbance spectrum given in Figure 3.4 is the absorbance spectrum given in Figure 2.42.

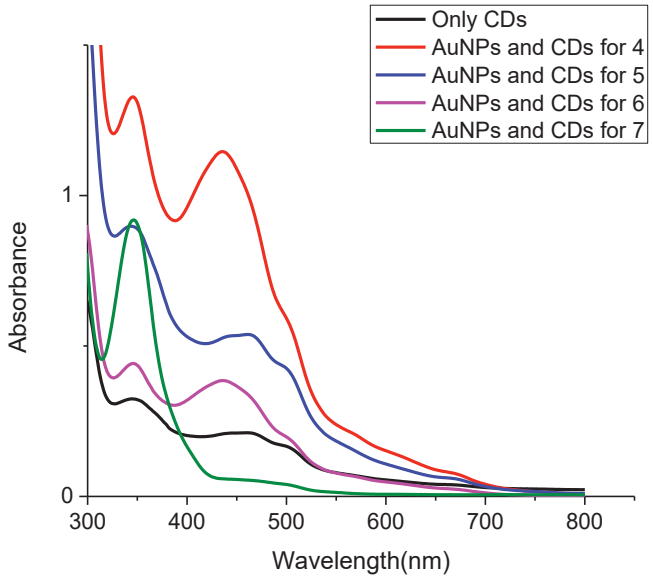

Figure 3.4. UV-visible Absorption Spectrum for all reactions

The maximum emission wavelength of the CDs solution is changeable when changed the exciting wavelength of 350 to 500 nm for using different microliters of AuNPs. 200 microliters of AuNPs of PL emission peak were observed at 550 nm when excited at 470nm (Figure 3.5 b). However, in carbon dot synthesis prepared with 970 microliters of AuNPs, emission peaks are observed at 400 nm when excited at 460 nm as shown in Figure.3.5d). All spectrum was measured by Varian Cary Eclipse Fluorescence Spectrometer. Also, reaction images were shown in Figure 3.6 under visible and UV-irradiation. AuNPs with CDs synthesis of quantum yields were estimated and shown in

Table 3.4 for each excitation peak. When $3.5x10^9$ number of gold nanoparticle was added into the solution, the quantum efficiency was calculated as 3.0% at 450 nm. When $1.7x10^{10}$ number of gold nanoparticle was used, the quantum efficiency was calculated as 66.00% at 450 nm. However, when $3.5x10^9$ number of gold nanoparticle was used, the quantum efficiency was calculated as 14.0% at 550 nm. When $1.7x10^{10}$ number of gold nanoparticle is used, the quantum efficiency cannot be calculated at 550 nm.

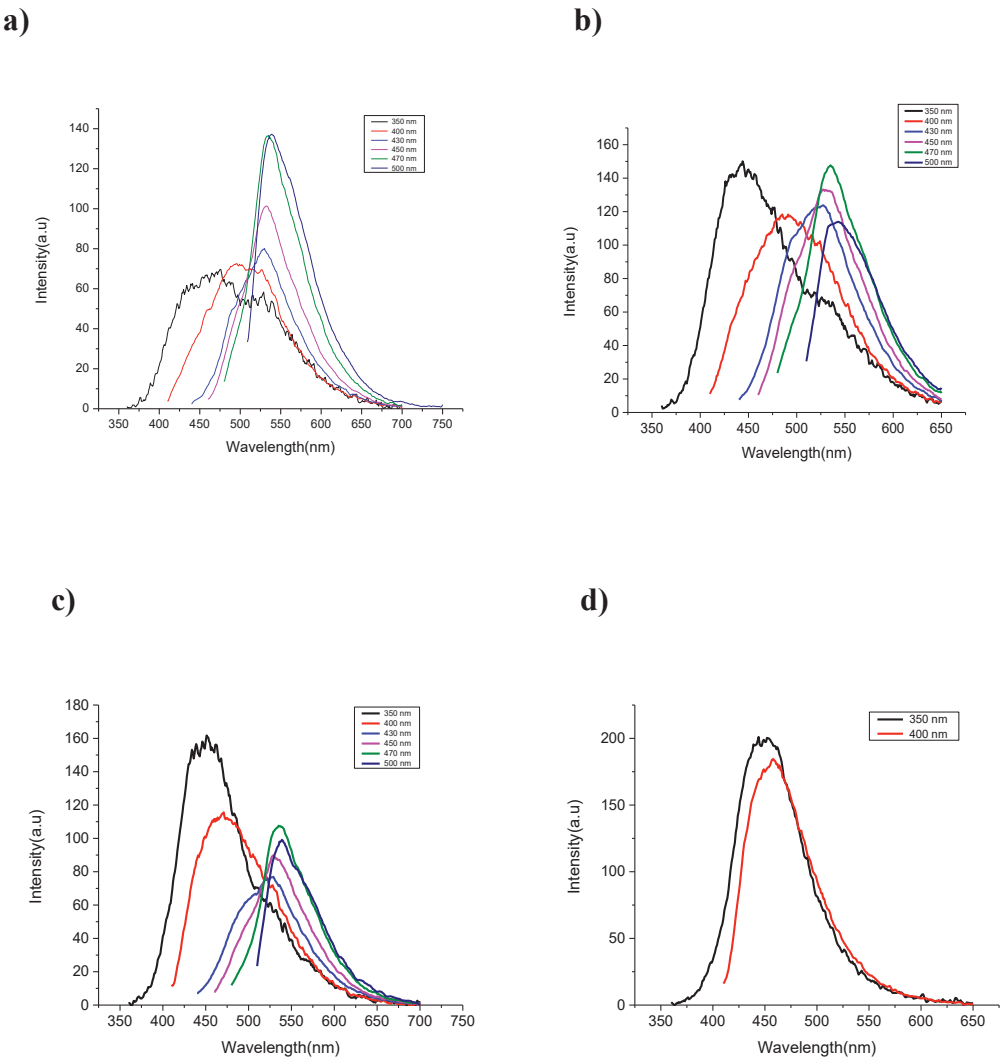

Figure 3.5. Fluorescence emission spectra of CDs for 4h with the excitation wavelength of 300 to 550 nm in 15 mL DMF at 240 °C with different amounts of AuNPs a)$1.5x10^{10}$ AuNPs/mL b)$2.5x10^{10}$ AuNPs/mL and c)$3.0x10^{10}$ AuNPs/mL d) $7.4x10^{10}$ AuNPs/mL

Table 3.4. All quantum yields for synthesizing N,S-CDs in the presence of AuNPs for the second synthesis

Number	Number of AuNPs/mL	QY (%)	Excitation Wavelength (nm)	PL Emission peak(nm)	Time (h)	Figures
4	$3.5x10^9$	3	350	460	4	Figure 3.5 a)
		14.9	470	537		
5	$5.8x10^9$	6	350	443	4	Figure 3.5 b)
		23.8	470	535		
6	$1.06x10^{10}$	14.5	350	450	4	Figure 3.5 c)
		37	470	537		
7	$1.7x10^{10}$	66.4	350	450	4	Figure 3.5 d)

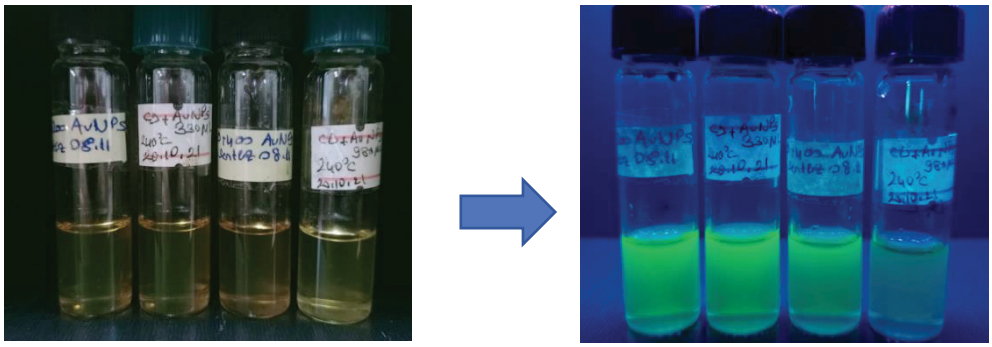

Figure 3.6. Reaction images for AuNPs with N,S-CDs under visible and UV-irradiation for $1.5x10^{10}$ AuNPs/mL, $2.5x10^{10}$ AuNPs/mL, $3.0x10^{10}$ AuNPs/mL, $7.4x10^{10}$ AuNPs/mL from left to right

3.3.3. Synthesizing AuNPs with N,S-CDs for High QY of CDs

After the synthesis of gold nanoparticles with N,S-CDs with high photoluminescence intensity, it was solidified after the characterization process applied to the material. The resulting material was dissolved in DMF and absorbance and PL emission were measured using Edinburgh FS5 Spectrophotometer. According to literature, do not obtain direct synthesis without linkers. According to Figure 3.7, UV-visible absorption spectra of 350 nm, 460 nm and short shoulder peak at 500 nm for N, S-CDs synthesis in the presence of gold nanoparticles. In addition, after the characterization process of the material in Figure 2.42, the absorbance points give at 350 nm, 470 nm and short shoulder peak at 500 nm for N,S-CDs synthesis.

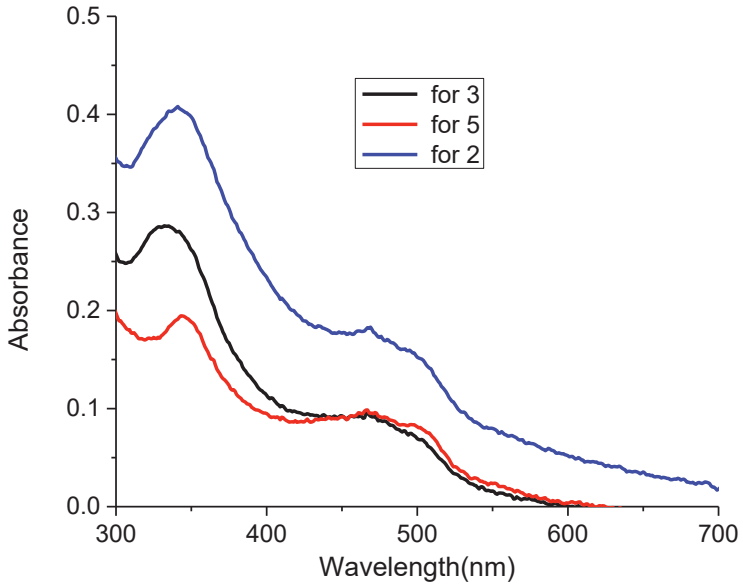

Figure 3.7. UV-visible Absorption Spectrum for AuNPs and N,S-CDs ($1.0x10^{10}$ AuNPs/ mL for 3 , $5.8x10^{9}$ AuNPs/mL for 5, and $1.0x10^{10}$ AuNPs/mL for 2)

The maximum emission wavelength of the CDs solution is changeable from 450 to 550 nm when changed the exciting wavelength of 350 to 500 nm for using different number of AuNPs. In Figure 3.8, this type of carbon dots synthesis with gold nanoparticles has the highest photoluminescent intensity at 550 nm. Table 3.5, All

quantum yields were calculated by using a coumarin reference point. According to this result, the quantum yield of N,S-CDs was found as 14.2%. Also, the quantum yield of N,S-CDs with gold nanoparticles was changed when the concentration of AuNPs solutions was changed. If the gold nanoparticles concentration was stable 0.05 from the 0.1 and volume of concentration 250 to 400 microliters, the quantum yield of the reaction was increased with the addition of gold nanoparticles.

Table 3.5. All quantum yields for AuNPs with CDs

CDs	QY (%)	Excitation Wavelength (nm)	Pl Emission peak(nm)	Time (h)	Figures
N,S- CDs	14.20%	460	550	4	Figure 2.44
250 µL AuNPs + N,S- CDs	10.20%	460	537	4	Figure 3.8 a)
330 µL AuNPs + N,S- CDs	19.20%	460	534	4	Figure 3.8 b)
400 µL AuNPs + N,S- CDs	17.10%	460	535	4	Figure 3.8 c)

a)

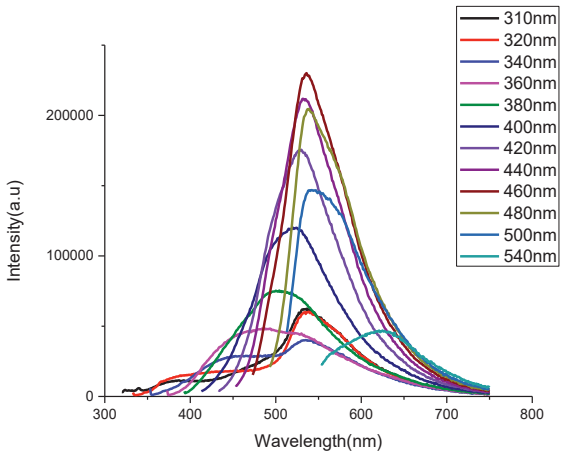

b)

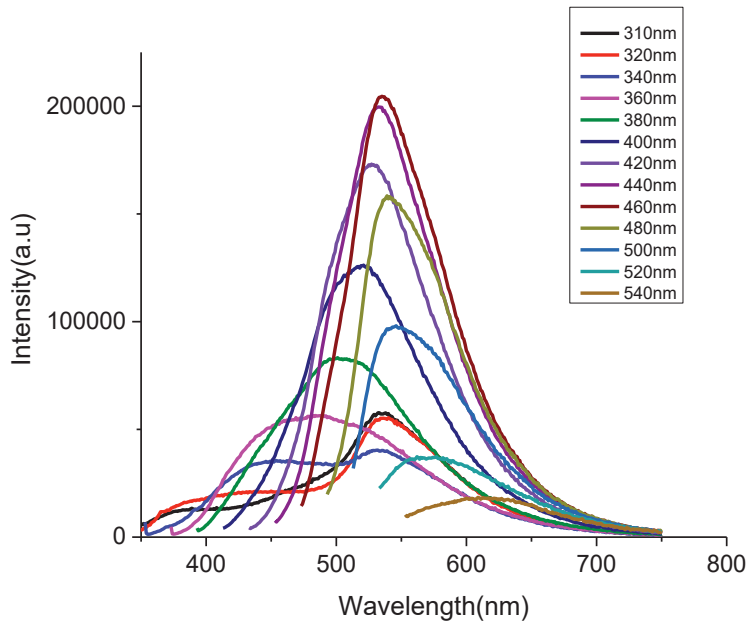

c)

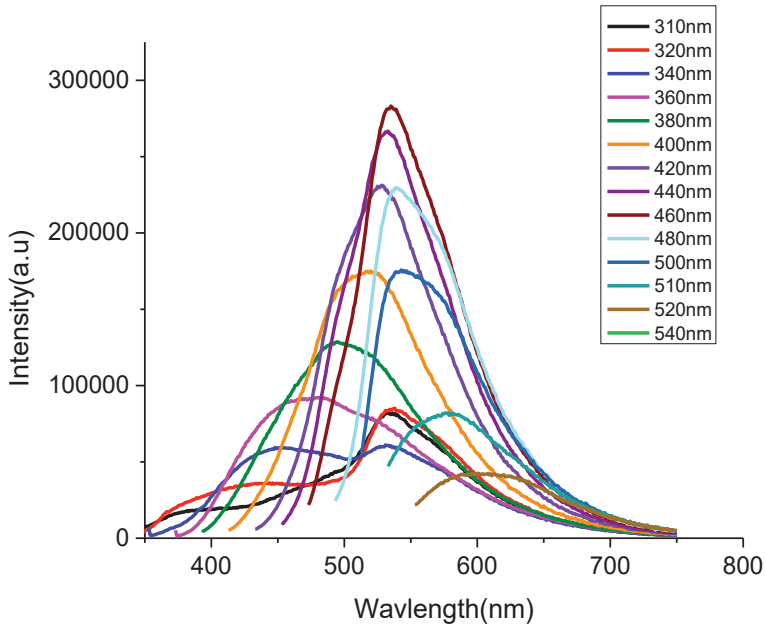

Figure 3.8. Fluorescence emission spectra of CDs for 4h with the excitation wavelength of 300 to 550 nm in 15 mL DMF at 240 °C with different amounts of a)$3.0x10^{10}$AuNPs/mL b)$2.5x10^{10}$AuNPs/mL and c) $1.9.0x10^{10}$AuNPs/mL

3.3.4. FTIR results for All Synthesis

The functional groups of N,S-CDs synthesis were analyzed by the FT-IR spectroscopy (Perkin Elmer Frontier) whereas all possible chemical band was shown in Figure 3.9. The O-H bond make the wide band was centered at 3320 cm^{-1}. The presence of the band at 2974 cm^{-1} indicates the stretching vibration bond C-H bending. Another band at 2067 cm^{-1} indicated the stretching vibration mode of N-C=O. The presence of amide bonds is visible in the FTIR spectrum, as indicated by their usual peaks of 1648 cm^{-1} and 1180 cm^{-1}, which correspond to C=O and C-N stretching vibrations. In addition, the C-O=C stretching vibration has a distinctive peak at 1348 cm^{-1}. The absence of the band at 1044 cm^{-1} indicating the stretching vibration mode C=S proved that the thiourea ligand was bound to the nanoparticle surface successfully. And the final bands at 878 cm^{-1} indicate the stretching vibration mode of N-H.

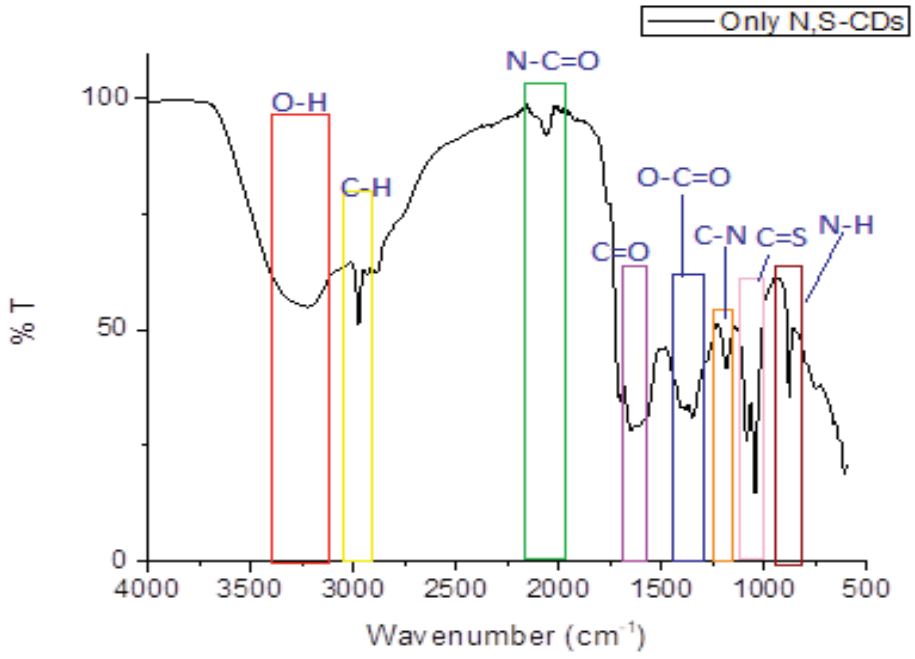

Figure 3.9. FT-IR spectra for synthesizing N,S-CDs

Another FTIR spectra of gold nanoparticles with N,S-CDs were shown in Figure 3.10. The bands at 3320 cm^{-1} 2067 cm^{-1} 1648 cm^{-1}, 1180 cm^{-1}, and 1348 cm^{-1} are assigned to O-H N-C=O, to C=O, C-N, C-O=C stretching. The absence of the bands at 1044 cm^{-1} and 887 cm^{-1} indicating the stretching vibration mode of C=S and N-H bonds demonstrated that gold nanoparticles were bounded to carbon dots via sulfur atoms.

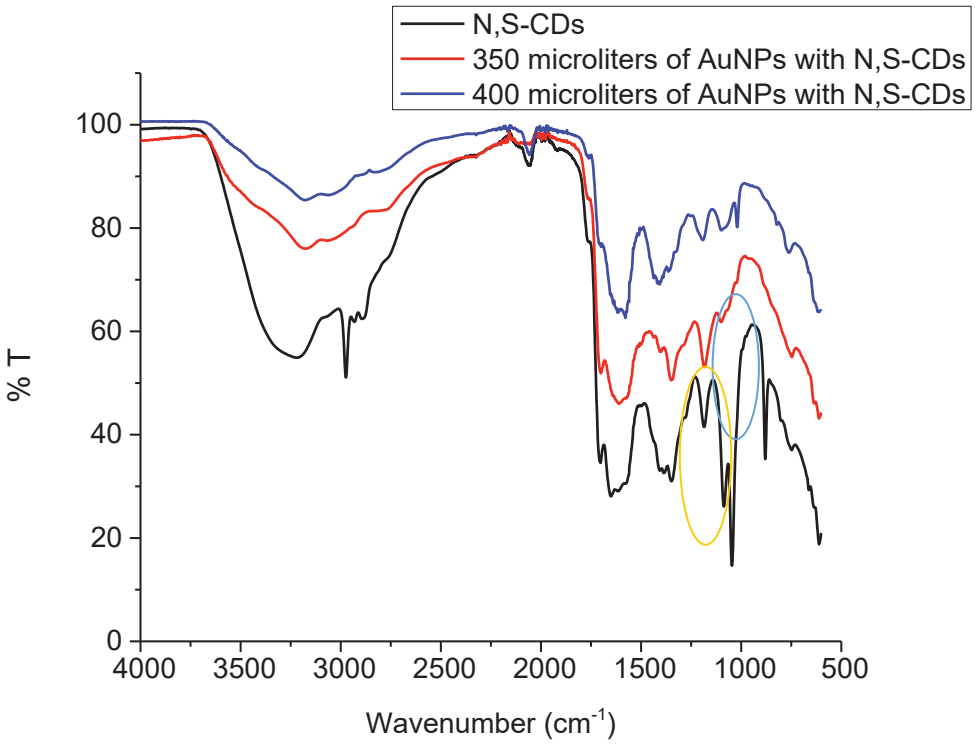

Figure 3.10. FT-IR spectra for synthesizing N,S-CDs in the presence of AuNPs

3.3.5. XRD Results for AuNPs with CDs

In Figure 3.11 measurement of the XRD pattern of CDs(red line) and AuNPS with CDs(black line) exhibits a broad peak at around 25° confirming the formation of these structures, corresponding to the interlayer gap of 3.2 Å and the characteristic diffraction peak (002) of graphite. The honeycomb structure based on sp^2 hybridized carbon atoms corresponds to the reflection. Also, the blue line is the AuNPs, a sharp peak was observed.

AuNPs with N, S-CDs synthesis of the black line did not see a sharp peak because our percentage of AuNPs was very low. SEM-EDS result also proved this.

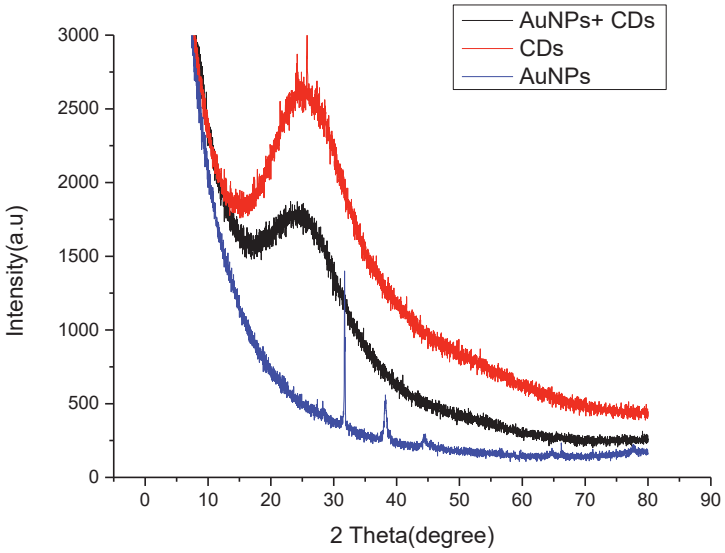

Figure 3.11. XRD pattern for CDs (N,S-CDs) (red line), AuNPs CDs (N,S-CDs +AuNPs) (black line) c)only AuNPs (blue line)

3.3.6. Scanning Electron Transmission Microscope (STEM) Results for All Results

Another widely utilized approach is electron microscopy, which may provide structural information over a wide variety of modifications. Using electrons instead of light, the morphology and topography of materials are provided by Scanning Electron Microscopy (SEM), producing an image with a resolution of 100 Å to 10 micrometers. Also, the size and shape information of CDs due to their higher resolution information can be detectable by using Scanning Electron Transmission Microscope (STEM) when compared to SEM due to its transmission detector. The energy dispersive X-ray detector, or EDS, is the most often used SEM device. Using the EDS detector makes it possible to analyze the composition of the sample taken from a region, point, or line. It is possible to provide an EDX analysis spectrum with data expressed as an atomic percent or weight percent. STEM images of carbon dots were shown in Figure 3.12 which has obtained from 30-50 nm carbon nanoparticles. All images proved that N,S-CDs particles have a

spherical form. And also, implying that the applied potential as 15.000 kV was important in determining the size of the C-dots The smaller the C-dots produced, the higher the applied potential.

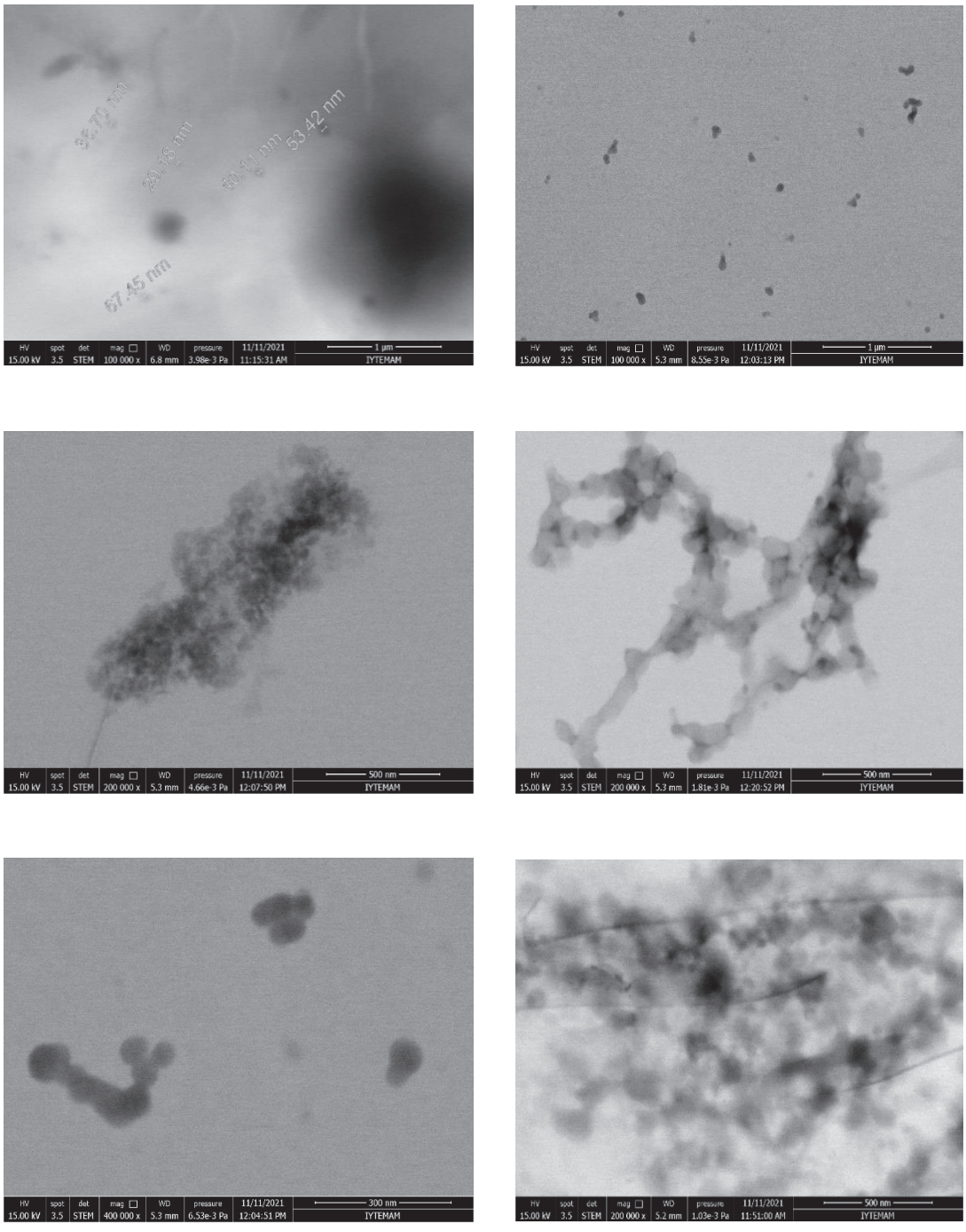

Figure 3.12. Typical STEM images for Carbon Dot synthesis

In addition to this, according to the SEM-EDS analysis, carbon dots were formed, while the carbon and oxygen source in it was provided by citric acid, while the nitrogen and sulfur source came from thiourea. The increase in N, S, O, and C fractions in these materials proves the formation of N,S-CDs. Figure 3.13, shows SEM-EDS results of N,S-CDs. In addition, SEM-EDS analysis was carried out in carbon dots synthesized 3 months ago and no difference was found proportionally as shown in Figure 3.14.

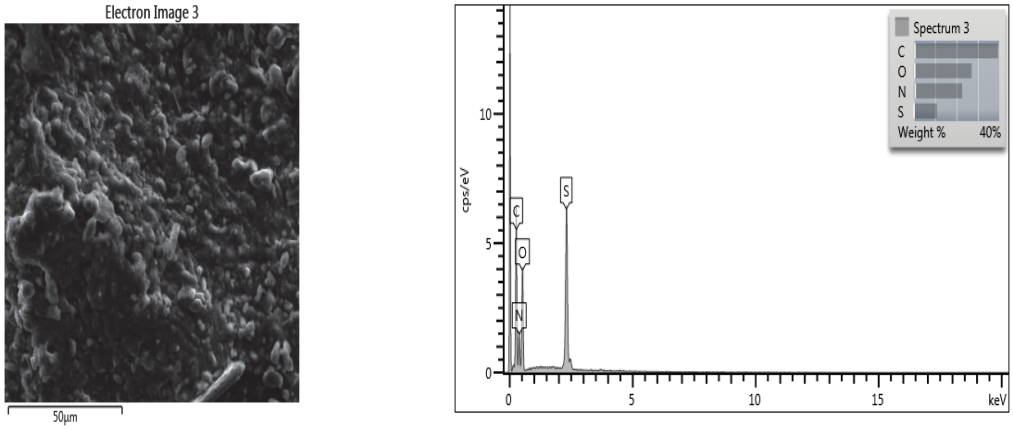

Element	Wt%	Atomic %
C	39.43	47.37
N	22.65	23.34
O	27.08	24.42
S	10.84	4.88
Total:	100.00	100.00

Figure 3.13. SEM-EDS analysis for N,S-CDs

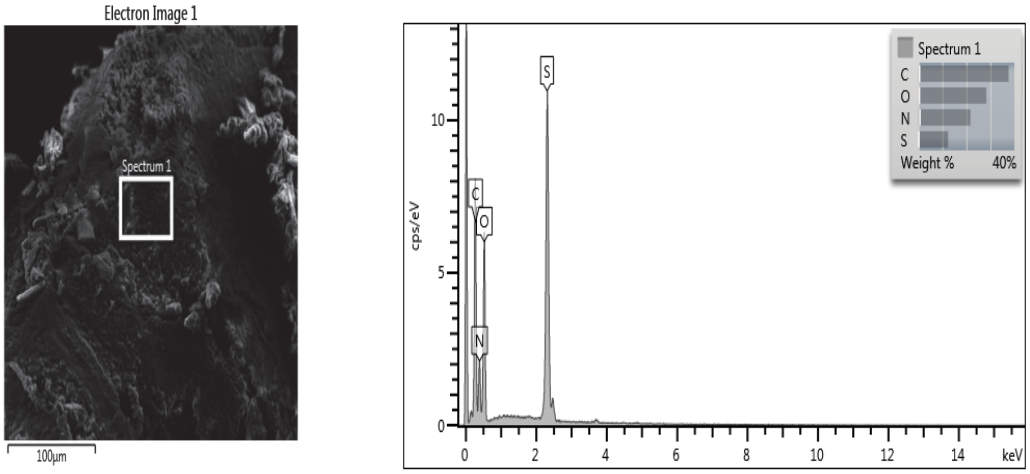

Element	Wt%	Atomic %
C	37.63	45.82
N	21.69	22.65
O	28.30	25.88
S	12.38	5.65
Total:	100.00	100.00

Figure 3.14. SEM-EDS analysis for N,S-CDs for synthesized 3 months ago

Then, to find out how gold nanoparticles and carbon dots affect each other, an image was obtained by applying. Because gold has a greater molecular weight and is denser than carbon dots, electrons pass through this point more. Thus, while electrons encountering more atoms appear darker, they take on a lighter color as they pass through the less dense area, which shows us the carbon dots formed as shown in Figure 3.15.

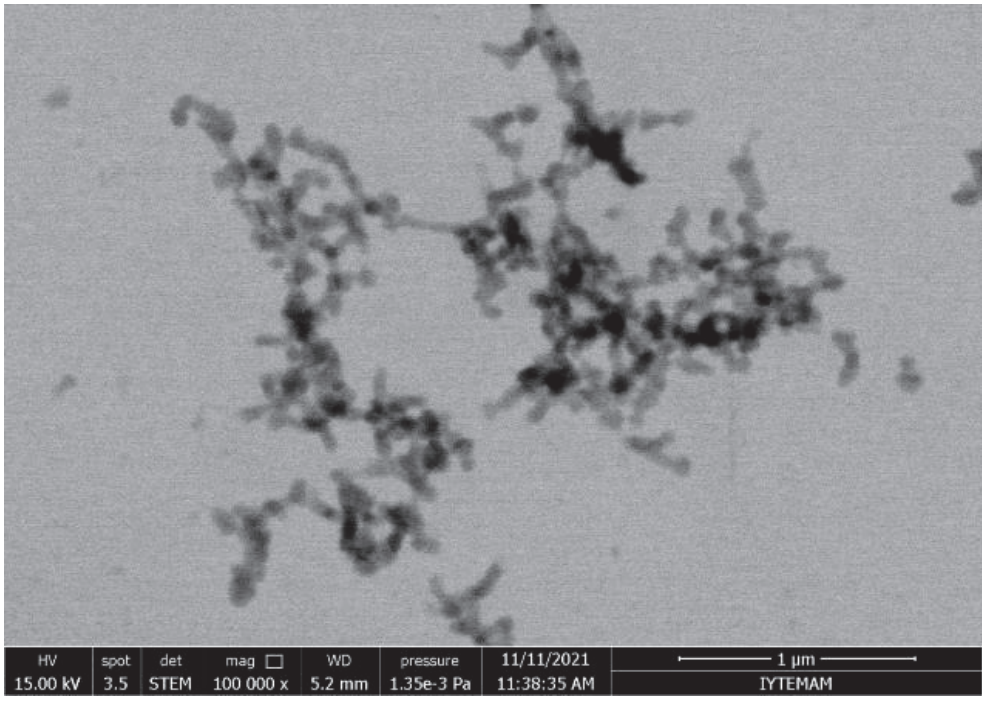
HV
15.00 kV
spot
3.5
det
STEM
mag
100 000 x
WD
5.2 mm
pressure
1.35e-3 Pa
11/11/2021
11:38:35 AM
1 µm
IYTEMAM

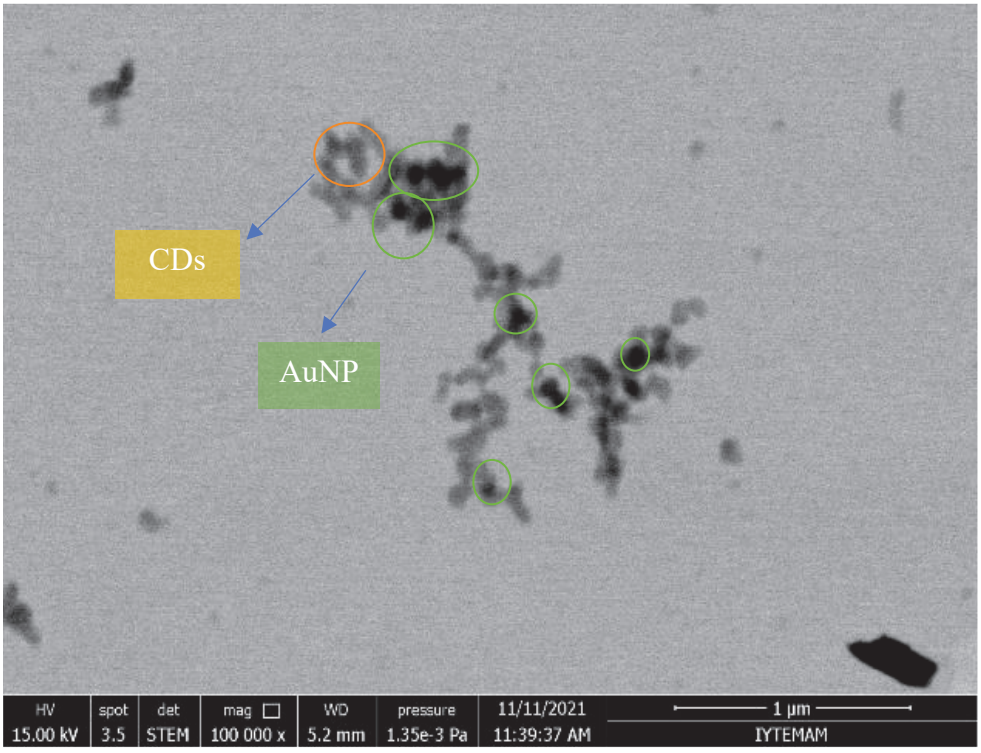
CDs
AuNP
HV
15.00 kV
spot
3.5
det
STEM
mag
100 000 x
WD
5.2 mm
pressure
1.35e-3 Pa
11/11/2021
11:39:37 AM
1 µm
IYTEMAM

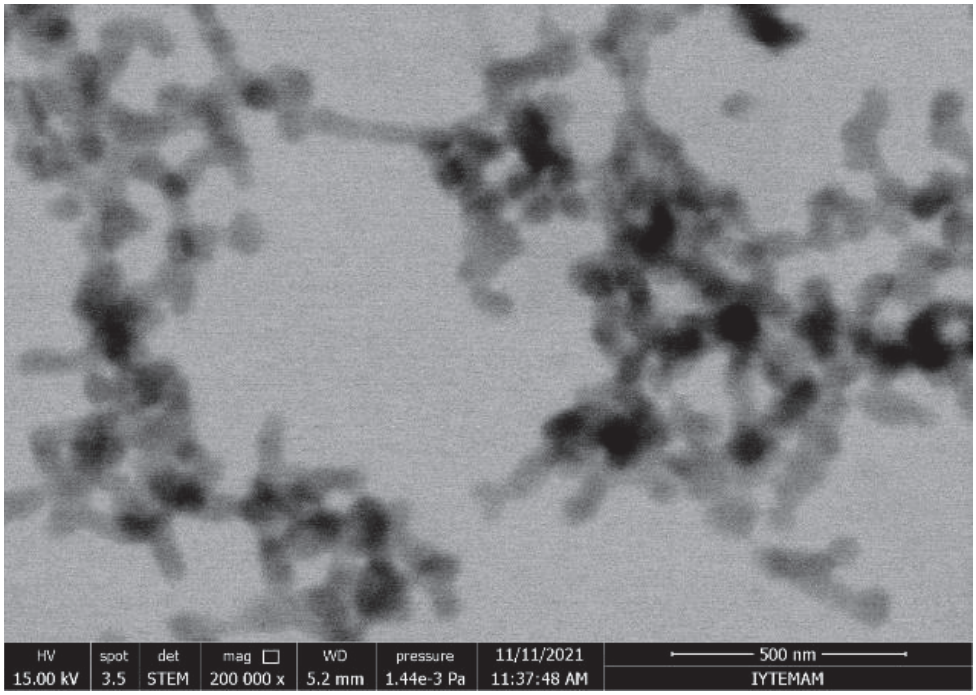

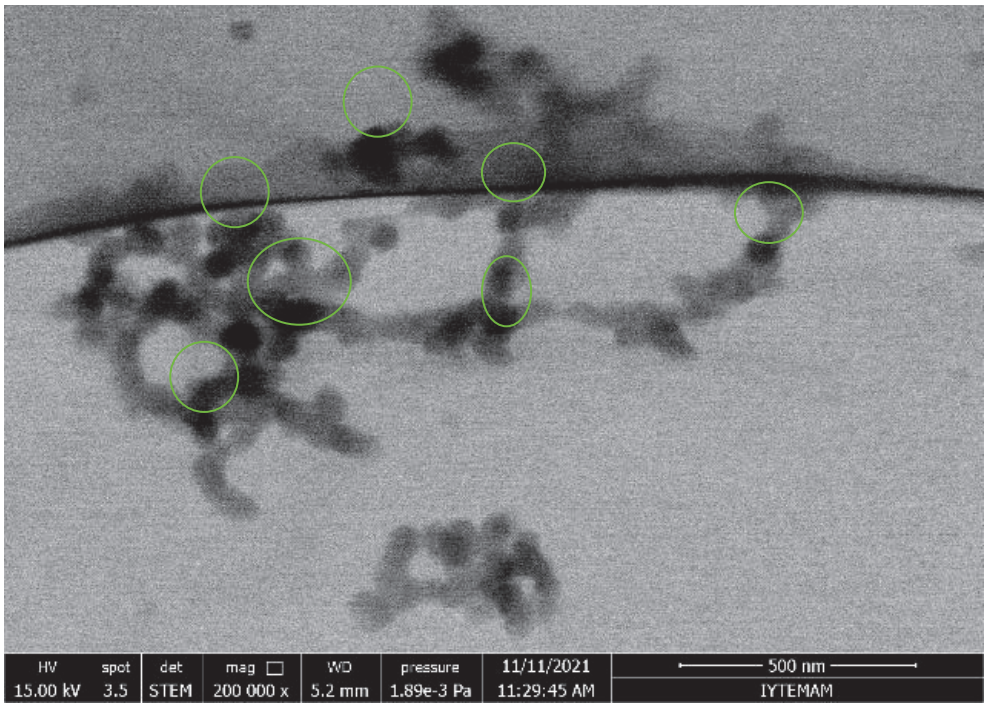

Figure 3.15. Typical STEM images for N,S-CDs synthesizing in the presence of AuNPs

Also, SEM-EDS results of gold nanoparticles with N,S-CDs solution was analyzed and all atomic percentage of these compounds was shown in Figure 3.16. High-resolution images showing the distribution of an element are obtained from high-energy electrons, and a backscattering detector was used for this. Backscattered electrons differ according to the weight of the elements, and so because of their larger nuclei, heavier elements can deflect incoming electrons more strongly than lighter elements. Heavy elements with a larger atomic number appear brighter than other lighter elements because more backscattered electrons are emitted from the sample surface. Here, gold nanoparticles percentages are very low as found in particles because my material looks dark because it is a carbon dot, and the device has difficulty detecting it because gold is embedded in the material.

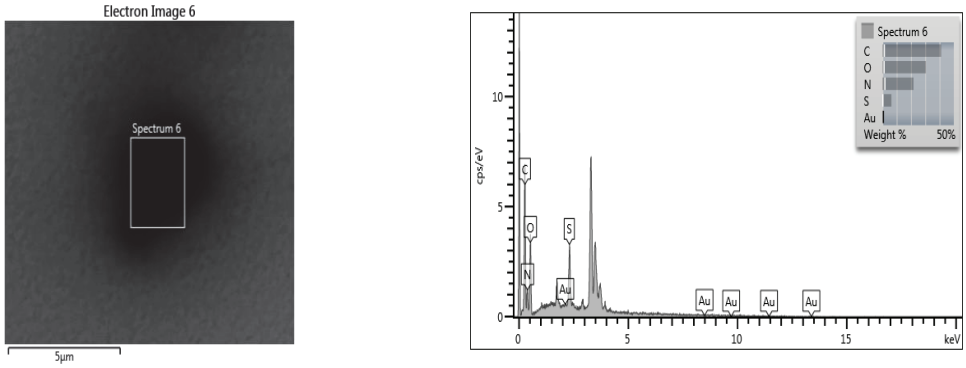

Element	Wt%	Atomic %
C	41.12	48.37
N	21.74	21.93
O	30.48	26.91
S	6.27	2.76
Au	0.39	0.03
Total:	100.00	100.00

Figure 3.16. SEM-EDS analysis of N,S-CDs synthesizing in the presence of AuNPs

CHAPTER 4

BIOLOGICAL IMAGING OF CARBON DOTS

4.1. Introduction

In general, CDs are used mostly for fluorescence imaging, particularly bioimaging. Carbon dots that emit blue are difficult to apply in bioimaging because of the blue autofluorescence of the biological background and the destructiveness of ultraviolet or blue light for excitation. For this reason, the synthesis of carbon dots with red fluorescence emitting with high photoluminescence emission and low cytotoxicity has an important place for biomedical applications to obtain high-quality bioimaging.[9899] Zhang et al.[100] succeeded in synthesizing N, S-CD in 16 hours at 160 degrees using p-phenylenediamine and cysteamine hydrochloride. They were able to visualize carbon dots with minimal cytotoxicity and excellent biocompatibility, showing bright yellow-green emission when excited with a 405 nm laser, in MCF-7 cells by in vitro cellular uptake. Lin et al. [101] succeeded in synthesizing multicolor CDs that emit ions in different regions by solvothermal pathway using o-PD, m-PD, and p-PD. These different nitrogen-doped carbon dots have been used for low cytotoxicity and cellular imaging under single wavelength excitation. In addition, these carbon dots performed bioimaging proving that they are in the cytoplasmic regions of MCF-7 cells with confocal micrographs as a result of 405 nm laser excitation.

Gao et al.,[102] using (3-aminopropyl)trimethoxysilane (APTMS) and glycerol, were able to synthesize fluorescent emission carbon dots by hydrothermal route at 260 °C for 12 h. These carbon dots, which have easy synthesis, water solubility, appropriate biocompatibility and high fluorescence properties, can efficiently distinguish cancerous cells from normal cells and visualize their mitochondria. Guo et al.[103] succeeded in synthesizing fluorescent carbon dots at 160 degrees for 10 hours by microwave method using citric acid and N,N-dimethylaniline.

In this study, it was used in unique cell imaging and biological applications without a washing process that can switch between mitochondria and nucleolus. Using m-phenylenediamine and L-cysteine, Hua et al.[104] succeeded in synthesizing fluorescent

carbon quantum dots that are easily dispersed in water by a hydrothermal route at 160 °C for 10 hours. Perform nucleus imaging and nucleus targeting at the end of synthesis uses drug delivery in organelle-targeted imaging for cancer therapy. Ji et al.[105] succeeded in synthesizing carbon nanodots by microwave using citric acid and urea. Considering that these dots perform an energy-dependent transport within the cell with low cytotoxicity, they mostly target mitochondria, and as a result, they have been used in applications of bioimaging and antioxidation fields in A549 cells. Su et al[106] succeeded in synthesizing red carbon dots emitting in the red region after 1 hour at 195 ºC by hydrothermal route using 4-Aminophenol and KIO4. As a result, they used carbon dots with 20.1% quantum efficiency, which are water-soluble, can be synthesized in one dimension and enter the nucleus, and exhibit a killing effect on tumor cells. As a result of all these studies, it has been tried to synthesize carbon dots with high quantum efficiency, water solubility feature, no toxic effect in the cell, and high photoluminescence feature to be used for imaging in cancer cells.

4.2. Experimental

4.2.1. Materials

Citric acid and DMF were used for synthesizing carbon dot solution was purchased from supplier Sigma Aldrich. Also, Thiourea was a supplier from Alfa Easer. Cell mediums DMEM/F-12 (Dulbecco's Modified Eagle Medium/Nutrient Mixtıure) and other solutions FBS(Fetal Bovine Serum), L-glutamine, Pen-strep (penicillin), Trypsin EDTA were obtained from Biological Industries.

4.2.2. Instrumentation

Optical and structural techniques were characterized for synthesizing carbon dots. Absorbance and Photoluminescence and quantum yields measurement by Edinburg FS5 Spectrophotometer. Particle size measurements were measured by DLS (Malvern ZS-Zetasizer) (İYTE) SEM analysis SEM-EDS and High-Resolution SEM images analysis was measured by using FEI, QUANTA 250 FEG. Fourier transform infrared

Spectroscopy was measured by using PERKIN ELMER FRONTIER. Also, Confocal Microscope (Andor Revolution) was used to image cells by taking 20X and 40X objectives as shown in Figure 4.1.

Figure 4.1. The Confocal Microscope

4.2.3. Cell Culture

The cellular uptake and distribution of produced carbon dots were investigated using an A549 cell which was obtained from the ATTC (Amerikan Culture Collection). The basal medium contains these solid materials, 10% FBS (fetal bovine serum),%1 penicillin, and L-glutamine. In a humidified incubator with 5% CO_2, cell culture was kept at 37°C. Discard the old medium from the cell culture. After 1 mL of PBS buffer was used to wash, discarded into the PBS buffer into the cell culture. 1 mL of trypsin was added to the solution and put in the incubator for 3 minutes at 37°C with 5% CO_2. After 7 mL of medium was added because inactivating of trypsin solution. Finally, these cells were a seed in the six-wall plate.

4.2.4. Cytotoxicity Assay

4.2.4.1. MTT Assay

The intracellular viability of carbon dots was determined using the colorimetric MTT assay by using A549 cells. 4500 cells were seed in 100 μL DMEM solution for each well in 96 well plates. Cell medium was removed after overnight incubation and replaced with 100 μL of medium treated with different concentrations of carbon dot solution (0.1/1.0/50.0/100.0 μg/mL). Cells were incubated for another 24 hours to investigate the toxicity of carbon dots added to the cell.

After the incubation process, carbon dot with the medium was removed, and then, 10 μL MTT in including 100 μL medium was added and incubated for 4h.

After 4h incubation, 100 μL DMSO was added to each well and kept on shaker another 15 minutes. The absorbance of each cell was measured by using a spectrophotometer at 540 nm.

4.2.4.2. Colony Formation Assay (CFA)

1500 cells (A549) were seeded into each well in 6 wall plate. Before this procedure, cell number was optimized for CFA assay. After this procedure cell was incubated for 24h because of the attachment of these cells to the bottom of the flask. After the carbon dot in different concentrations (0.1/1.0/50.0/100.0 μg/mL) was added and waited in an incubator for another 24h.

After CD was included, the medium was replaced with a fresh medium. After, 7 days was waited because of controlling colon information process.

Finally, removed the media, each cell was fixed and cell colony staining was performed with a crystal violet solution containing paraformaldehyde (PFA). ImageJ was used to count for stained cell colonies.

4.2.5. Immunofluoresence Imaging of C-dots

Immunofluoresence imaging procedure was applied to. 250.000 cells (A549) were seeded into each well in 35 mm of the cell culture dish. After, the cell was incubated for 24h. 50 μg/mL of carbon dot solution was added to the dish. Live-cell images were taken with confocal microscopy 3 hours later. In addition to this, the carbon dot solution was taken and washed with PBS solution. After 6 hours, imaging was taken again. Another procedure is that remove the medium and rinse with PBS and fixation methanol was added to fix the cells. Permeabilize cells with PBS buffer containing Triton-X-100 for 5 minutes gentle rockings. After rinsing once with PBS and add 70% of ethanol and pick up coverslip to dry. After the dried process, DAPI was added to visualize nuclei of cells. Finally, cell images were taken with confocal microscopy.

4.3. Result and Discussion

4.3.1. Confocal Imagining for Live Cells

To detect intracellular localization of CDs A549 cells were treated with 50 μg/mL of carbon nanoparticles. To detect nanoparticles with or without targeting capabilities, optical approaches rely on scattering contrast**.** After 3 hours of the incubation process, light scattering characteristics of CDs were imaged by confocal microscope using a bright field and 532 nm laser as shown in Figure 4.1. After 6h of incubation, CDs medium removed and cells rinsed with PBS and fresh media added. Live cell imaging was taken in the period of incubation and after the washing process by using bright field and 488 nm, 532 nm laser in the confocal microscope.

Red spots were observed in all treated cells, which are referred to as carbon dots and these dots were imaged by using a 532 mm laser. Green spots were observed in all treated cells, which are referred to as carbon dots and these dots were imaged by using a 488 mm laser. All confocal imaged of A549 cells were shown in Figure 4.2.

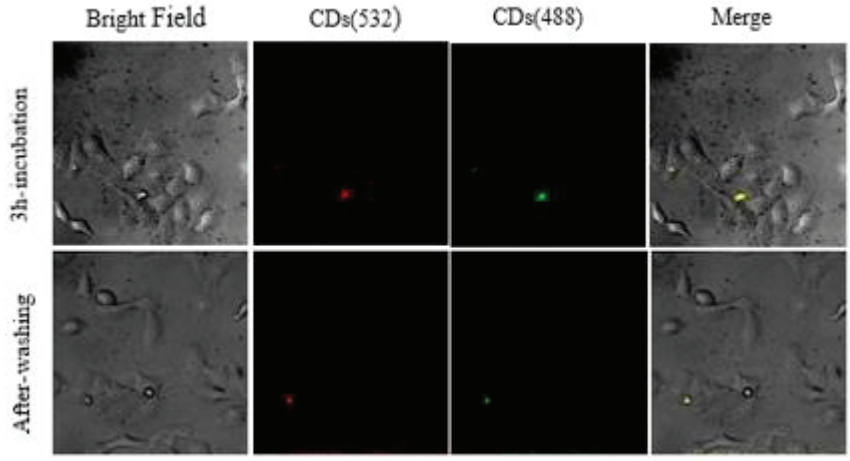

Figure 4.2. Confocal images of A549 living cells incubated with 50.0 μg/mL for 24 hours by using 532 nm laser and 488 nm laser. Cells observed bright fields by using confocal microscopy.

Live cell imaging of CDs treated A549 cells, confocal imaging taken in the period (3 h) of incubation, shows CDs targets nucleus. After 6 h of incubation, CDs were removed, cells rinsed with PBS, and the culture medium was replaced with a fresh one. After-washing images show that CDs are still located in the nucleus. To make sure about CDs targets, the same treatment procedure was applied and cells fixed, afterward, DAPI was used as a nucleus dye.

4.3.2. Confocal Imagining for Fixed Cells Treated with CDs

A549 cells were treated with 50 μg/mL of carbon dots after 6 for analyzing nuclear localization of CDs. After that cells were fixed by methanol and the cell nuclei stained blue with DAPI and cell imaged captured by the confocal microscope. After staining the nucleus of the cell with DAPI, images taken with carbon dots were compared. Immunofluorescence images show that carbon dots target the nucleus as shown in Figure 4.3. In here, nucleus stained by DAPI which shown in Figure 4.3, it is blue imaged captured. And also, After CDs were imaged by confocal microscope using and 532 nm laser as shown in Figure 4.3 and red spots were observed.

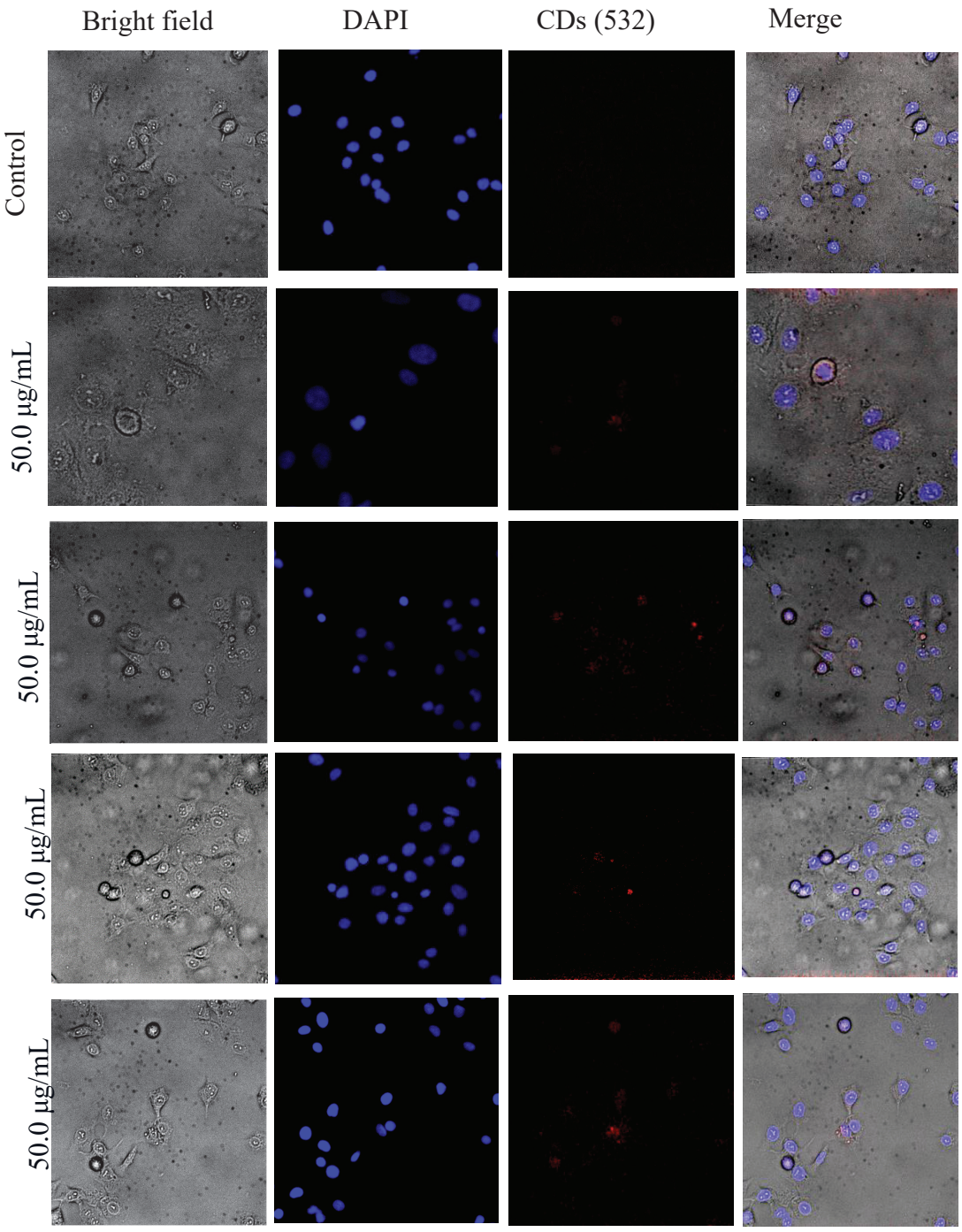

Figure 4.3. Confocal images of A549 living cells incubated with 50.0 µg/mL for 24 hours by using a 532 nm laser. Cells observed bright fields by using confocal microscopy. Nucleus was stained DAPI (blue), merged images of darkfield and blue fluorescence

Confocal image of fixed A549 cells treated with 50 ug/mL CDs for 6h, stained with DAPI. CDs detected by 488 (A) and 532 nm (B) channels. Colocalization analysis between CDs and DAPI made by Coloc2 plugin in ImageJ. Analyzed only a region of interest by making an ROI (region of interest) as shown in Figure 4.4.

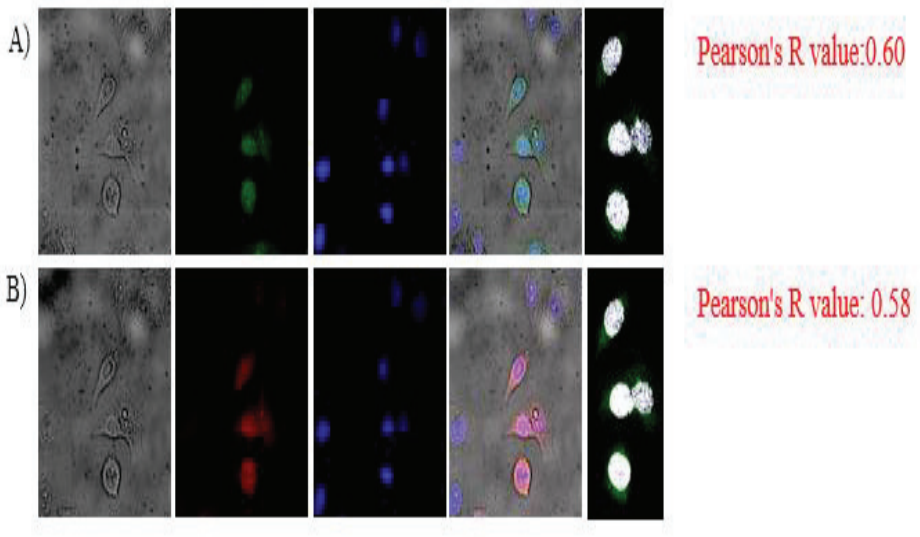

Figure 4.4. Colocalization Analysis (A) 488 and (B) 532 nm channels

4.3.3. Results for MTT Assay

The cytotoxicity of the prepared CDs was tested on A549 cells by colorimetric MTT assay. Cells were treated with concentrations of 0.1, 1, 10, 50, 100 and 150 µg/mL of CDs solution. After 24 h labeling, the viability of the cancer cells was measured by MTT assay. In Figure 4.5, CDs stimulated proliferation at a very low concentration (0.1 µg/mL) up to 10 µg/mL, after which viability declined with increasing concentration. The apparent low toxicity of CDs is consistent with previous studies, showing CDs exhibit IC50 values from 100 µg/mL. This indicates low cytotoxicity and superior biocompatibility of the CDs, ensuring their feasibility for intracellular imaging. MTT results obtained after 48 and 72 hours showed a decrease in cell viability as the

concentration increased. MTT results obtained after 48 and 72 hours showed a decrease in cell viability as the concentration increased.

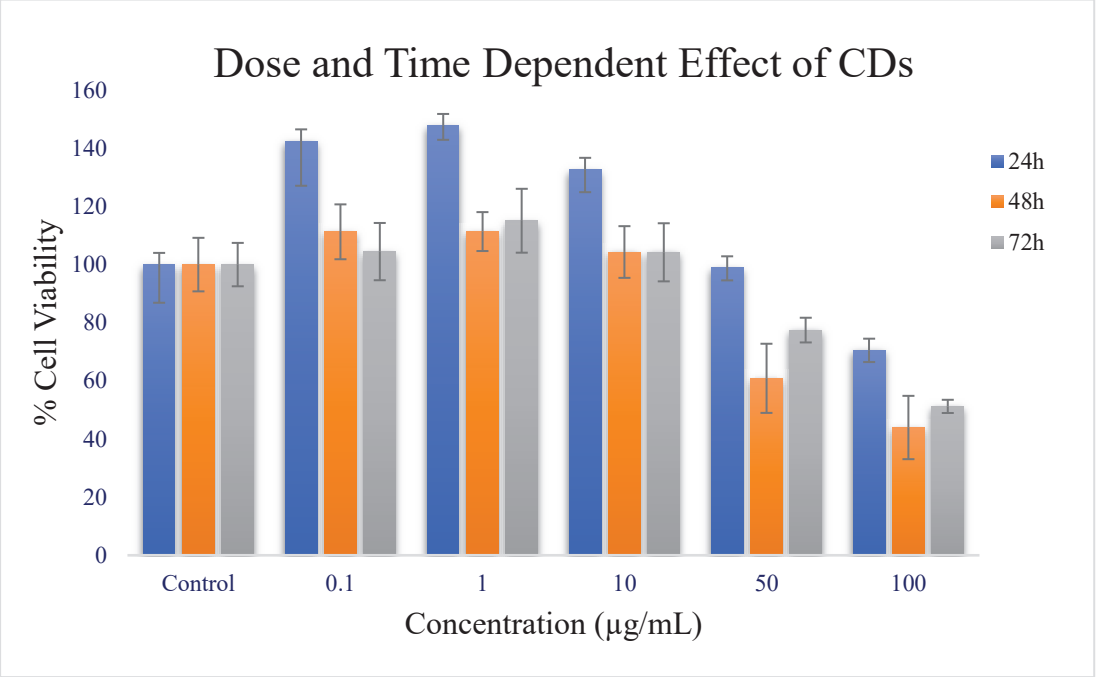

Figure 4.5. The cell viability of A549 cells treated with 0.1, 1, 10, 50, 100, and 150 µg/mL of CDs for 24h, 48h, 72h

4.3.4. Results for Colony Formation Assay

The cytotoxicity was further validated via colony formation assay(CFA), which confirmed MTT results after treatment with CDs. This assay is an in vitro cell proliferation assay based on the ability of a single cell to grow in a colony. The viability of A549 cells (Figure 4.6) was still maintained at approximately, 110%. These cells did not decrease below 60% for 24h. It is seen that a little toxic effect was observed after the addition of 100 µg/mL of CDs.

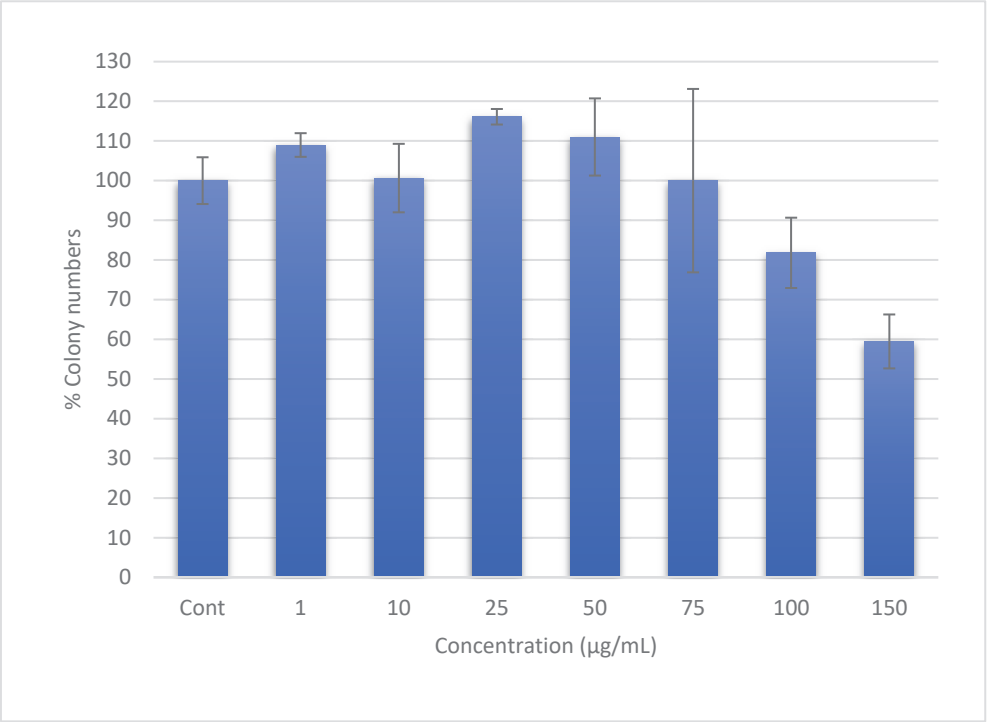

Figure 4.6. Effect of Carbon Dots on cell Colony Formation Ability for A549 for 24h

CHAPTER 5

CONCLUSION

We developed the various kind of carbon dots and N,S-CDs with gold nanoparticles by using different synthesis methods and precursors to obtain highly efficient carbon dot nanoparticles. Reactant concentrations, reaction time, and volume were optimized to obtain carbon dots with high photoluminescence quantum efficiency. Absorption and photoluminescence spectra, confocal microscope for microphotoluminescence measurements were performed for optical characterization. To investigate the elemental composition and crystal structure, X-ray powder diffraction (XRD), scanning electron microscopy and its X-ray energy dispersive spectroscopy detector (SEM and SEM-EDS), Scanning Electron Transmission Microscope (STEM), dynamic light scattering (DLS), were used. Citric acid and thiourea were used to synthesize N,S-doped CDs by hydrothermal treatment. Results show that temperature range and solvent effect are also important to synthesize high efficient green-emitting CDs. Absorption peak, optimum emission peaks exhibit at 340 nm, 470 nm and give a shoulder peak at 500 nm. And these peaks relevant to the π–π* transition gives the C=C band, while the n–π* transition gives the C=N band. Our carbon dot solution contains different particle sizes of carbon nanoparticles. This particle size dependence is consistent with the quantum confinement effect. If increase the particle size can be explained by decreasing bandgap due to p-electron delocalization the quantum confinement effect. Therefore, we have different emission wavelengths for carbon dot synthesize because of different particle sizes. Also, the solvent effect was analyzed to observe PL property of carbon dots is dependent on the H bond affect hydrogen bonding in aprotic solvents is weaker than in protic solvent, therefore obtaining larger spectral shifts and resulting in shorter fluorescence lifetimes. DMSO is more polar than DMF and Methanol solvent. When the polar aprotic DMSO solvent is added to the solution, the nitrogen bonds form strong hydrogen bonds with the DMSO, causing the emission energy level to increase and shift to the red zone. Also, the same procedure was repeated by changing time and temperature. If the reaction temperature increase, time can be reducible. We obtained optimum procedure when time stable at 160 ^{o}C for 6h and quantum yield was obtained as %17.9 for preparing 15 mL of DMF solvent and %18.4 for 20 mL of DMF solvent. After

the characterization process, the quantum yield of carbon dots was estimated as 14.2% for preparing 15 ml of DMF solvent at 240 ºC for 4h. After the optimum condition was done, we tried to synthesize carbon dots in the presence of AuNPs. Firstly, different amounts of AuNPs such as $2.5x10^9$, $5.0x10^9$, and $1.0x10^{10}$ were added to the reaction at the start of carbon dot synthesis, and the reaction concentration of AuNPs is also important to obtain high photoluminescence of carbon dots. When using these numbers of AuNPs, quantum yields of reaction were estimated as %18.7, %21.3, %31.2, respectively. And also we tried to optimize the synthesis carbon dots in the presence of gold nanoparticles. Another experimental procedure is that different amount of $3.5x10^9$, $5.8x10^9$, $1.06x10^{10}$, and $1.7x10^{10}$ of AuNPs was used to synthesize carbon dots in the presence of gold nanoparticles solution. If the carbon dot synthesis prepared with $3.5x10^9$ of gold nanoparticles/volume, emission peak was observed at 460 nm when excited at 350 nm. Also quantum yield was estimated as % 3.0 at 460 nm. If the carbon dot synthesis prepared with $1.7x10^{10}$ of gold nanoparticles/volume, emission peaks are observed at 450 nm when excited at 350 nm and quantum yield was extimated 66.4 percentage at 450 nm. And also quantum yield was estimated as %14.9, %23.8, %37.0 when emission wavelength at 550 nm for each $3.5x10^9$, $5.8x10^9$, $1.06x10^{10}$ number of gold nanoparticles /volume. As a results, ıf the number of gold nanoparticles was increased, emission of the gold nanoparticle was shifted to the blue-site. After the purification process, agglomeration can occur and radiative recombination is reduced and thus the quantum yield can be lower. After all procedures, the best results were repeated for analysis after the purification process. $1.9x10^{10}$ $3.0x10^{10}$ $2.5x10^{10}$ number of AuNPs/µL components was centrifuged using 40.000rpm at 15 minutes and powder was diluted with DMF and reaction of quantum yield was estimated as %10.2, %19.2 and 17.1%. These results show that ıf the amount of gold nanoparticle amount is kept from $5.0x10^9$ to $1.0x10^{10}$ and its concentration is kept from 0.05 mol to 1 mol, it will give high photoluminescence green emission at 550 nm. Also, explaining AuNPs with carbon dot was demonstrated that FTIR results and SEM results. FTIR results proved that this carbon dot has a rich carboxyl group. The stretching vibrations (2067, 1180, and 1044 cm^{-1}) suggested the presence of S- and N-containing groups, as well as a conjugated aromatic structure. The peak at 1044 cm^{-1} and 887 cm^{-1}were attributed to v(C=S) and v(N-H) groups of carbon dot. These groups disappeared after being treated with AuNPs. The disappearance of the C=S band could be explained by the direct binding of sulfur to the empty surface of AuNPs.

Similarly, the disappearance of the N-H signal stems from the bond between nitrogen and oxygen of the citrates which are on the surface of the AuNPs. According to the HTEM analysis, the particle size is found out as 30-50 nm in diameter for CDs synthesis and the increase in the sulfur, nitrogen amounts of carbon dots results in a red shift. The results of optical spectra and proved with SEM-EDS results. The decrease in sulfur as atomic percentage in SEM-EDS results supports this FTIR theory for AuNPs with CDs synthesis. Also, The HTEM images revealed the presence of gold nanoparticles on the surface of the carbon dots. Electrons flow through this spot more easily because gold has a higher molecular weight and is denser than carbon dots. As a result, while electrons pass through more dense atoms, the point appeared darker, but they travel through the less dense area, they appear lighter which proved that the lighter area is carbon dot and another darker point is AuNPs. SEM-EDS results of carbon dot peresence of gold nanoparticles was analyzed and our atomic percentages of gold very low as shown in Figure 3.13. Since the amount of gold nanoparticles is low at the beginning of the experiment, the SEM-EDS analysis prove this result. Also, SEM-EDS results proved that XRD pattern of black line. Finally, obtaining carbon dot solution, a cell imaging study was applied. 50 μg/mL of carbon nanoparticles was treated with A549 cells. After 3 hours of the incubation process, light scattering characteristics of CDs were imaged by confocal microscope using a bright field and 532 nm laser. Before and after the washing process, images demonstrated that CDs were still located in the nucleus. To ensure that CDs targets, the same procedure was applied cell fixation and DAPI procedure. IC-50 values estimated as 100 μg/mL, this results proved that the low toxicity of CDs is consistent with previous studies. Also, the cytotoxicity was subsequently verified using a colony formation assay (CFA), which corroborated MTT findings following CD treatment. The viability of these cells was calculated as 110%. These MTT results do not decrease below the % 60. When the addition of 100 μg/mL of CDs, a slightly toxic effect was observed. As a result of these investigations, carbon dots with high quantum efficiency, water-solubility, no hazardous impact on cells, and strong photoluminescence have been attempted to be employed for imaging in cancer cells.

REFERENCES

1. Xu X, Ray R, Gu Y, et al. Electrophoretic analysis and purification of fluorescent single-walled carbon nanotube fragments. *J Am Chem Soc*. 2004;126(40):12736-12737.

2. Ding H, Yu S-B, Wei J-S, Xiong H-M. Full-color light-emitting carbon dots with a surface-state-controlled luminescence mechanism. *ACS Nano*. 2016;10(1):484-491.

3. Wang R, Lu K-Q, Tang Z-R, Xu Y-J. Recent progress in carbon quantum dots: synthesis, properties and applications in photocatalysis. *J Mater Chem A*. 2017;5(8):3717-3734.

4. Hu S-L, Niu K-Y, Sun J, Yang J, Zhao N-Q, Du X-W. One-step synthesis of fluorescent carbon nanoparticles by laser irradiation. *J Mater Chem*. 2009;19(4):484-488.

5. Li X, Wang H, Shimizu Y, Pyatenko A, Kawaguchi K, Koshizaki N. Preparation of carbon quantum dots with tunable photoluminescence by rapid laser passivation in ordinary organic solvents. *Chem Commun*. 2010;47(3):932-934.

6. Cao L, Wang X, Meziani MJ, et al. Carbon dots for multiphoton bioimaging. *J Am Chem Soc*. 2007;129(37):11318-11319.

7. Yang S-T, Cao L, Luo PG, et al. Carbon dots for optical imaging in vivo. *J Am Chem Soc*. 2009;131(32):11308-11309.

8. Yang S-T, Wang X, Wang H, et al. Carbon dots as nontoxic and high-performance fluorescence imaging agents. *J Phys Chem C*. 2009;113(42):18110-18114.

9. Xi Y, Song J, Xu S, et al. Growth of ZnO nanotube arrays and nanotube based piezoelectric nanogenerators. *J Mater Chem*. 2009;19(48):9260-9264.

10. Shinde DB, Pillai VK. Electrochemical resolution of multiple redox events for graphene quantum dots. *Angew Chemie Int Ed*. 2013;52(9):2482-2485.

11. Deng J, Lu Q, Mi N, et al. Electrochemical synthesis of carbon nanodots directly from alcohols. *Chem Eur J*. 2014;20(17):4993-4999.

12. Lu J, Yang J, Wang J, Lim A, Wang S, Loh KP. One-pot synthesis of fluorescent carbon nanoribbons, nanoparticles, and graphene by the exfoliation of graphite in ionic liquids. *ACS Nano*. 2009;3(8):2367-2375.

13. Zhou J, Booker C, Li R, et al. An electrochemical avenue to blue luminescent nanocrystals from multiwalled carbon nanotubes (MWCNTs). *J Am Chem Soc*. 2007;129(4):744-745.

14. Li H, He X, Kang Z, et al. Water-soluble fluorescent carbon quantum dots and photocatalyst design. *Angew Chemie Int Ed*. 2010;49(26):4430-4434.

15. Ma Z, Zhang Y-L, Wang L, et al. Bioinspired photoelectric conversion system based on carbon-quantum-dot-doped dye--semiconductor complex. *ACS Appl Mater \& interfaces*. 2013;5(11):5080-5084.

16. Tang D, Zhang H, Huang H, et al. Carbon quantum dots enhance the photocatalytic performance of BiVO 4 with different exposed facets. *Dalt Trans*. 2013;42(18):6285-6289.

17. Liu M, Xu Y, Niu F, Gooding JJ, Liu J. Carbon quantum dots directly generated from electrochemical oxidation of graphite electrodes in alkaline alcohols and the applications for specific ferric ion detection and cell imaging. *Analyst*. 2016;141(9):2657-2664.

18. Zong J, Zhu Y, Yang X, Shen J, Li C. Synthesis of photoluminescent carbogenic dots using mesoporous silica spheres as nanoreactors. *Chem Commun*. 2011;47(2):764-766.

19. Tang L, Ji R, Cao X, et al. Deep ultraviolet photoluminescence of water-soluble self-passivated graphene quantum dots. *ACS Nano*. 2012;6(6):5102-5110.

20. Wang Y, Li Y, Yan Y, et al. Luminescent carbon dots in a new magnesium aluminophosphate zeolite. *Chem Commun*. 2013;49(79):9006-9008.

21. Yang Y, Cui J, Zheng M, et al. One-step synthesis of amino-functionalized fluorescent carbon nanoparticles by hydrothermal carbonization of chitosan. *Chem Commun*. 2012;48(3):380-382.

22. Park SY, Lee HU, Park ES, et al. Photoluminescent green carbon nanodots from food-waste-derived sources: large-scale synthesis, properties, and biomedical applications. *ACS Appl Mater \& interfaces*. 2014;6(5):3365-3370.

23. Li H, He X, Liu Y, Yu H, Kang Z, Lee S-T. Synthesis of fluorescent carbon nanoparticles directly from active carbon via a one-step ultrasonic treatment. *Mater Res Bull*. 2011;46(1):147-151.

24. Cheng L, Li Y, Zhai X, Xu B, Cao Z, Liu W. Polycation-b-polyzwitterion copolymer grafted luminescent carbon dots as a multifunctional platform for serum-resistant gene delivery and bioimaging. *ACS Appl Mater \& interfaces*. 2014;6(22):20487-20497.

25. Zhai X, Zhang P, Liu C, et al. Highly luminescent carbon nanodots by microwave-assisted pyrolysis. *Chem Commun*. 2012;48(64):7955-7957.

26. Titirici M-M, Antonietti M. Chemistry and materials options of sustainable carbon materials made by hydrothermal carbonization. *Chem Soc Rev*. 2010;39(1):103-116.

27. Zhu H, Wang X, Li Y, Wang Z, Yang F, Yang X. Microwave synthesis of fluorescent carbon nanoparticles with electrochemiluminescence properties. *Chem Commun*. 2009;(34):5118-5120.

28. Ma C-B, Zhu Z-T, Wang H-X, et al. A general solid-state synthesis of chemically-doped fluorescent graphene quantum dots for bioimaging and optoelectronic applications. *Nanoscale*. 2015;7(22):10162-10169.

29. Yang Z-C, Wang M, Yong AM, et al. Intrinsically fluorescent carbon dots with tunable emission derived from hydrothermal treatment of glucose in the presence of monopotassium phosphate. *Chem Commun*. 2011;47(42):11615-11617.

30. Zhu S, Meng Q, Wang L, et al. Highly photoluminescent carbon dots for multicolor

patterning, sensors, and bioimaging. *Angew Chemie*. 2013;125(14):4045-4049.

31. Zhang Z, Hao J, Zhang J, Zhang B, Tang J. Protein as the source for synthesizing fluorescent carbon dots by a one-pot hydrothermal route. *Rsc Adv*. 2012;2(23):8599-8601.

32. Li H, Kang Z, Liu Y, Lee S-T. Carbon nanodots: synthesis, properties and applications. *J Mater Chem*. 2012;22(46):24230-24253.

33. Li X, Zhang S, Kulinich SA, Liu Y, Zeng H. Engineering surface states of carbon dots to achieve controllable luminescence for solid-luminescent composites and sensitive Be 2+ detection. *Sci Rep*. 2014;4(1):1-8.

34. Bhunia SK, Saha A, Maity AR, Ray SC, Jana NR. Carbon nanoparticle-based fluorescent bioimaging probes. *Sci Rep*. 2013;3(1):1-7.

35. Qu S, Wang X, Lu Q, Liu X, Wang L. A biocompatible fluorescent ink based on water-soluble luminescent carbon nanodots. *Angew Chemie Int Ed*. 2012;51(49):12215-12218.

36. Pan D, Zhang J, Li Z, Wu C, Yan X, Wu M. Observation of pH-, solvent-, spin-, and excitation-dependent blue photoluminescence from carbon nanoparticles. *Chem Commun*. 2010;46(21):3681-3683.

37. Zhao Y, Liu X, Yang Y, et al. Carbon dots: from intense absorption in visible range to excitation-independent and excitation-dependent photoluminescence. *Fullerenes, Nanotub Carbon Nanostructures*. 2015;23(11):922-929.

38. Ding H, Wei J-S, Zhang P, Zhou Z-Y, Gao Q-Y, Xiong H-M. Solvent-controlled synthesis of highly luminescent carbon dots with a wide color gamut and narrowed emission peak widths. *Small*. 2018;14(22):1800612.

39. Sun Y-P, Zhou B, Lin Y, et al. Quantum-sized carbon dots for bright and colorful photoluminescence. *J Am Chem Soc*. 2006;128(24):7756-7757.

40. \cTucureanu V, Matei A, Avram AM. FTIR spectroscopy for carbon family study. *Crit Rev Anal Chem*. 2016;46(6):502-520.

41. Zheng M, Liu S, Li J, et al. Integrating oxaliplatin with highly luminescent carbon dots: an unprecedented theranostic agent for personalized medicine. *Adv Mater*. 2014;26(21):3554-3560.

42. Yuan C, Liu B, Liu F, Han M-Y, Zhang Z. Fluorescence “turn on” detection of mercuric ion based on bis (dithiocarbamato) copper (II) complex functionalized carbon nanodots. *Anal Chem*. 2014;86(2):1123-1130.

43. Shi Y, Pan Y, Zhang H, et al. A dual-mode nanosensor based on carbon quantum dots and gold nanoparticles for discriminative detection of glutathione in human plasma. *Biosens Bioelectron*. 2014;56:39-45.

44. Miao X, Qu D, Yang D, et al. Synthesis of carbon dots with multiple color emission by controlled graphitization and surface functionalization. *Adv Mater*. 2018;30(1):1704740.

45. Yan F, Sun Z, Zhang H, Sun X, Jiang Y, Bai Z. The fluorescence mechanism of carbon dots, and methods for tuning their emission color: a review. *Microchim*

Acta. 2019;186(8):1-37.

46. Pan L, Sun S, Zhang A, et al. Truly fluorescent excitation-dependent carbon dots and their applications in multicolor cellular imaging and multidimensional sensing. *Adv Mater*. 2015;27(47):7782-7787.

47. Dong Y, Pang H, Yang H Bin, et al. Carbon-based dots co-doped with nitrogen and sulfur for high quantum yield and excitation-independent emission. *Angew Chemie Int Ed*. 2013;52(30):7800-7804.

48. Liu H, Zhao X, Wang F, et al. High-efficient excitation-independent blue luminescent carbon dots. *Nanoscale Res Lett*. 2017;12(1):1-7.

49. Liu Y, Zhou L, Li Y, Deng R, Zhang H. Highly fluorescent nitrogen-doped carbon dots with excellent thermal and photo stability applied as invisible ink for loading important information and anti-counterfeiting. *Nanoscale*. 2017;9(2):491-496.

50. Yang Z, Xu M, Liu Y, et al. Nitrogen-doped, carbon-rich, highly photoluminescent carbon dots from ammonium citrate. *Nanoscale*. 2014;6(3):1890-1895.

51. Ogi T, Aishima K, Permatasari FA, Iskandar F, Tanabe E, Okuyama K. Kinetics of nitrogen-doped carbon dot formation via hydrothermal synthesis. *New J Chem*. 2016;40(6):5555-5561.

52. Xu Q, Pu P, Zhao J, et al. Preparation of highly photoluminescent sulfur-doped carbon dots for Fe (III) detection. *J Mater Chem A*. 2015;3(2):542-546.

53. Li J, Yang S, Deng Y, et al. Emancipating target-functionalized carbon dots from autophagy vesicles for a novel visualized tumor therapy. *Adv Funct Mater*. 2018;28(30):1800881.

54. Mohan R, Drbohlavova J, Hubalek J. Dual band emission in carbon dots. *Chem Phys Lett*. 2018;692:196-201.

55. Xu J, Wang C, Li H, Zhao W. Synthesis of green-emitting carbon quantum dots with double carbon sources and their application as a fluorescent probe for selective detection of Cu 2+ ions. *RSC Adv*. 2020;10(5):2536-2544.

56. Dong Y, Chen Y, You X, et al. High photoluminescent carbon based dots with tunable emission color from orange to green. *Nanoscale*. 2017;9(3):1028-1032.

57. Yang S, Sun X, Wang Z, Wang X, Guo G, Pu Q. Anomalous enhancement of fluorescence of carbon dots through lanthanum doping and potential application in intracellular imaging of ferric ion. *Nano Res*. 2018;11(3):1369-1378.

58. Yang Y, Hou J, Huo D, et al. Green emitting carbon dots for sensitive fluorometric determination of cartap based on its aggregation effect on gold nanoparticles. *Microchim Acta*. 2019;186(4):1-8.

59. Qu D, Zheng M, Du P, et al. Highly luminescent S, N co-doped graphene quantum dots with broad visible absorption bands for visible light photocatalysts. *Nanoscale*. 2013;5(24):12272-12277.

60. Liu Y, Xiao N, Gong N, et al. One-step microwave-assisted polyol synthesis of green luminescent carbon dots as optical nanoprobes. *Carbon N Y*. 2014;68:258-264.

61. Liu C, Zhang P, Zhai X, et al. Nano-carrier for gene delivery and bioimaging based on carbon dots with PEI-passivation enhanced fluorescence. *Biomaterials*. 2012;33(13):3604-3613.

62. Zhang QQ, Yang T, Li RS, et al. A functional preservation strategy for the production of highly photoluminescent emerald carbon dots for lysosome targeting and lysosomal pH imaging. *Nanoscale*. 2018;10(30):14705-14711.

63. Liu Y, Chao D, Zhou L, Li Y, Deng R, Zhang H. Yellow emissive carbon dots with quantum yield up to 68.6\% from manganese ions. *Carbon N Y*. 2018;135:253-259.

64. Jiang K, Sun S, Zhang L, Wang Y, Cai C, Lin H. Bright-yellow-emissive N-doped carbon dots: preparation, cellular imaging, and bifunctional sensing. *ACS Appl Mater \& interfaces*. 2015;7(41):23231-23238.

65. Hou J, Wang W, Zhou T, Wang B, Li H, Ding L. Synthesis and formation mechanistic investigation of nitrogen-doped carbon dots with high quantum yields and yellowish-green fluorescence. *Nanoscale*. 2016;8(21):11185-11193.

66. Song L, Cui Y, Zhang C, Hu Z, Liu X. Microwave-assisted facile synthesis of yellow fluorescent carbon dots from o-phenylenediamine for cell imaging and sensitive detection of Fe 3+ and H 2 O 2. *RSC Adv*. 2016;6(21):17704-17712.

67. Yan F, Bai Z, Zu F, et al. Yellow-emissive carbon dots with a large Stokes shift are viable fluorescent probes for detection and cellular imaging of silver ions and glutathione. *Microchim Acta*. 2019;186(2):1-11.

68. Wang W, Peng J, Li F, Su B, Chen X, Chen X. Phosphorus and chlorine co-doped carbon dots with strong photoluminescence as a fluorescent probe for ferric ions. *Microchim Acta*. 2019;186(1):1-9.

69. Geng X, Sun Y, Guo Y, et al. Fluorescent carbon dots for in situ monitoring of lysosomal ATP levels. *Anal Chem*. 2020;92(11):7940-7946.

70. Ding Y-Y, Gong X-J, Liu Y, et al. Facile preparation of bright orange fluorescent carbon dots and the constructed biosensing platform for the detection of pH in living cells. *Talanta*. 2018;189:8-15.

71. Wu M, Zhan J, Geng B, et al. Scalable synthesis of organic-soluble carbon quantum dots: superior optical properties in solvents, solids, and LEDs. *Nanoscale*. 2017;9(35):13195-13202.

72. Vedamalai M, Periasamy AP, Wang C-W, et al. Carbon nanodots prepared from o-phenylenediamine for sensing of Cu 2+ ions in cells. *Nanoscale*. 2014;6(21):13119-13125.

73. Liu J, Li D, Zhang K, Yang M, Sun H, Yang B. One-step hydrothermal synthesis of nitrogen-doped conjugated carbonized polymer dots with 31\% efficient red emission for in vivo imaging. *Small*. 2018;14(15):1703919.

74. Huang S, Yang E, Yao J, Liu Y, Xiao Q. Red emission nitrogen, boron, sulfur co-doped carbon dots for “on-off-on” fluorescent mode detection of Ag+ ions and L-cysteine in complex biological fluids and living cells. *Anal Chim Acta*. 2018;1035:192-202.

75. Li C, Wang Y, Zhang X, et al. Red fluorescent carbon dots with phenylboronic acid tags for quick detection of Fe (III) in PC12 cells. *J Colloid Interface Sci*. 2018;526:487-496.

76. Sun S, Zhang L, Jiang K, Wu A, Lin H. Toward high-efficient red emissive carbon dots: facile preparation, unique properties, and applications as multifunctional theranostic agents. *Chem Mater*. 2016;28(23):8659-8668.

77. Wang Z, Yuan F, Li X, et al. 53\% efficient red emissive carbon quantum dots for high color rendering and stable warm white-light-emitting diodes. *Adv Mater*. 2017;29(37):1702910.

78. Liu Y, Duan W, Song W, et al. Red emission B, N, S-co-doped carbon dots for colorimetric and fluorescent dual mode detection of Fe3+ ions in complex biological fluids and living cells. *ACS Appl Mater \& interfaces*. 2017;9(14):12663-12672.

79. Ali H, Bhunia SK, Dalal C, Jana NR. Red fluorescent carbon nanoparticle-based cell imaging probe. *ACS Appl Mater \& interfaces*. 2016;8(14):9305-9313.

80. Ju YJ, Li N, Liu SG, et al. Proton-controlled synthesis of red-emitting carbon dots and application for hematin detection in human erythrocytes. *Anal Bioanal Chem*. 2019;411(6):1159-1167.

81. Zhao J, Li F, Zhang S, An Y, Sun S. Preparation of N-doped yellow carbon dots and N, P co-doped red carbon dots for bioimaging and photodynamic therapy of tumors. *New J Chem*. 2019;43(16):6332-6342.

82. Zuo G, Jiao Y, Gao R, et al. Lipophilic red-emitting oligomeric organic dots for moisture detection and cell imaging. *ACS Appl Nano Mater*. 2020;3(2):1942-1949.

83. Ding H, Wei J-S, Zhong N, Gao Q-Y, Xiong H-M. Highly efficient red-emitting carbon dots with gram-scale yield for bioimaging. *Langmuir*. 2017;33(44):12635-12642.

84. Ghosh S, Ali H, Jana NR. Water dispersible red fluorescent carbon nanoparticles via carbonization of resorcinol. *ACS Sustain Chem \& Eng*. 2019;7(14):12629-12637.

85. Yuan R, Liu J, Xiang W, Liang X. Red-emitting carbon dots phosphors: a promising red color convertor toward warm white light emitting diodes. *J Mater Sci Mater Electron*. 2018;29(12):10453-10460.

86. Lan M, Zhao S, Zhang Z, et al. Two-photon-excited near-infrared emissive carbon dots as multifunctional agents for fluorescence imaging and photothermal therapy. *Nano Res*. 2017;10(9):3113-3123.

87. Li H, He X, Liu Y, et al. One-step ultrasonic synthesis of water-soluble carbon nanoparticles with excellent photoluminescent properties. *Carbon N Y*. 2011;49(2):605-609.

88. Du F, Min Y, Zeng F, Yu C, Wu S. A targeted and FRET-based ratiometric fluorescent nanoprobe for imaging mitochondrial hydrogen peroxide in living cells. *Small*. 2014;10(5):964-972.

89. Bao L, Zhang Z-L, Tian Z-Q, et al. Electrochemical tuning of luminescent carbon

nanodots: from preparation to luminescence mechanism. *Adv Mater*. 2011;23(48):5801-5806.

90. Liu L, Li Y, Zhan L, Liu Y, Huang C. One-step synthesis of fluorescent hydroxyls-coated carbon dots with hydrothermal reaction and its application to optical sensing of metal ions. *Sci China Chem*. 2011;54(8):1342.

91. Song T, Zhao Y, Wang T, Li J, Jiang Z, Yang P. Carbon dots doped with N and S towards controlling emitting. *J Fluoresc*. 2020;30(1):81-89.

92. Kimling J, Maier M, Okenve B, Kotaidis V, Ballot H, Plech A. Turkevich method for gold nanoparticle synthesis revisited. *J Phys Chem B*. 2006;110(32):15700-15707.

93. Li H, Su D, Gao H, et al. Design of red emissive carbon dots: robust performance for analytical applications in pesticide monitoring. *Anal Chem*. 2020;92(4):3198-3205.

94. Liu R, Liu J, Kong W, et al. Adsorption dominant catalytic activity of a carbon dots stabilized gold nanoparticles system. *Dalt Trans*. 2014;43(28):10920-10929.

95. Zheng C, Ke W, Yin T, An X. Intrinsic peroxidase-like activity and the catalytic mechanism of gold@ carbon dots nanocomposites. *RSC Adv*. 2016;6(42):35280-35286.

96. Song J, Zhao L, Wang Y, et al. Carbon quantum dots prepared with chitosan for synthesis of CQDs/AuNPs for iodine ions detection. *Nanomaterials*. 2018;8(12):1043.

97. Zhu Y, Du J, Peng Q, et al. The synthesis of highly active carbon dot-coated gold nanoparticles via the room-temperature in situ carbonization of organic ligands for 4-nitrophenol reduction. *RSC Adv*. 2020;10(33):19419-19424.

98. Fan Y, Guo X, Zhang Y, Lv Y, Zhao J, Liu X. Efficient and stable red emissive carbon nanoparticles with a hollow sphere structure for white light-emitting diodes. *ACS Appl Mater \& interfaces*. 2016;8(46):31863-31870.

99. Liu ML, Chen B Bin, Li CM, Huang CZ. Carbon dots: synthesis, formation mechanism, fluorescence origin and sensing applications. *Green Chem*. 2019;21(3):449-471.

100. Zhang Z, Pei K, Yang Q, Dong J, Yan Z, Chen J. A nanosensor made of sulfur--nitrogen co-doped carbon dots for “off--on” sensing of hypochlorous acid and Zn (II) and its bioimaging properties. *New J Chem*. 2018;42(19):15895-15904.

101. Jiang K, Sun S, Zhang L, et al. Red, green, and blue luminescence by carbon dots: full-color emission tuning and multicolor cellular imaging. *Angew chemie*. 2015;127(18):5450-5453.

102. Gao G, Jiang Y-W, Yang J, Wu F-G. Mitochondria-targetable carbon quantum dots for differentiating cancerous cells from normal cells. *Nanoscale*. 2017;9(46):18368-18378.

103. Guo S, Sun Y, Li J, et al. Fluorescent Carbon Dots Shuttling between Mitochondria and the Nucleolus for in Situ Visualization of Cell Viability. *ACS Appl Bio Mater*. 2020;4(1):928-934.

104. Hua X-W, Bao Y-W, Wu F-G. Fluorescent carbon quantum dots with intrinsic nucleolus-targeting capability for nucleolus imaging and enhanced cytosolic and nuclear drug delivery. *ACS Appl Mater \& interfaces*. 2018;10(13):10664-10677.

105. Ji Z, Yin Z, Jia Z, Wei J. Carbon nanodots derived from urea and citric acid in living cells: Cellular uptake and antioxidation effect. *Langmuir*. 2020;36(29):8632-8640.

106. Su W, Guo R, Yuan F, et al. Red-emissive carbon quantum dots for nuclear drug delivery in cancer stem cells. *J Phys Chem Lett*. 2020;11(4):1357-1363.